Interdisciplinary Research Centre

in

Materials for High Performance Applications

Final Proceedings of The EOARD/IRC-sponsored International Workshop on Gamma Aluminide Alloy Technology

held from 1 to 3 May 1996
at The IRC in Materials for High Performance Applications
The University of Birmingham

SECTION FOUR

THE UNIVERSITY OF BIRMINGHAM

UNIVERSITY OF WALES SWANSEA

THE UNIVERSITY OF BIRMINGHAM AND UNIVERSITY OF WALES SWANSEA CONSORTIUM

Funded by the Engineering and Physical Sciences Research Council

Final Proceedings of The EOARD/IRC-sponsored International Workshop on Gamma Aluminide Alloy Technology

held from 1 to 3 May 1996
at The IRC in Materials for High Performance Applications
The University of Birmingham

SECTION FOUR

The organisers wish to thank the United States Air Force European Office of Aerospace Research and Development for its contributions to the success of this conference

The Role of the Initial Steps of Oxidation for High Temperature Oxidation Resistance

C. Lang, M. Schütze
Karl Winnacker - Institut
DECHEMA
D - 60061 Frankfurt / M.

1 Introduction

- insufficient oxidation resistance of γ - titanium aluminides above 800°C.
- formation of a complex mixture of TiO_2 and Al_2O_3 instead of a thin, protective Al_2O_3 layer

gas / TiO_2 / (Al_2O_3) / $TiO_2 + Al_2O_3$ / Al depl. metal

- detrimental effect of nitrogen containing atmospheres
- niobium additions improve oxidation resistance

→ investigation of the initial stages of oxidation

2 Experimental Procedure

- materials: Ti36Al (mass - %)
  Ti35Al5Nb (mass - %)

Experimental Procedure

TEM sample preparation

foil samples

- electrolytic jet thinning with the solution H_2SO_4 : CH_3OH 1:9 at -25°C
- subsequent short ion thinning for cleaning of the surface
- oxidation in air from 800°C to 1000°C

cross sections

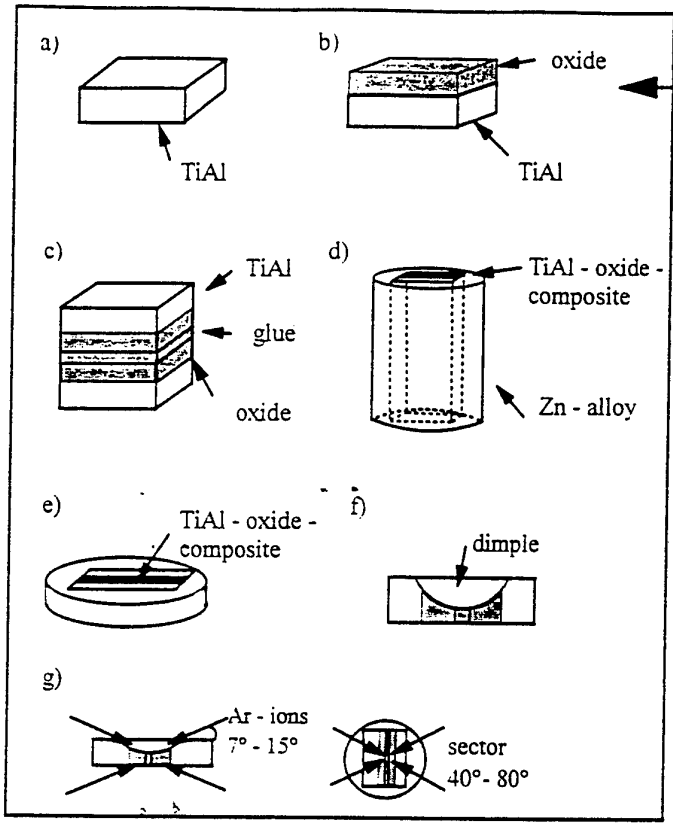

SEM + EDX

TEM investigation

energy dispersive X - ray analysis (EDX) → chemical composition

bright / dark field images → scale structure and morphology

selected area diffraction (SAD)

convergent - beam electron diffraction (CBED)

→ computer aided analysis of diffraction patterns

calculation of interplanar spacings d by the equation:

$$\lambda * L = R * d$$

d: interplanar spacing

R: distance of the reflex to the origin on the pattern

λ*L: camera constant

indexing of the diffraction patterns by the calculated interplanar spacings and identification of the phase

→ oxide scale structure, orientation relationship to the substrate

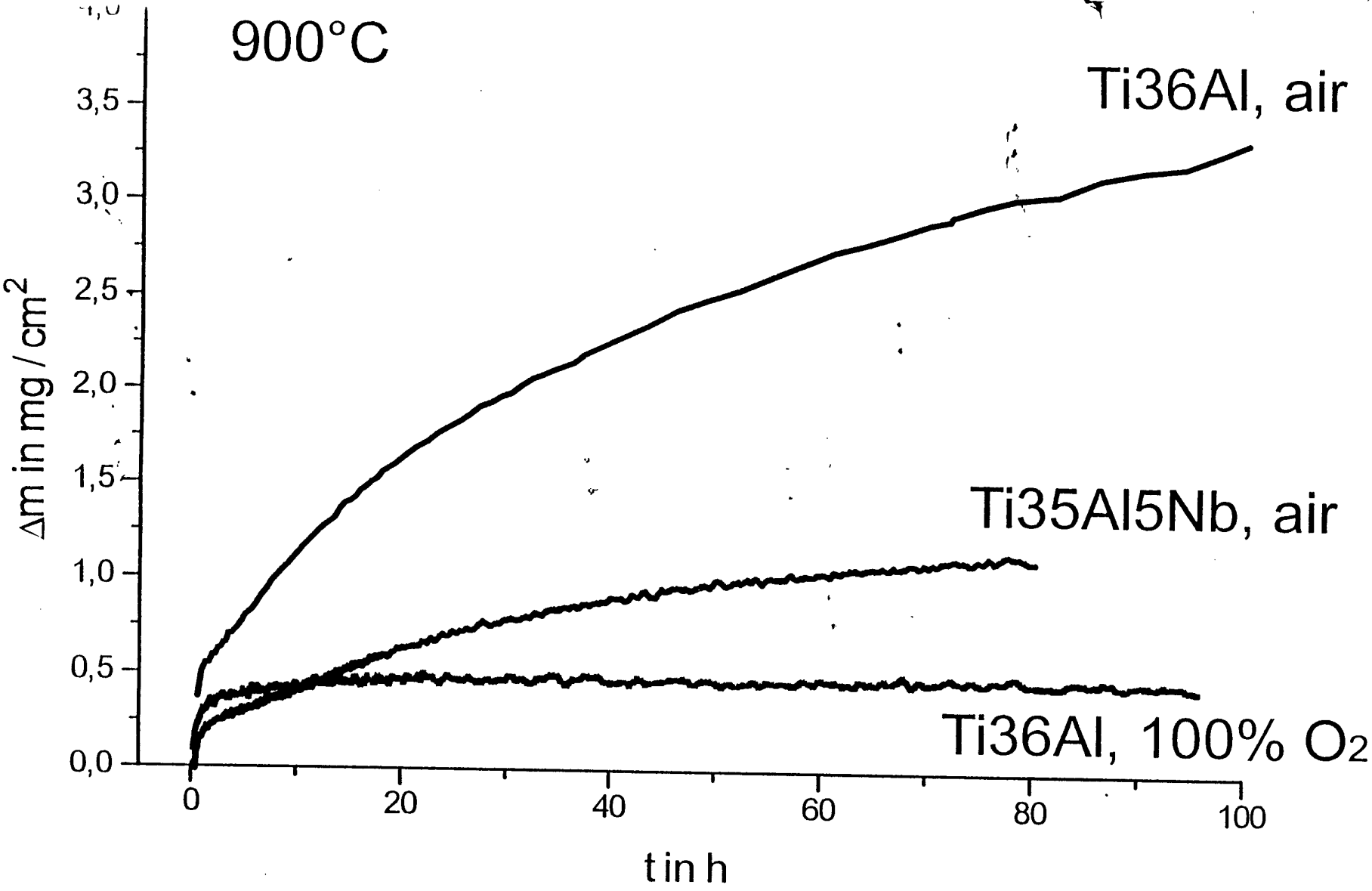
900°C
Ti36Al, air
Ti35Al5Nb, air
Ti36Al, 100% O2
Δm in mg / cm2
t in h
0,0
0,5
1,0
1,5
2,0
2,5
3,0
3,5
0
20
40
60
80
100

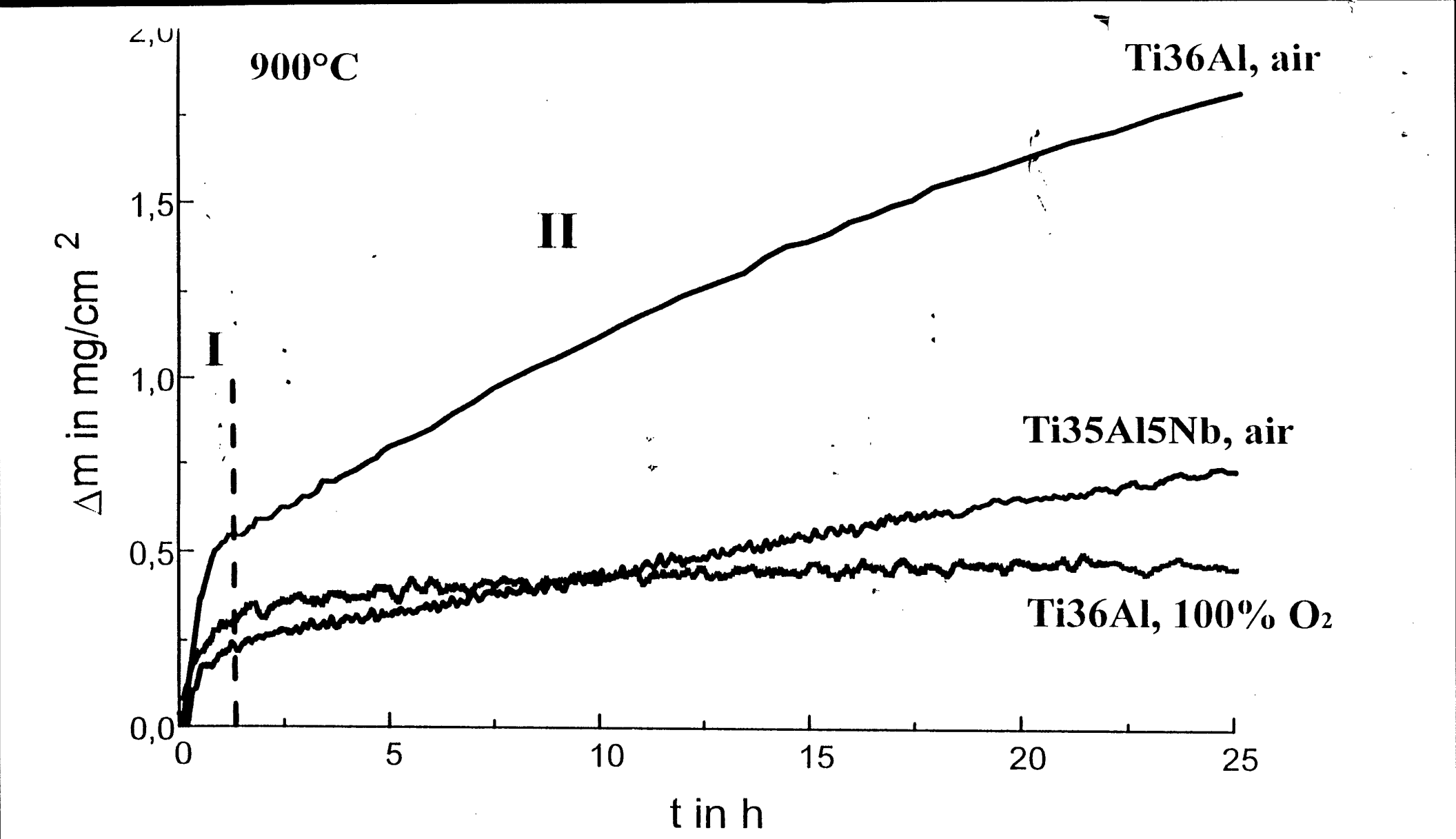
900°C
Ti36Al, air
II
I
Ti35Al5Nb, air
Ti36Al, 100% O2
Δm in mg/cm 2
t in h
0,0
0,5
1,0
1,5
0
5
10
15
20
25

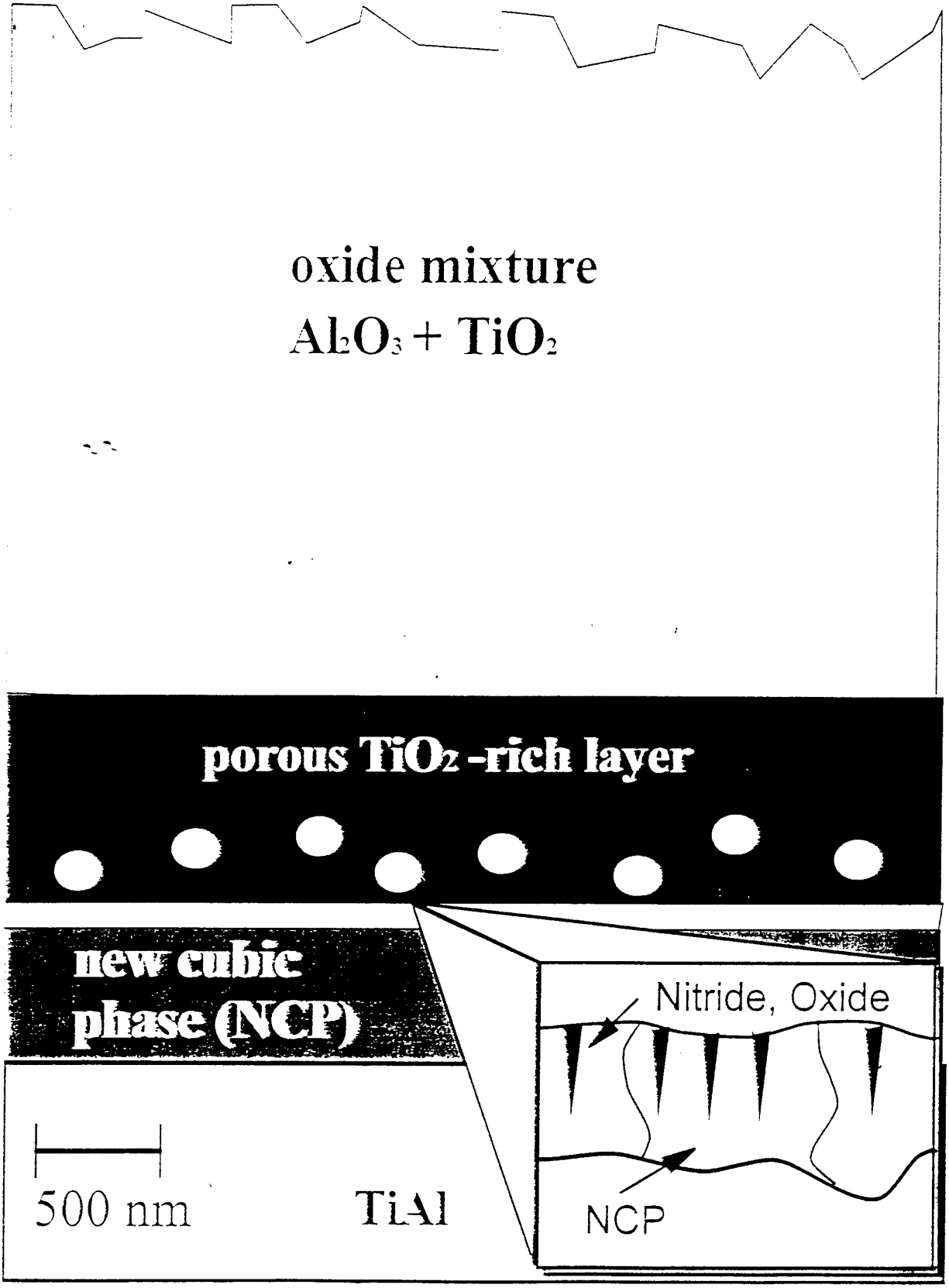

Schematic illustration of the oxide scale and the metal subsurface layer of Ti36Al after oxidation for 0.5 h at 900°C in air.

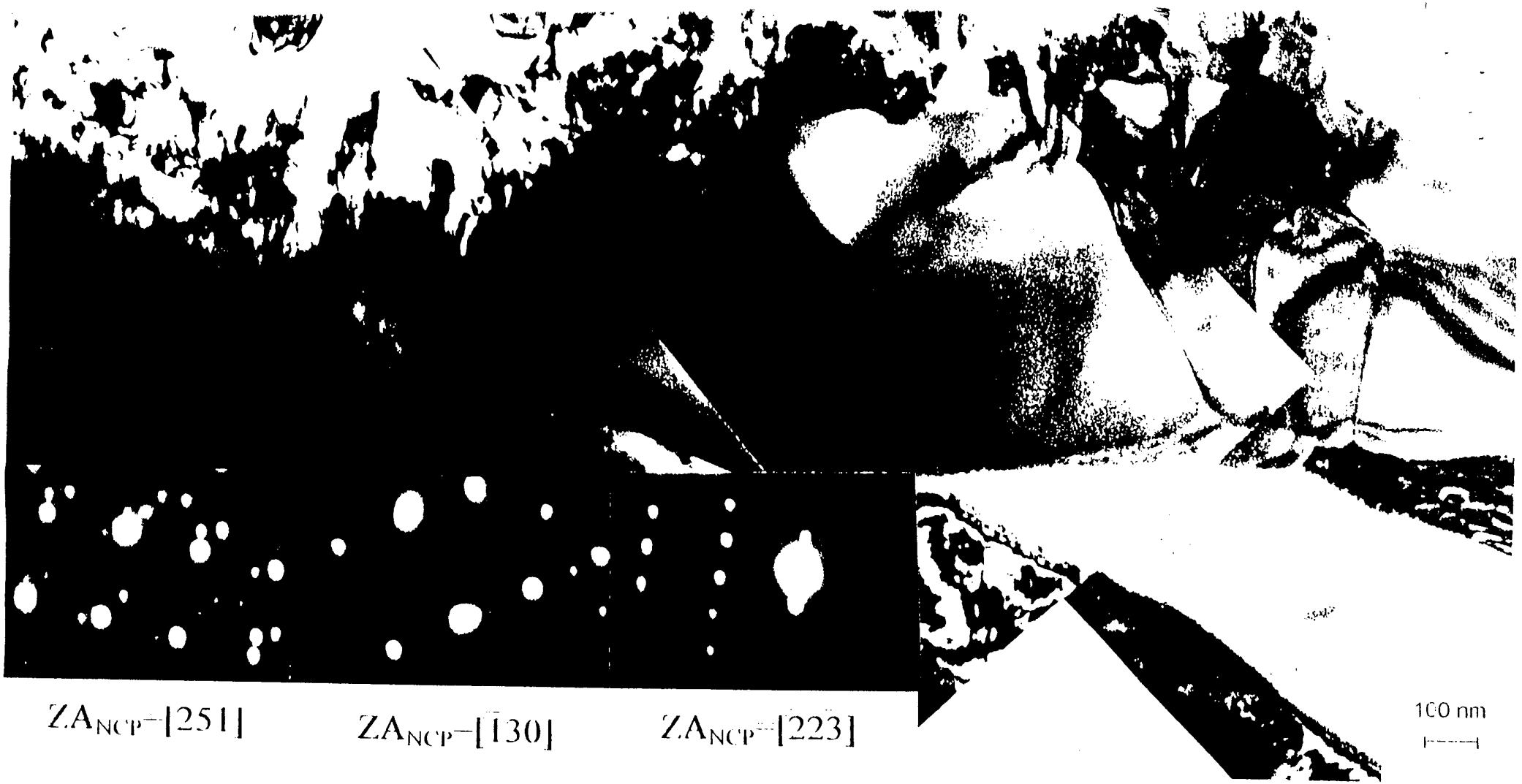

Metal subsurface zone of Ti36Al after 0.5 h of oxidation at 900°C in air.

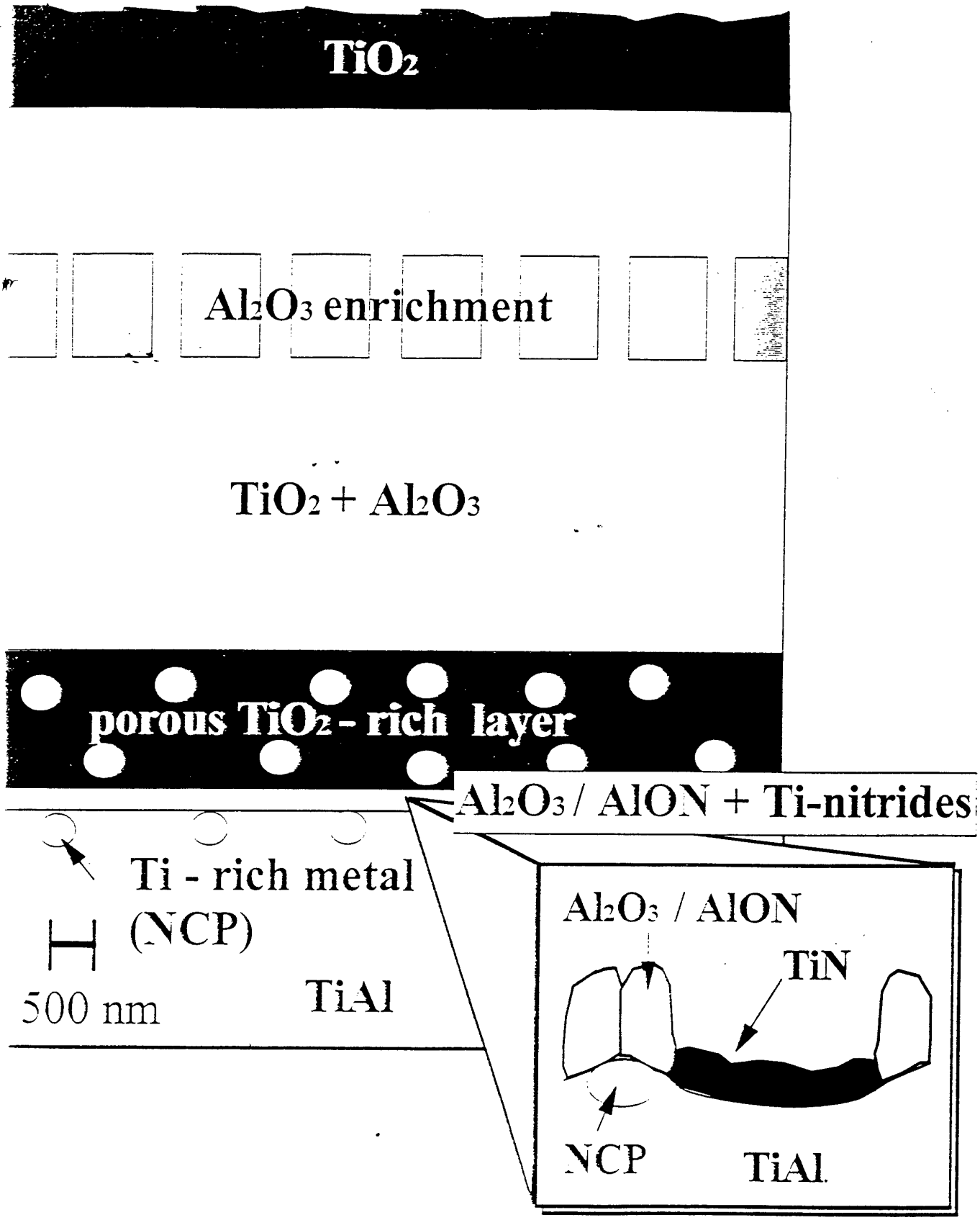

Schematic illustration of the oxide scale on Ti36Al after
h of oxidation at 900°C in air.

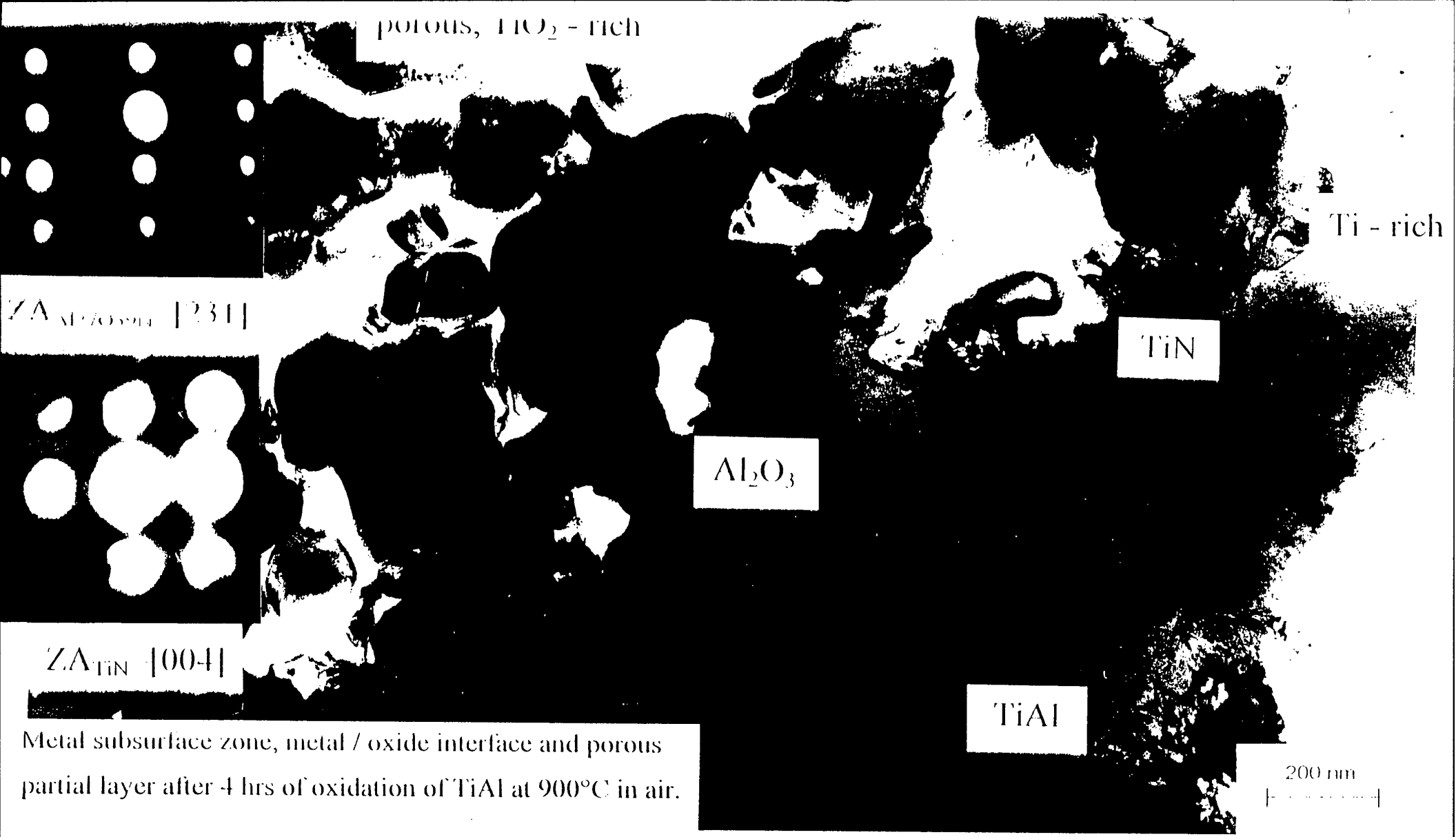

Metal subsurface zone, metal / oxide interface and porous partial layer after 4 hrs of oxidation of TiAl at 900°C in air.

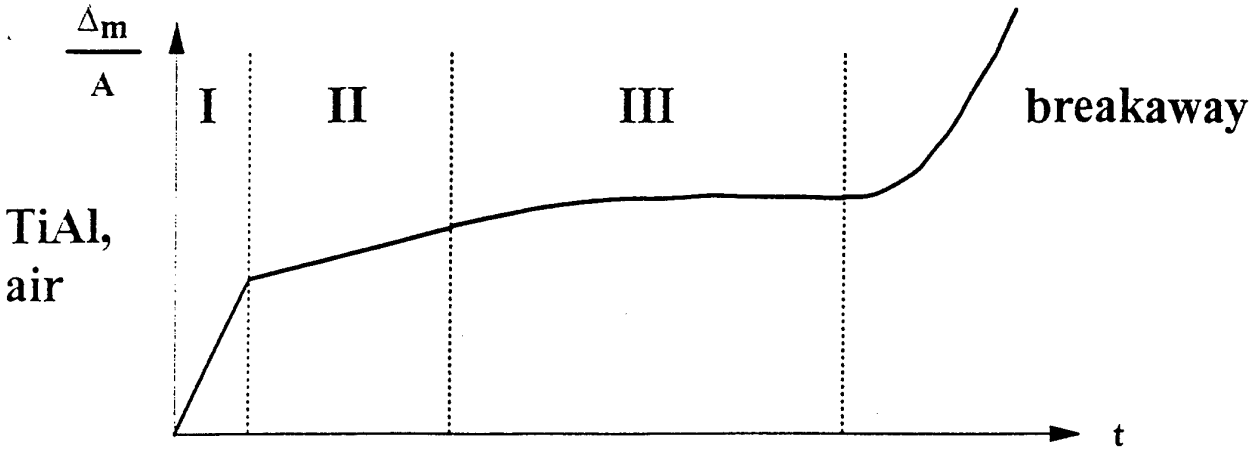

I:

- initial formation of Al_2O_3 and TiO_2

➡ Al depletion and subsequent for - mation of Ti - rich subsurface zone

➡ increase of Ti - activity and decrease of Al - activity

➡ formation of Ti - nitrides / oxides at the metal / oxide interface caused by the nonprotective oxide scale

➡ rapid oxide growth until consumption of the Ti - rich subsurface zone

II:

- change of the subsurface zone from Ti - rich to TiAl

➡ oxidation behaviour different to stage I because of the already formed oxide scale

➡ linear oxide growth through repeated formation of Ti - nitrides, Al_2O_3 and Ti_3Al at the metal oxide interface

III:

- formation of the outer Al_2O_3 barrier

➡ parabolic oxide growth

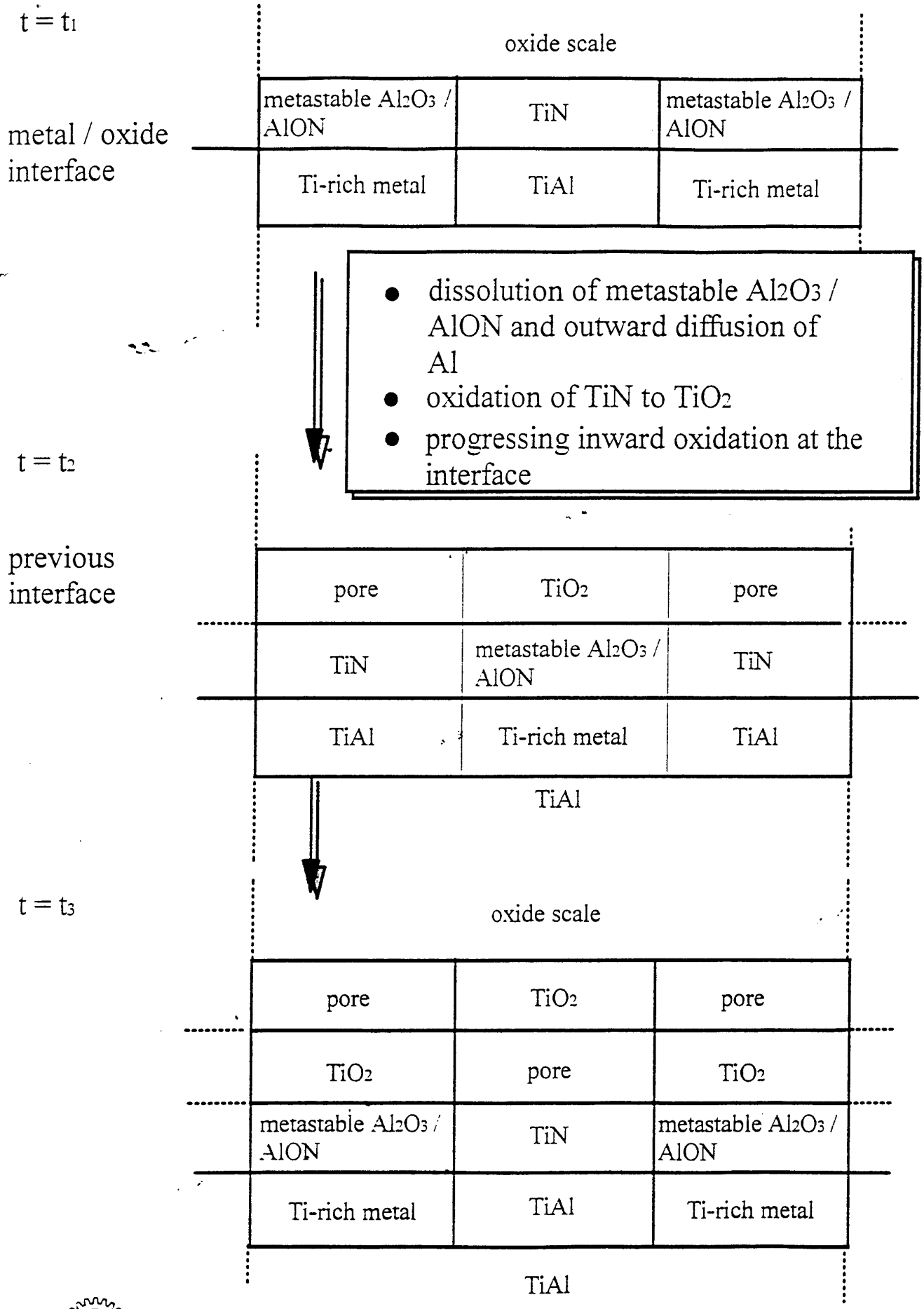
t = t1
oxide scale
metastable Al2O3 / AlON
TiN
metastable Al2O3 / AlON
metal / oxide interface
Ti-rich metal
TiAl
Ti-rich metal
dissolution of metastable Al2O3 / AlON and outward diffusion of Al
oxidation of TiN to TiO2
progressing inward oxidation at the interface
t = t2
previous interface
pore
TiO2
pore
TiN
metastable Al2O3 / AlON
TiN
TiAl
Ti-rich metal
TiAl
TiAl
t = t3
oxide scale
pore
TiO2
pore
TiO2
pore
TiO2
metastable Al2O3 / AlON
TiN
metastable Al2O3 / AlON
Ti-rich metal
TiAl
Ti-rich metal
TiAl

oxide mixture

α - $Al_2O_3 + TiO_2$

coarse-grained Ti - oxide

Ti - nitride + - oxide (porous)

$Al_{27}O_{39}N$

TiAl + internal Al - oxide
+ Al - rich metal

500 nm

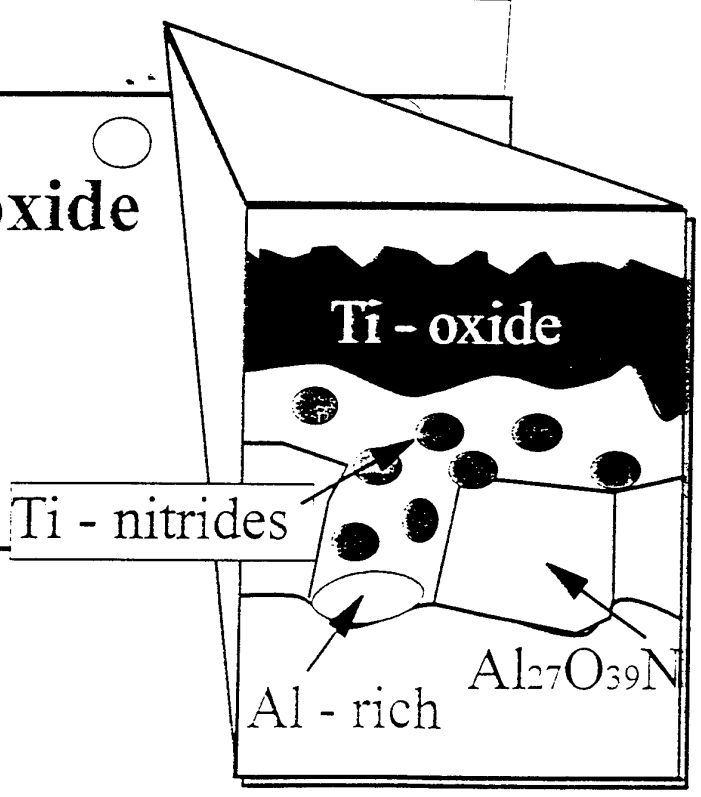

Schematic illustration of the oxide scale on Ti35Al5Nb after 4 h of oxidation at 900°C in air

Metal – oxide interface of Ti35Al5Nb after oxidation at 900°C for 4 h in air.

● Effect of niobium addition

- ● no formation of an Al depleted metal subsurface zone
- ● stabilizing of a thin Al_2O_3 / AlON layer at the metal / oxide interface

- – influence on γ - TiAl phase field
- – influence on the diffusion of Al and O in the metal and the oxide scale (doping of TiO_2)
- – influence on the solubility of Al in TiO_2

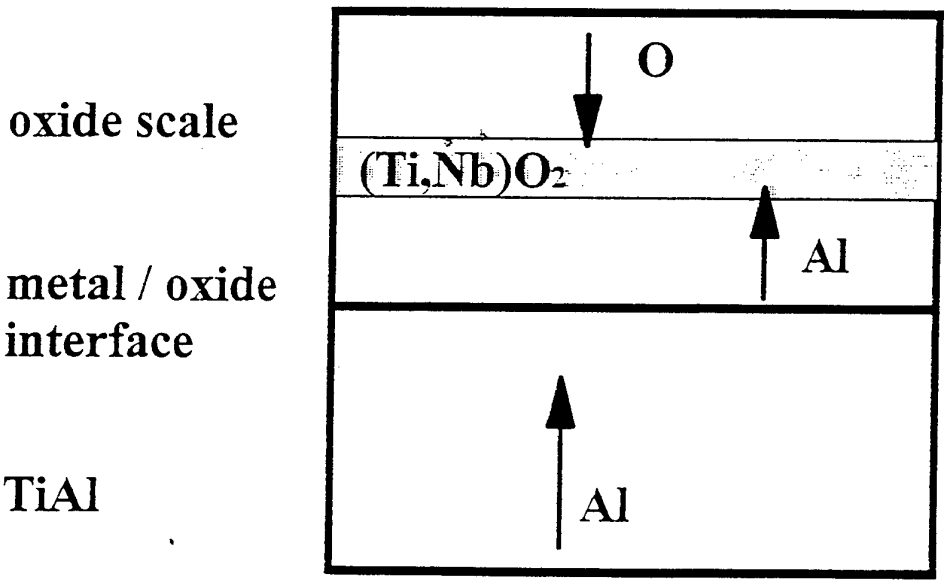

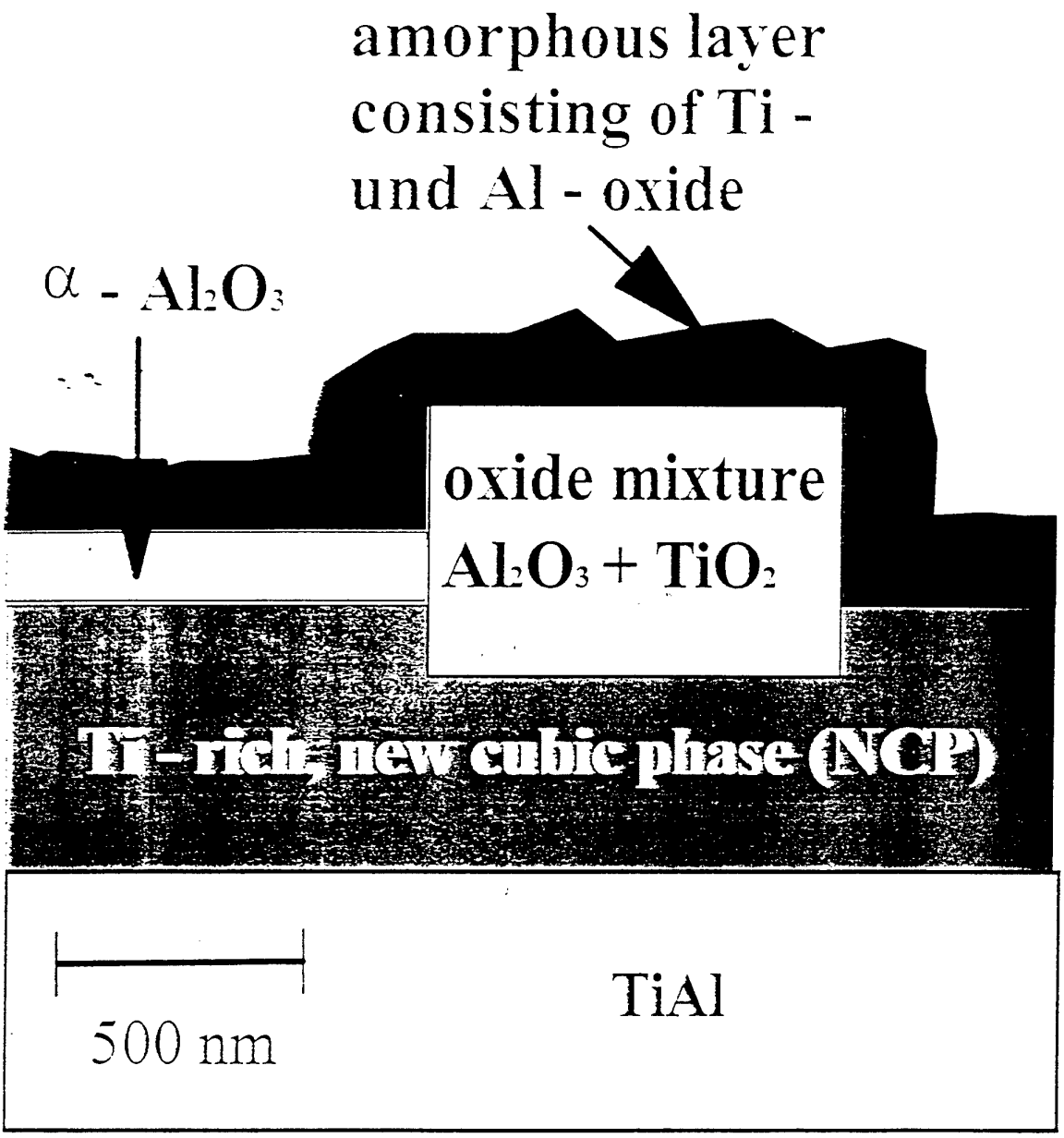

Schematic illustration of the oxide scale and the metal subsurface layer of Ti36Al after oxidation at 900°C for 4 h in pure oxygen.

Oxide scale and metal subsurface layer on Ti36Al after 4 h of oxidation at 900°C in pure oxygen

● Effect of nitrogen

- formation of Ti - nitrides at the metal / oxide interface
- formation of metastable Al_2O_3 or AlON, respevtively, at the metal / oxide interface instead of α - Al_2O_3

● Summary

- In nitrogen containing atmospheres metastable Al_2O_3 or AlON, respectively, is formed at the metal / oxide interface instead of α - Al_2O_3.
- In the metal / subsurface zone of Ti36Al Al depletion takes place and a new cubic phase (NCP) with a composition between α_2 - Ti_3Al and γ - TiAl exists.
- During air exposure Ti - nitrides are formed at the metal / oxide interface if an Al depletion occurs in the metal subsurface zone. Thus a continuous, protective Al_2O_3 layer is impeded.
- Niobium additions, which prevent Al depletion in the metal subsurface zone and stabilize Al_2O_3 / AlON formation at the interface, improve the oxidation resistance of γ - titanium aluminides

Development and Microstructural Assessment of TiAl-based Alloys at the IRC

Three general points concerning low alloy additions.

(i) Additions of 2at% of elements such as Ta and W changed yield and UTS very little, but improved creep with respect to our base alloy of Ti 48Al 2Mn 2Nb.

(ii) All other low alloying additions did little that could not be better accomplished by processing.

(iii) Grain size refinement by B addition straightforward in base alloy but complicated in Ta and W-containing alloys.

High Alloying additions

(i) Additions totalling about 8 - 10at% of elements such as Nb, Ta and Zr increase properties very signficantly. Life more complex with B2, $\alpha 2$ and γ phases and thermomechanical processing on these at early stage in IRC.

Property Targets Based on Industrial Specifications for LP Turbine Blades

Elongation ≈ 2%; K_{1C} ≈ 30MPa $m^{0.5}$
Yield ≈ 400MPa; UTS ≈ 550MPa

Alloys/processing based on derivatives of Ti45Al2Nb2Mn, ie. low alloying additions to Ti45Al

---

Property Targets Based on Industrial Specifications for HP Compressor Blades

Elongation 3%; K_{1c} 30MPa $m^{0.5}$;
Yield 700MPa UTS 1000MPa

Alloys/processing based on derivatives of Ti45Al with alloying additions of ≈ 8at% to Ti45Al

---

In neither case was a creep specification forthcoming! 1000h rupture tests at two temperatures and two stress levels are used to define relative primary and secondary creep strains

---

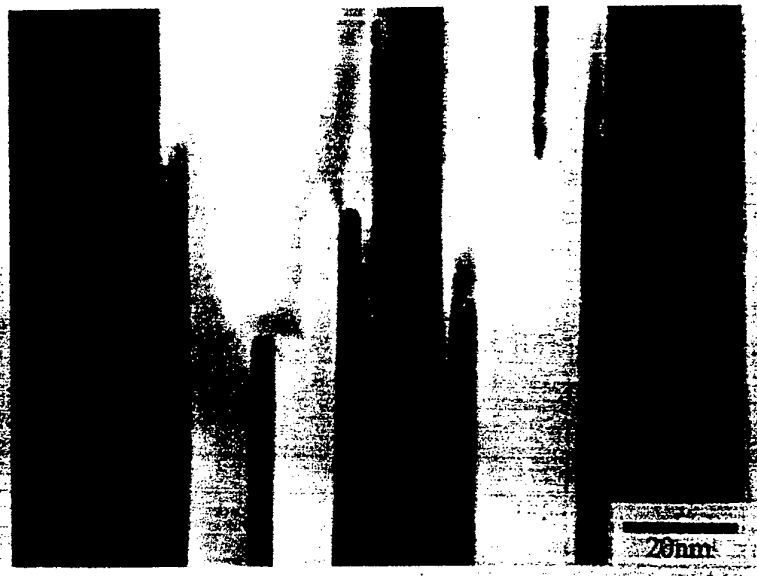

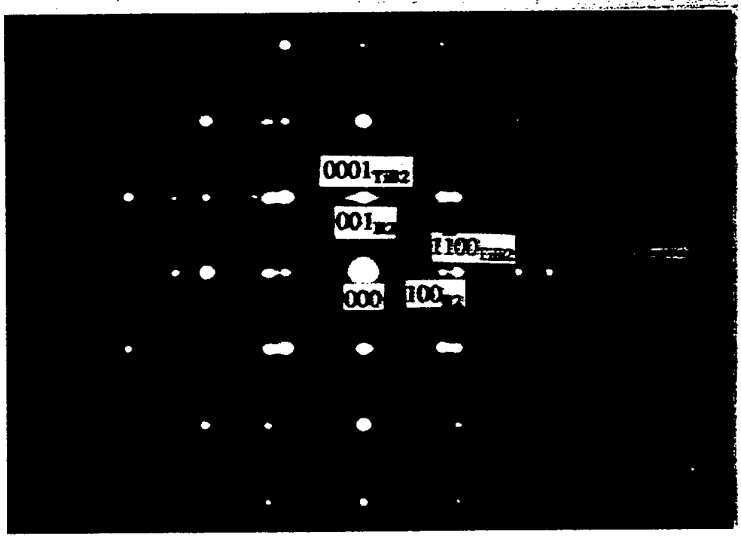

{1100} $_{TiB2}$// {100} $_{B2}$ and [0001] $_{TiB2}$//<001>$_{B2}$

TiB2	**a=303pm**	**B2**	**cubic**	**a=322pm**
hex	**c=322pm**			

UNIVERSITY COLLEGE OF SWANSEA

IRC in Materials for High Performance Applications

THE UNIVERSITY OF BIRMINGHAM

The Effect of Non-Turbulent Solidification

Ti-47Al-2Cr-2Nb

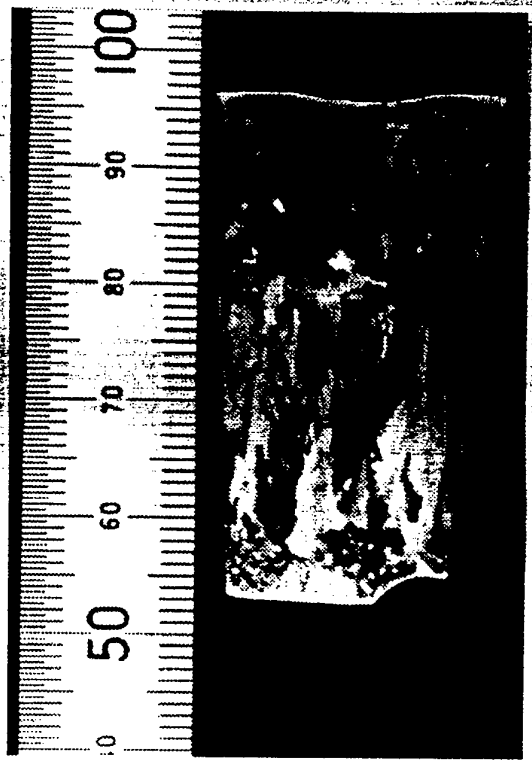

Ti-47Al-2Cr-2Nb-1B

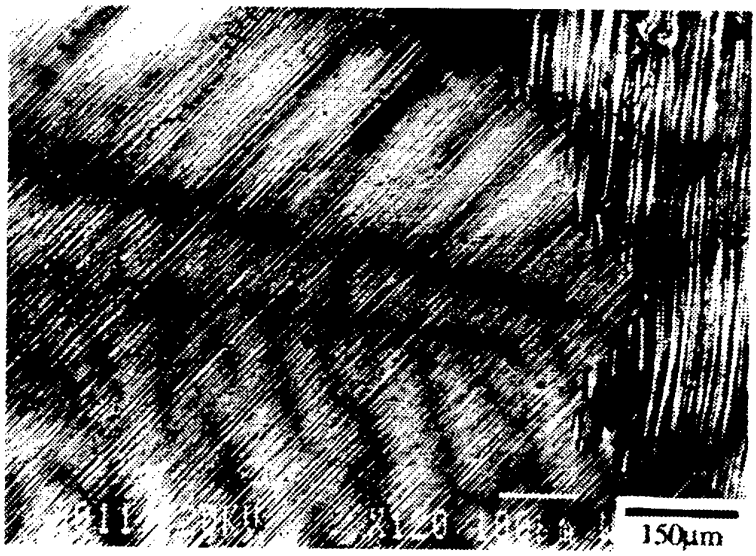

BSEI of Ti-47Al-2Cr-2Nb-1B

UNIVERSITY COLLEGE OF SWANSEA

IRC in Materials for High Performance Applications

THE UNIVERSITY OF BIRMINGHAM

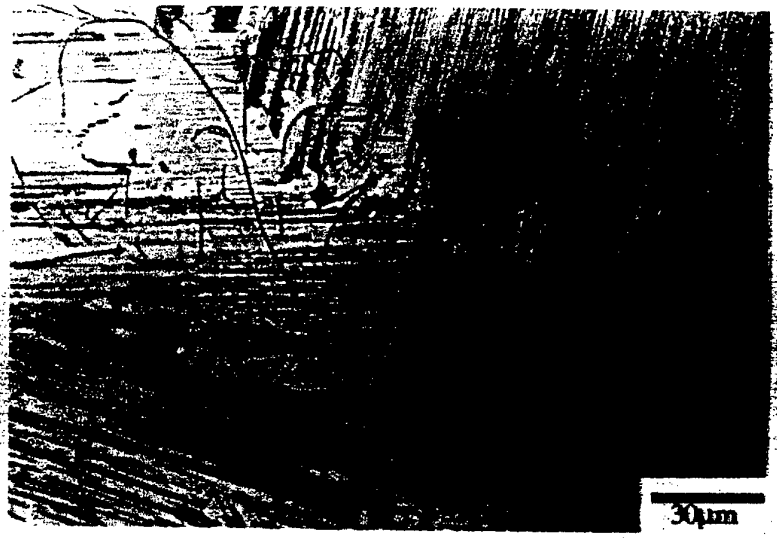

Boride morphology in Ti-47Al-2Cr-2Nb-1B

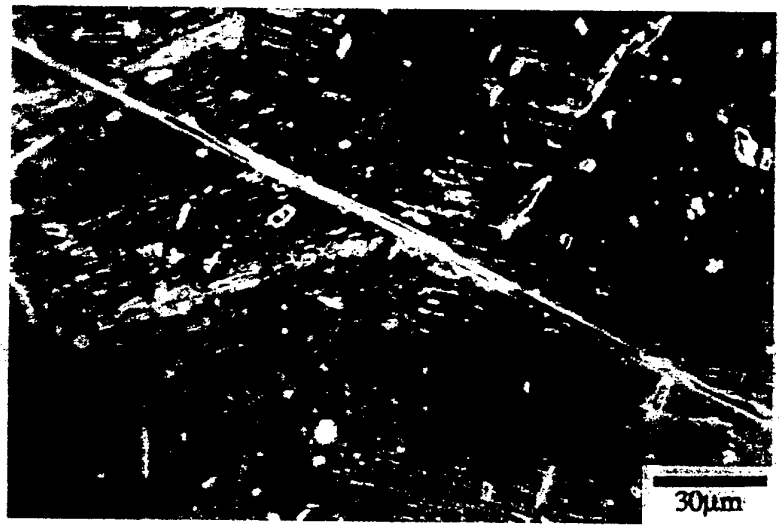

Boride morphology in Ti-47Al-2Ta-1Mn-1Cr-1B-0.2Si.

UNIVERSITY COLLEGE OF SWANSEA

IRC in Materials for High Performance Applications

THE UNIVERSITY OF BIRMINGHAM

Boride Agglomerates in Ti-47Al-2Ta-1Cr-1Mn-1B-0.2Si

As-cast — Bright field

As-cast — Dark field

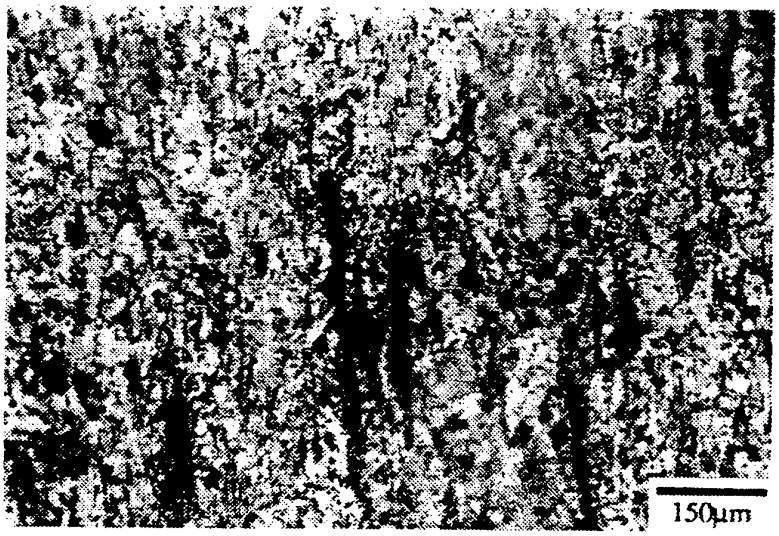

As-forged — forging axis ←→

UNIVERSITY COLLEGE OF SWANSEA

IRC in Materials for High Performance Applications

THE UNIVERSITY OF BIRMINGHAM

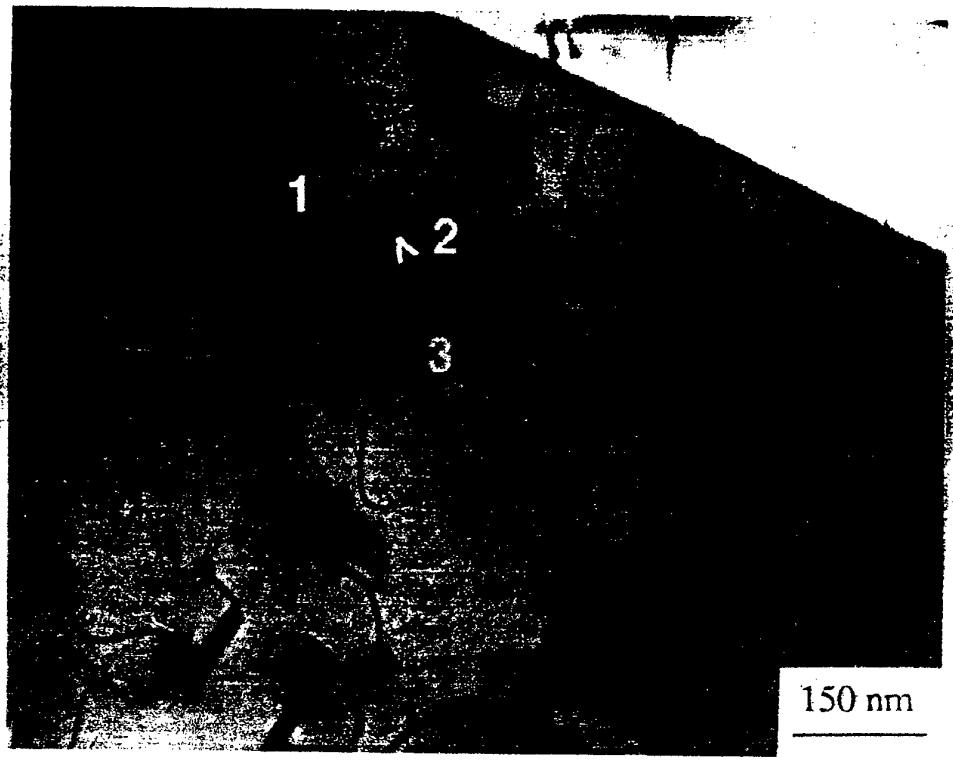

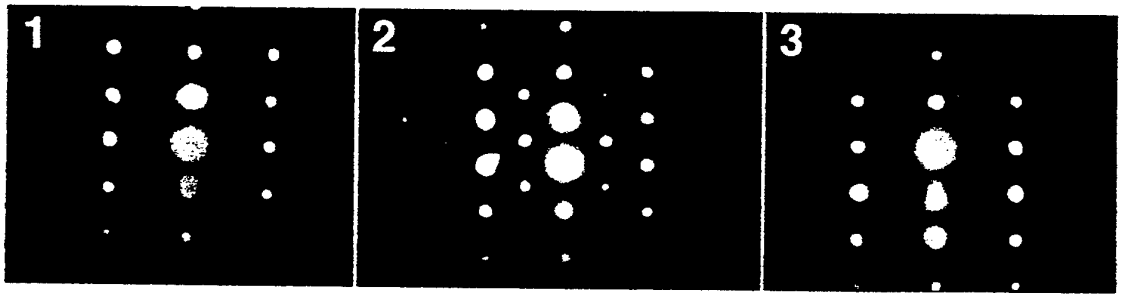

Typical APDBs in quenched Ti - 49Al and diffraction patterns from regions 1 - 3

UNIVERSITY COLLEGE OF SWANSEA

IRC in Materials for High Performance Applications

THE UNIVERSITY OF BIRMINGHAM

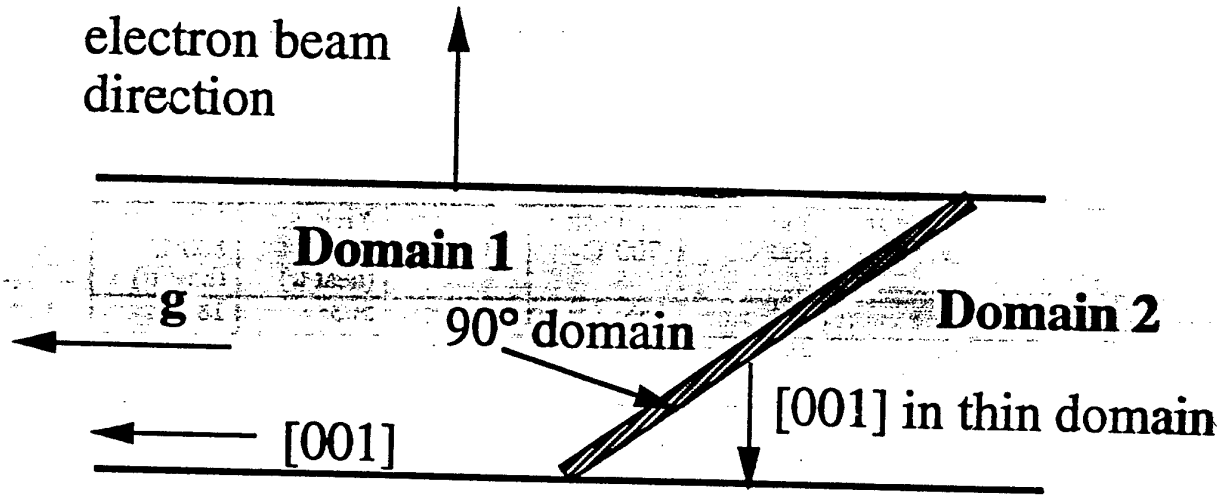

1/2 <101> displacement between domains 1 and 2

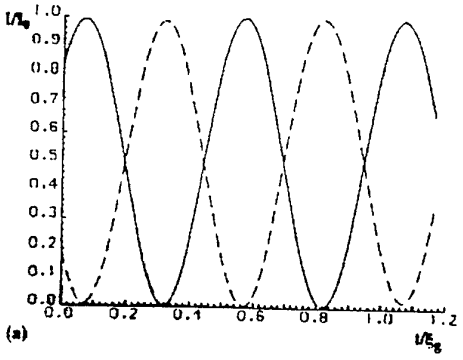

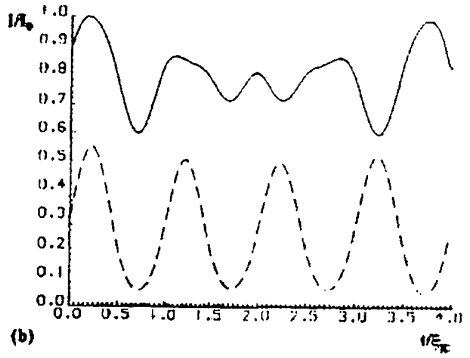

BF and DF micrographs with g = 001 (left) and g = 111 (right) each at Bragg. Computed images assume ΔR of 0.05 and appropriate deviations from Bragg for 90° domain

UNIVERSITY COLLEGE OF SWANSEA

IRC in Materials for High Performance Applications

THE UNIVERSITY OF BIRMINGHAM

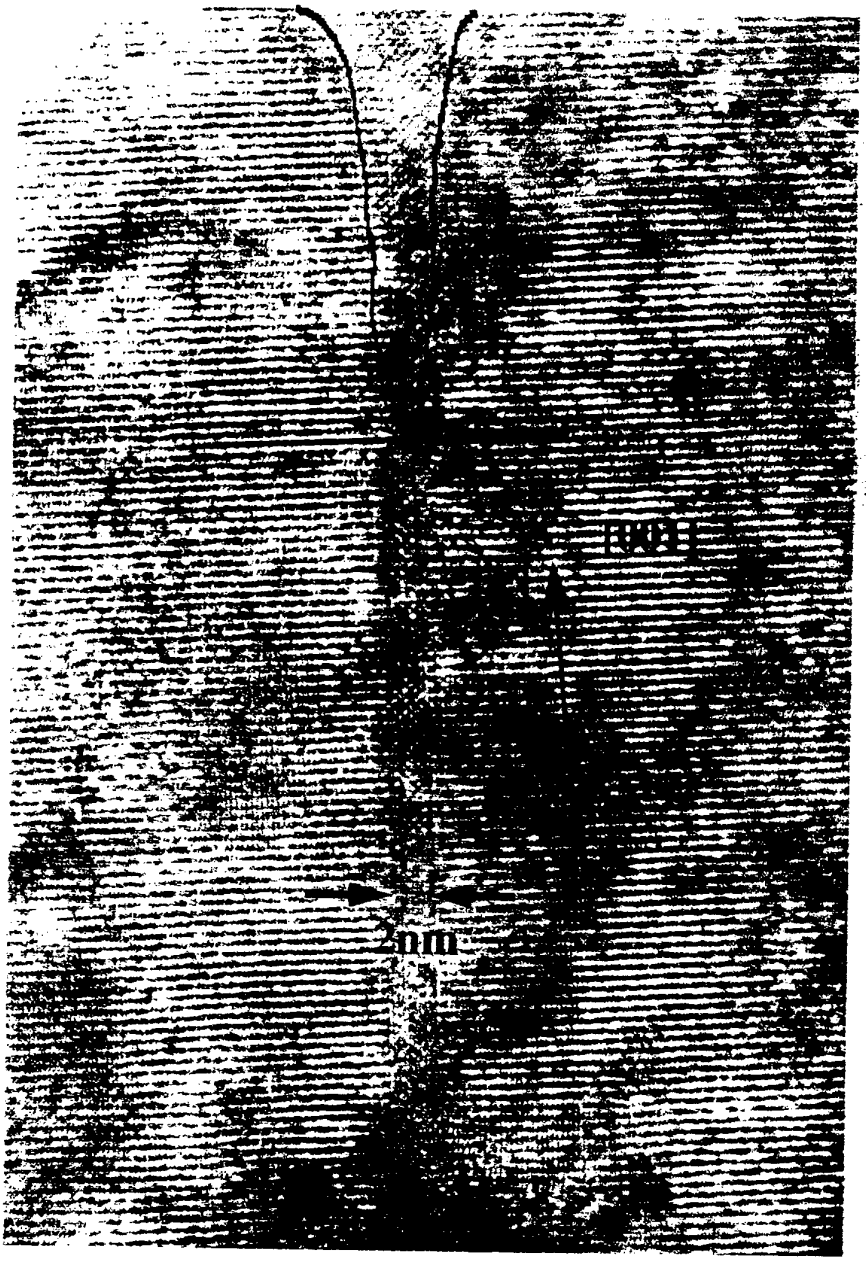

HREM of APDB in Ti-48Al-0.5Mo

UNIVERSITY COLLEGE OF SWANSEA

IRC in Materials for High Performance Applications

THE UNIVERSITY OF BIRMINGHAM

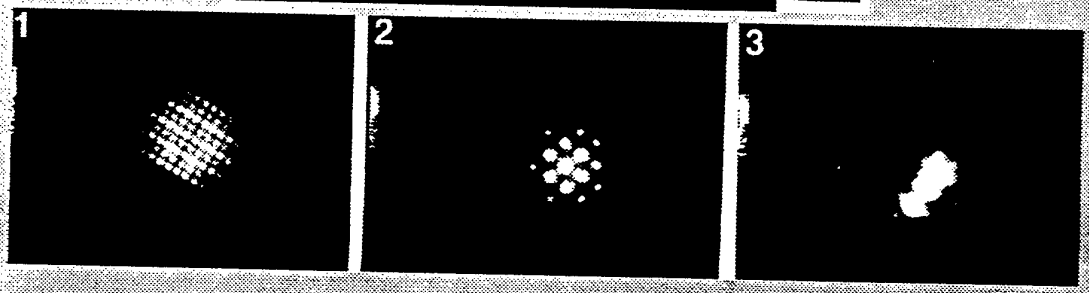

Dark field with reflection from γ_i showing relation between γ_i (area 1) and massive γ_m (area 2) and absence of relation between α (area 3) and γ_m

UNIVERSITY COLLEGE OF SWANSEA

IRC in Materials for High Performance Applications

THE UNIVERSITY OF BIRMINGHAM

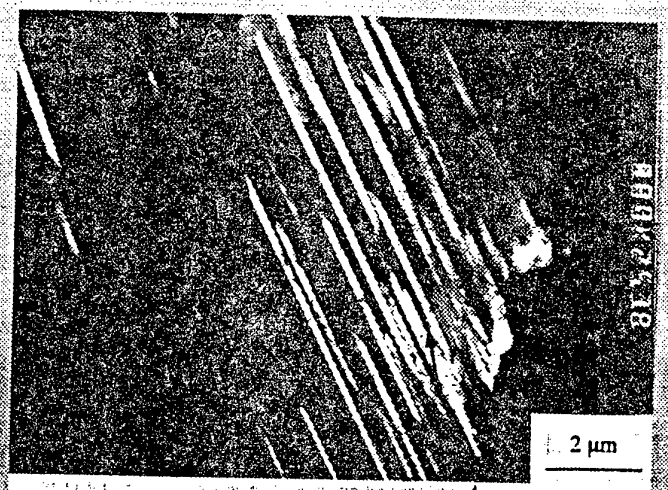

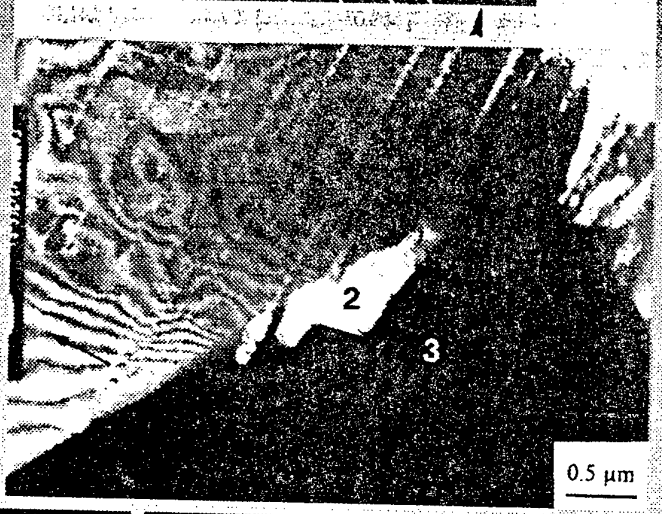

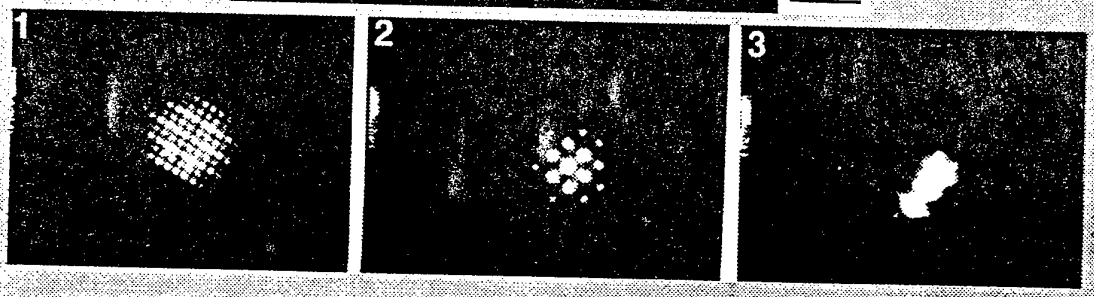

Dark field with reflection from γ_l showing relation between γ_l (area 1) and massive γ_m (area 2) and absence of relation between α (area 3) and γ_m

UNIVERSITY COLLEGE OF SWANSEA

IRC in Materials for High Performance Applications

THE UNIVERSITY OF BIRMINGHAM

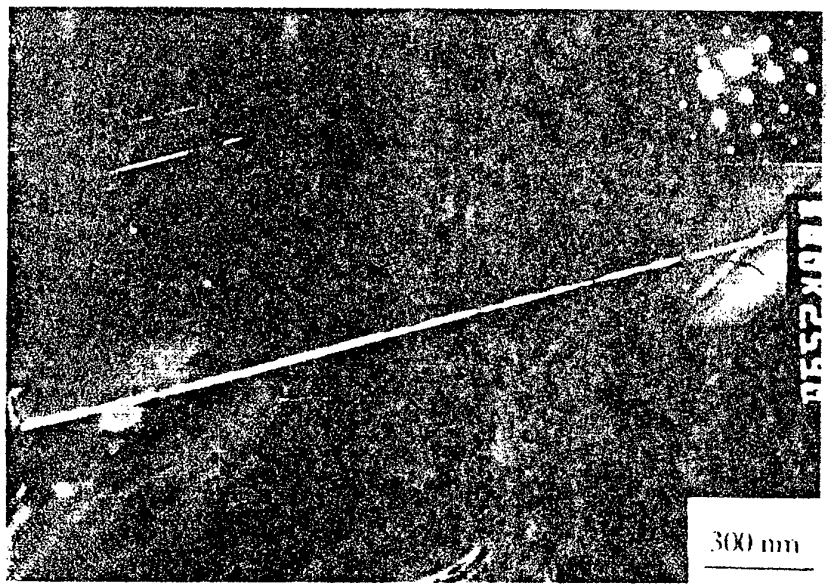

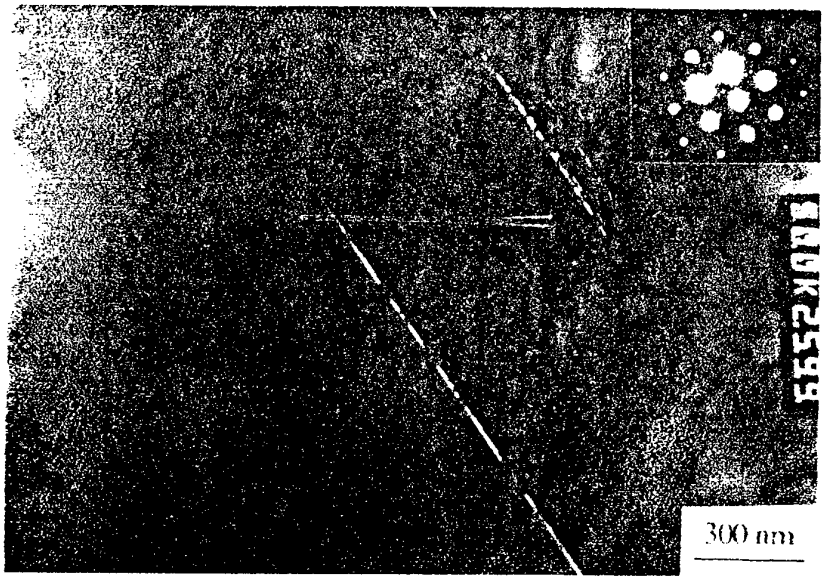

Dark field images of thin γ and thin $\alpha 2$ in γ_m

UNIVERSITY COLLEGE OF SWANSEA

IRC in Materials for High Performance Applications

THE UNIVERSITY OF BIRMINGHAM

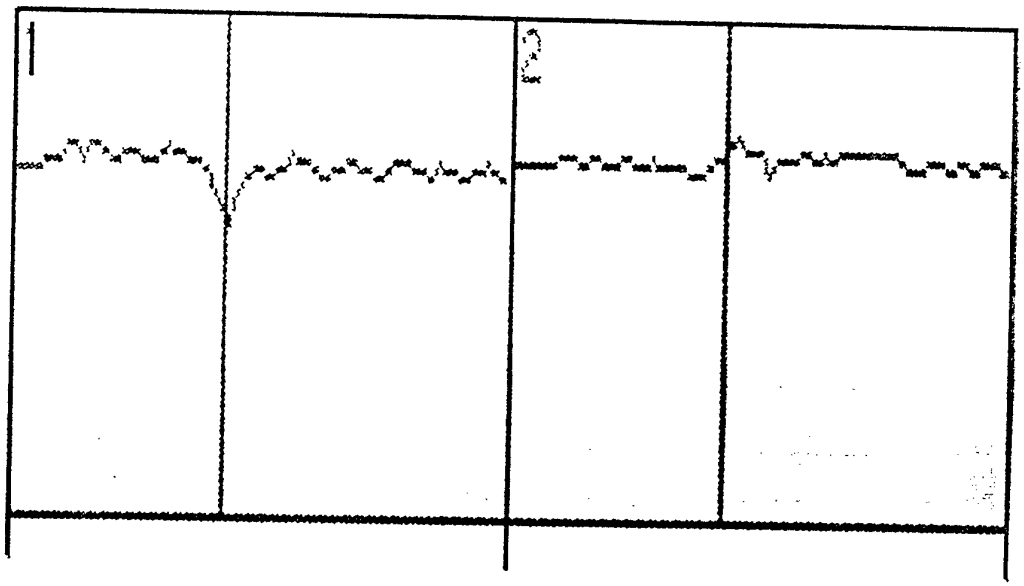

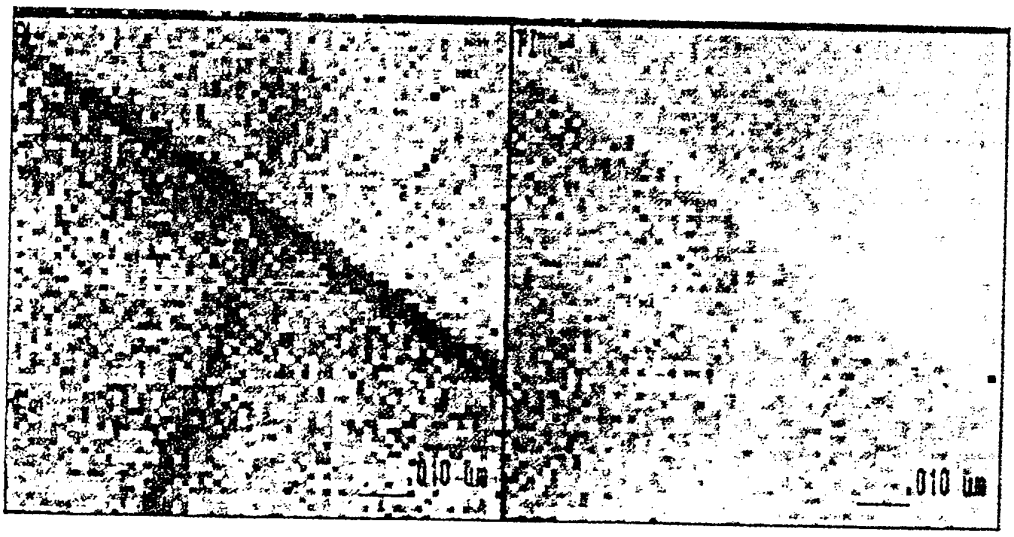

EDX trace and map showing Al depletion across thin $\alpha 2$

UNIVERSITY COLLEGE OF SWANSEA

IRC in Materials for High Performance Applications

THE UNIVERSITY OF BIRMINGHAM

Hardness traverse across sample extruded at 1380°C reduction in area 8.5 (Ti 48Al 2Cr 2Nb 1B)

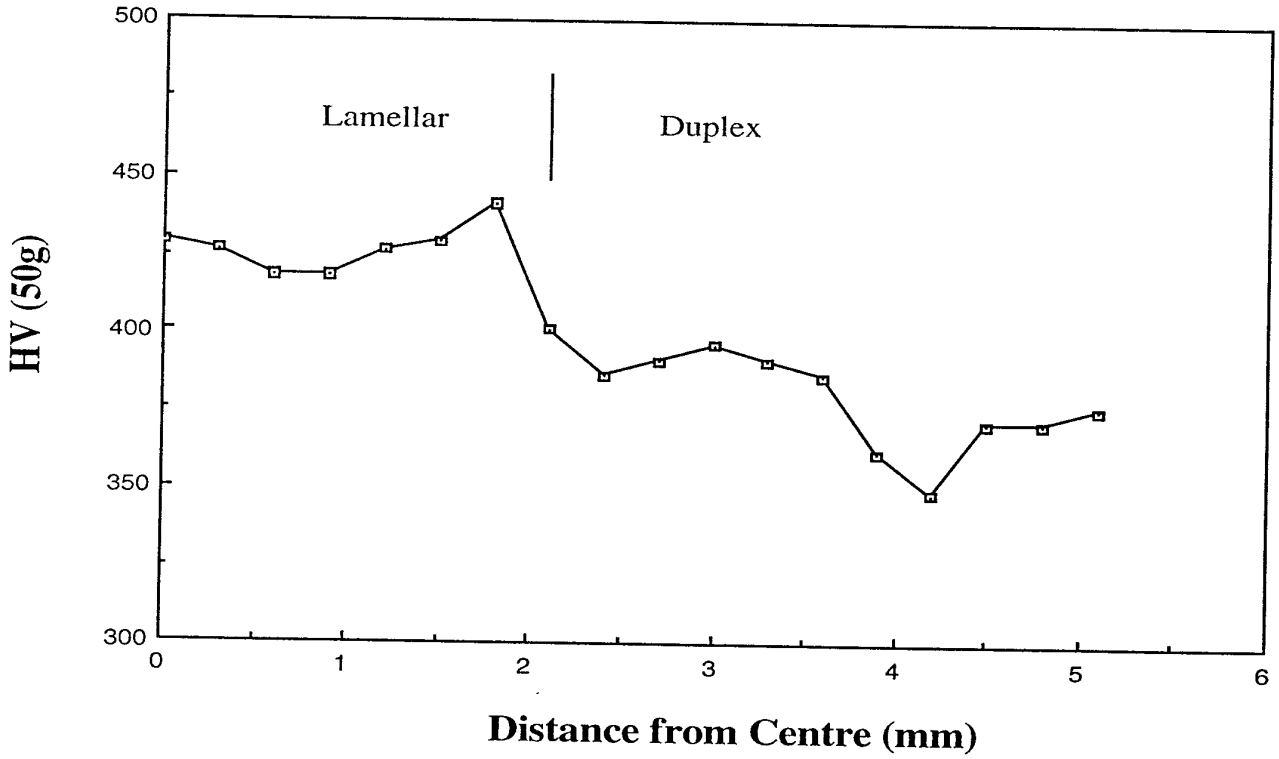

Recent Activities and Future Directions in the Study of Microstructures in Gamma Titanium Aluminides

Shigehisa Naka

ONERA

29, Av. de la Division Leclerc, 92322 Châtillon CEDEX, France

Collaborations: CEMES-CNRS of Toulouse (A. Couret, S. Zghal)

University of Orsay (R. Penelle, T. Baudin, M.L. Dupont)

ONERA

Numerous issues

1) Case of two-phase $\gamma+\alpha_2$ alloys such as the GE one
   - solidification texture
     - is it possible to reduce or suppress this texture by heat treatments or by thermomechanical processings ?
   - new types of transformation modes
     - Widmannstätten microstructure, "feather-like" microstructure
     - is it possible to take advantage of these transformation modes ?
   - quantitative analysis of the lamellar structure
     - information on the distribution of orientation variants → texture on a microscopic scale ?

2) Case of three-phase $\gamma+\alpha_2+\beta$ alloys (very good creep properties with reasonable tensile ductility)
   - reduction of solidification texture
   - more information required both on phase diagrams and on phase transformations
   - thermal stability of the β phase
     - observed β phase: residual or in equilibrium ?
     - ω phase precipitation

Solidification texture

Texture

During solidification

$L \Rightarrow \alpha$

α : HCP $\Rightarrow$ crystal growth direction // [0001]

During the formation of lamellar structure

$\alpha \Rightarrow \alpha+\gamma \Rightarrow \alpha_2+\gamma$ (or $\alpha \Rightarrow \alpha_2 \Rightarrow \alpha_2+\gamma$)

$(0001)\alpha$ or α_2 // $\{111\}\gamma$

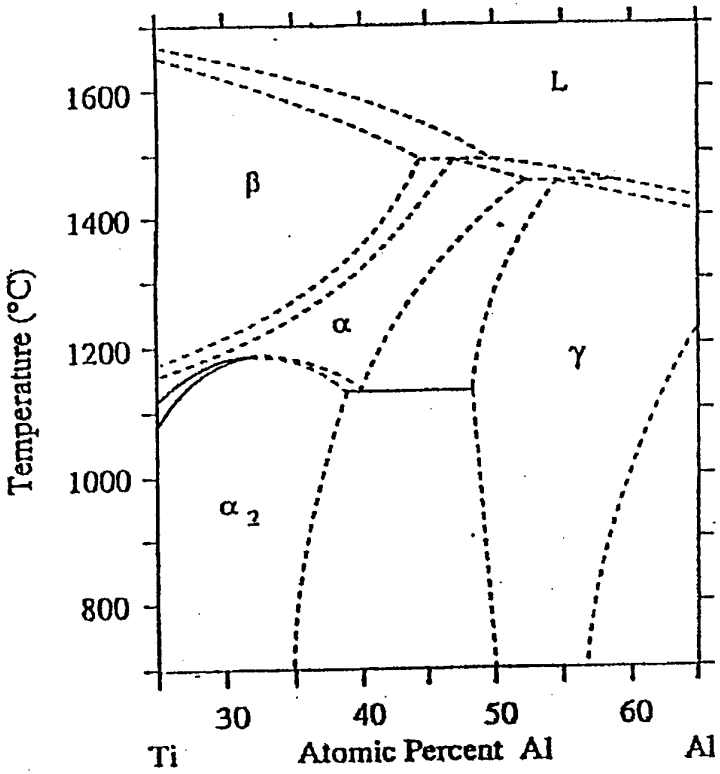

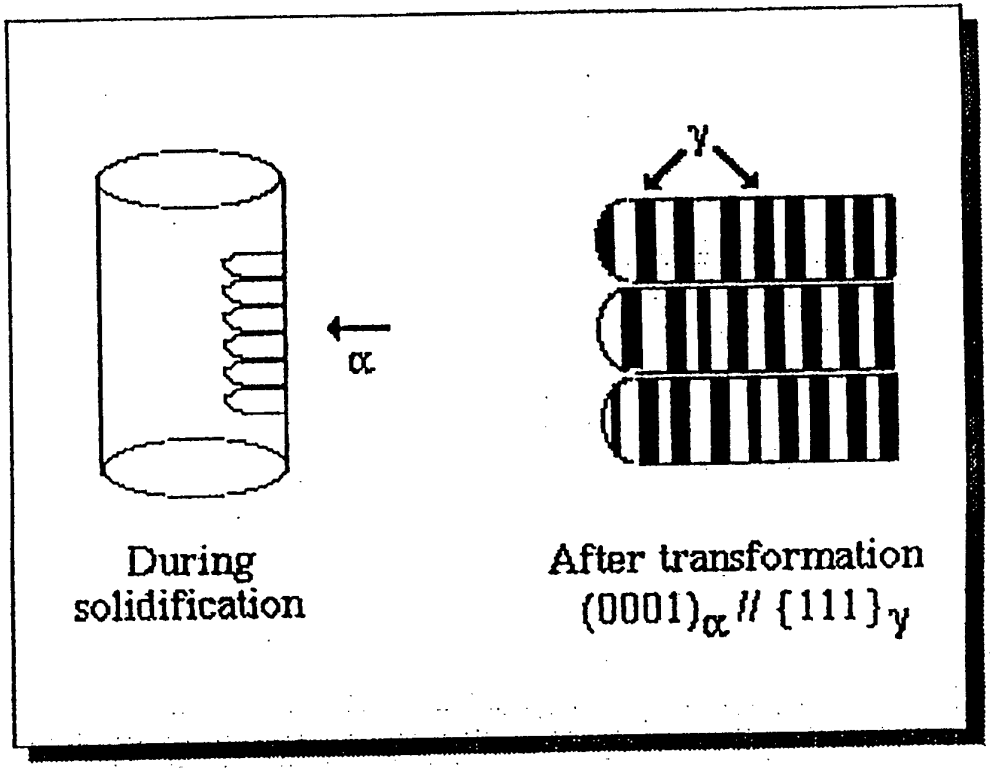

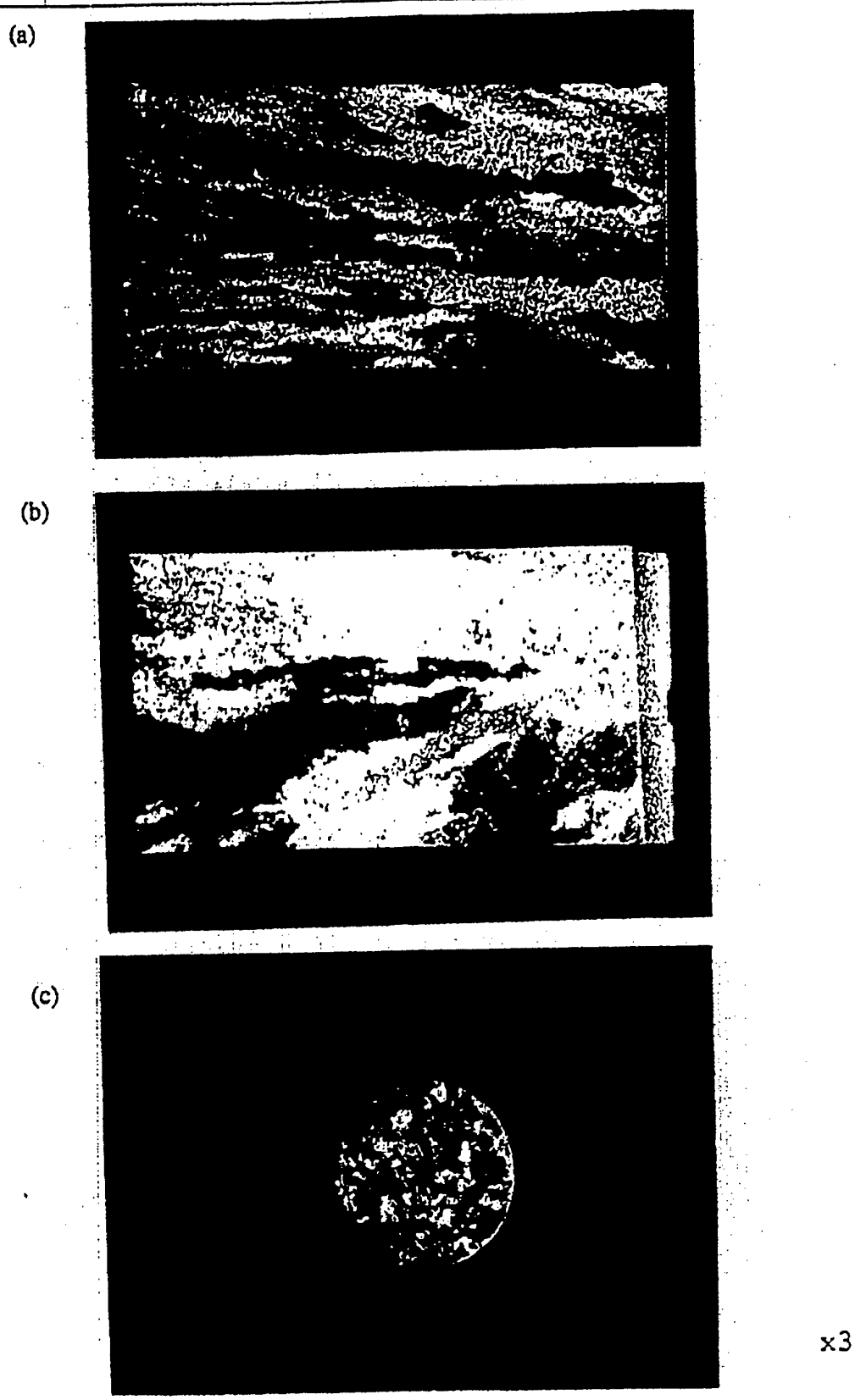
(a)
(b)
(c)
x3
transfix centre

(a)

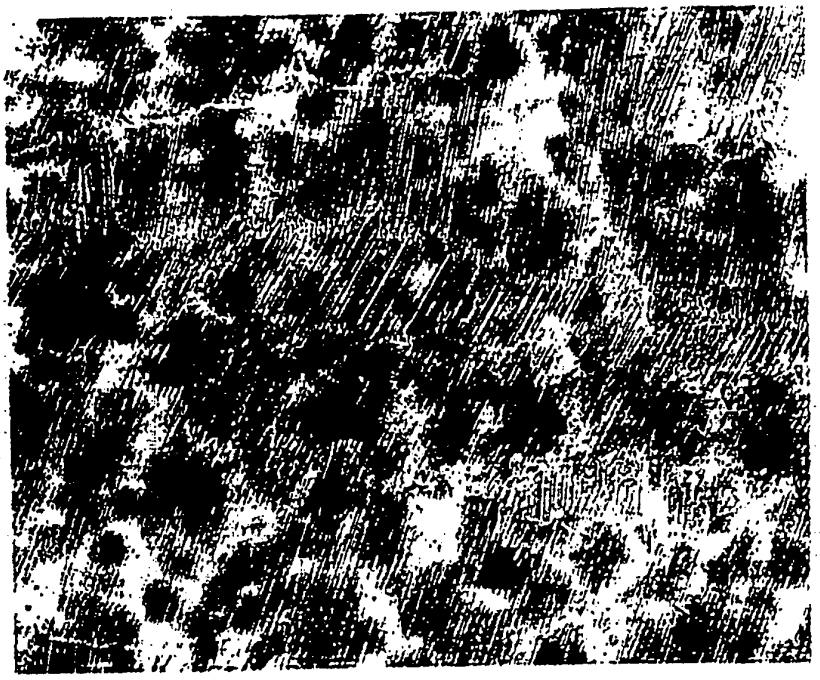

x50

(b)

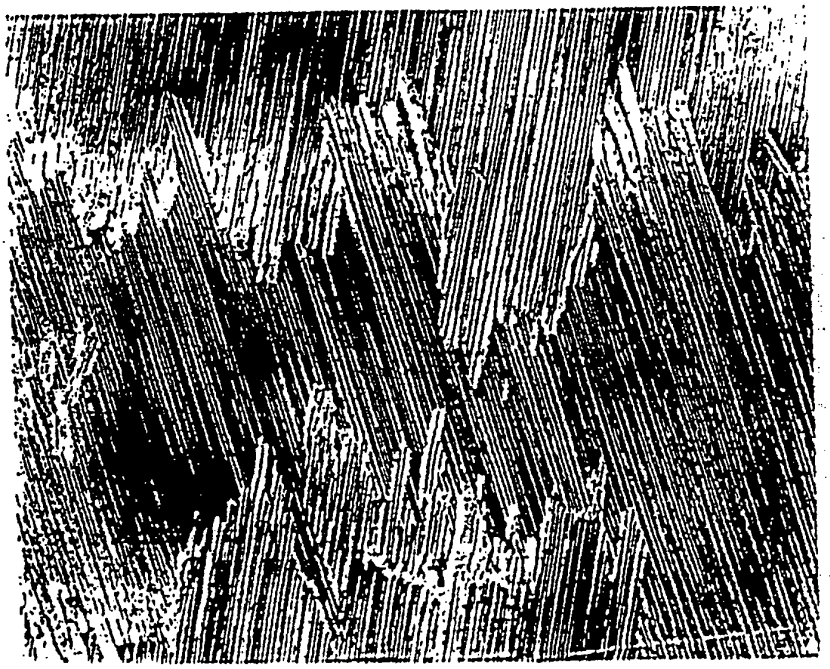

x200

Evolution of the texture during heat treatments

Collaboration with University of Orsay

• Texture analyses using neutron diffraction and SEM-EBSD show that the solidification texture cannot be reduced through heat treatments: the 111 (parallel to the axis of the rod cut from the ingot and following its radial direction) texture is even reinforced in many cases.

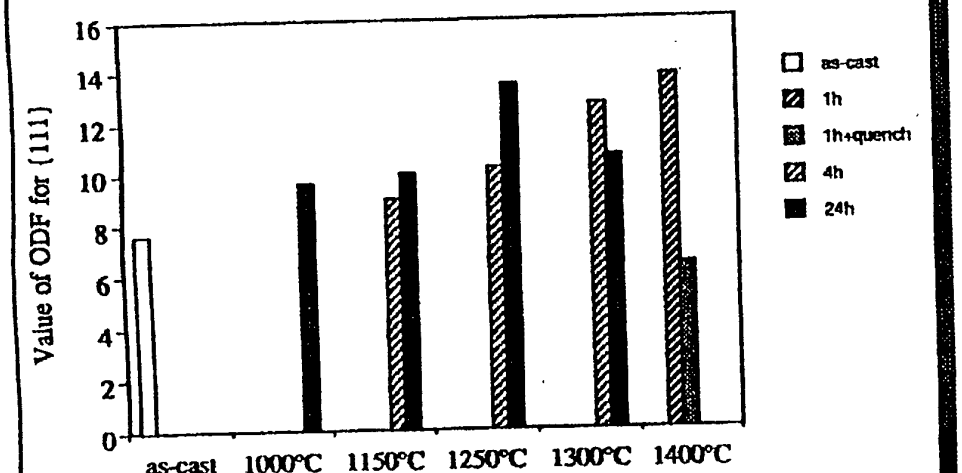

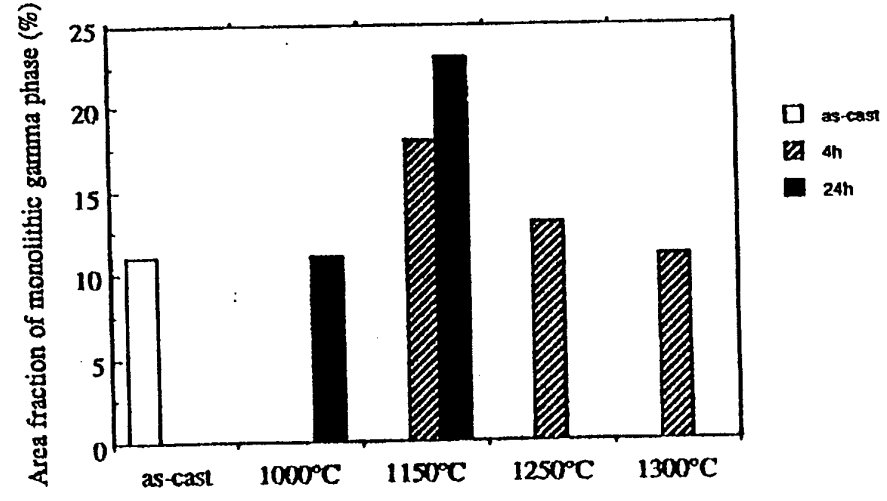

ONERA

Thermomechanical processings of strongly textured alloy ingots

- **Forging**
  - Forging is not difficult to conduct but deformation may be heterogeneous.
  - Forged products show a banded structure.
    recrystallized grains alternating with non recrystallized lamellar zones
  - Crystallographically, the texture is not suppressed but modified.
- **Extrusion**
  - Extrusion is difficult partly because of the orientation of columar grains.

- Industrial processing route: extrusion + forging
  Is the route (forging + extrusion + forging) economically viable?!!!

ONERA

High temperature deformability

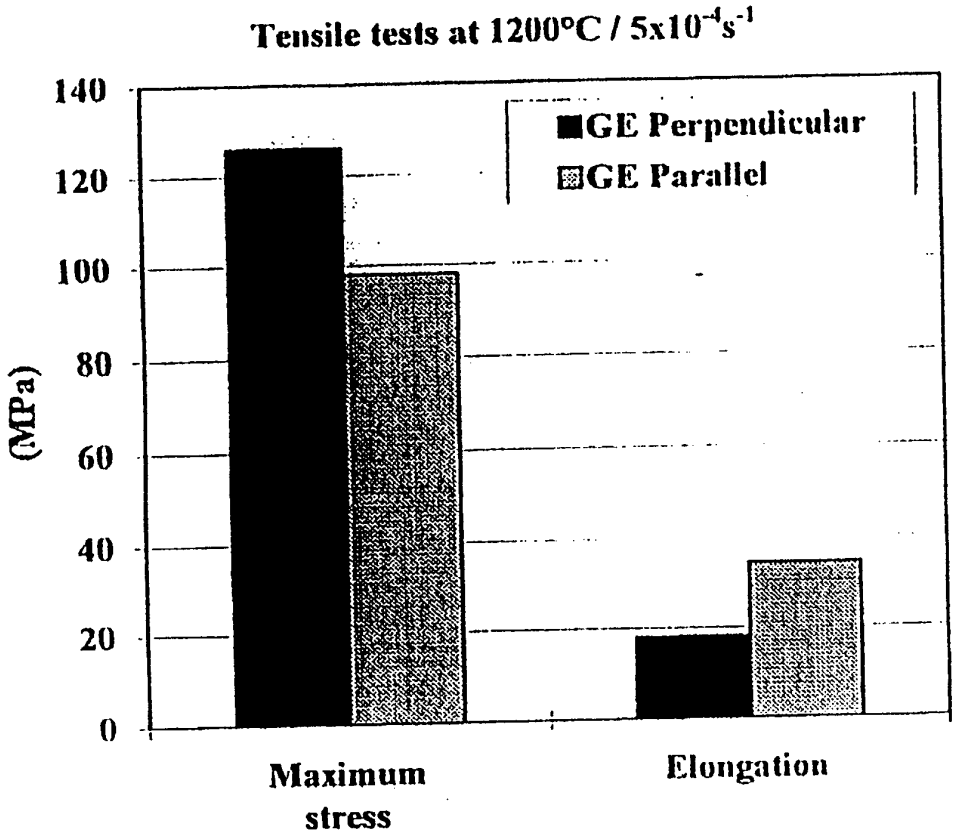

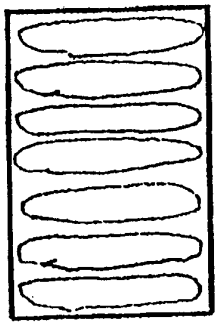

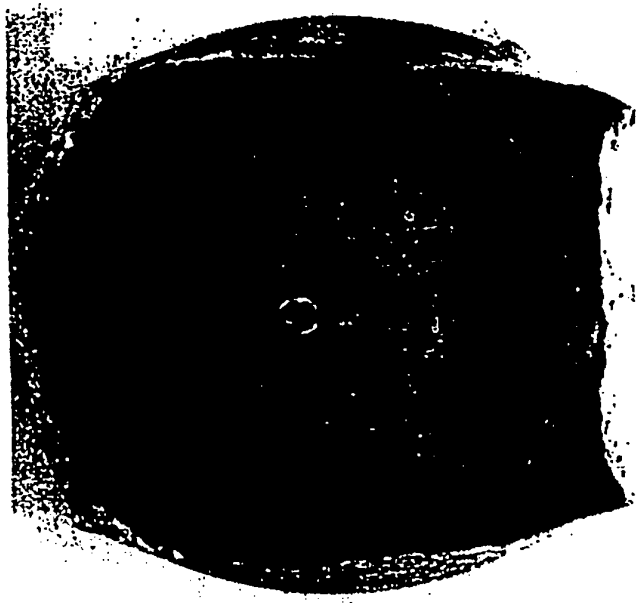

1 cm

ONERA

Shape of forged pancakes

Forging conditions : 1150°C and 5×10^{-3} s^{-1}

$Ti_{49}Al_{47}Nb_2Mn_2 + 2.4vol.\%TiB_2$

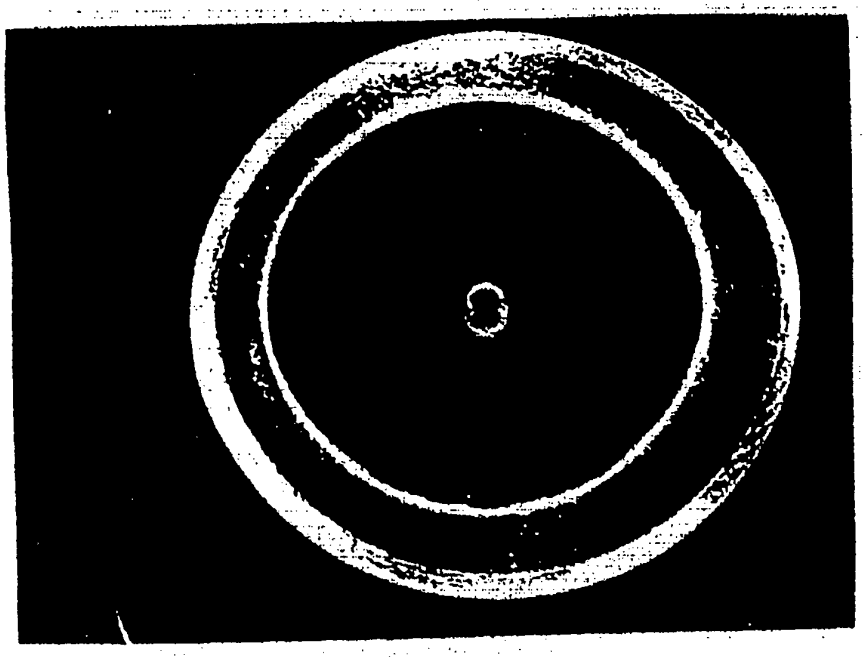

homogeneous deformation

1 cm

$Ti_{48}Al_{48}Nb_2Cr_2$

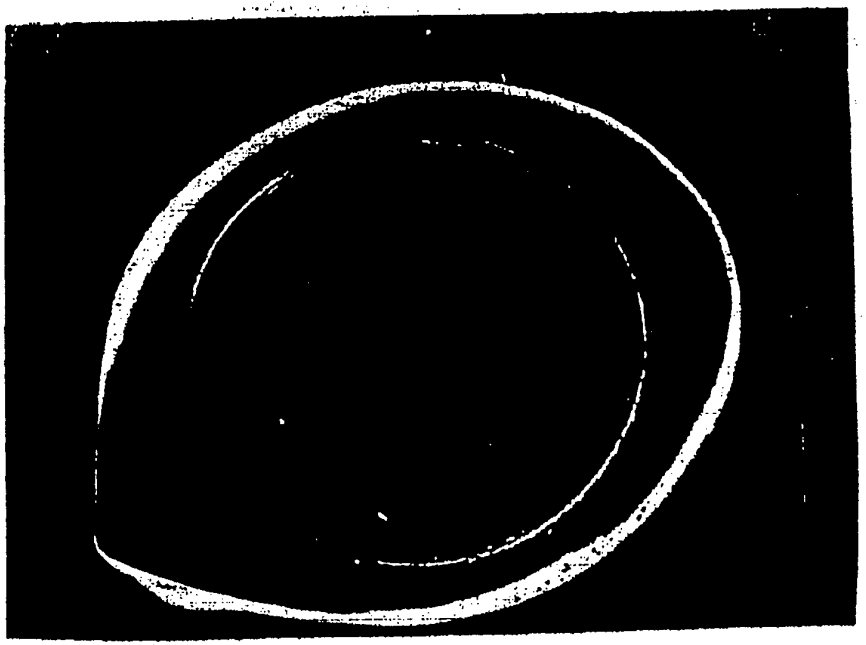

Heterogeneous deformation due to solidification texture

ONERA

As-forged microstructure

Forging at 1150°C - 80%

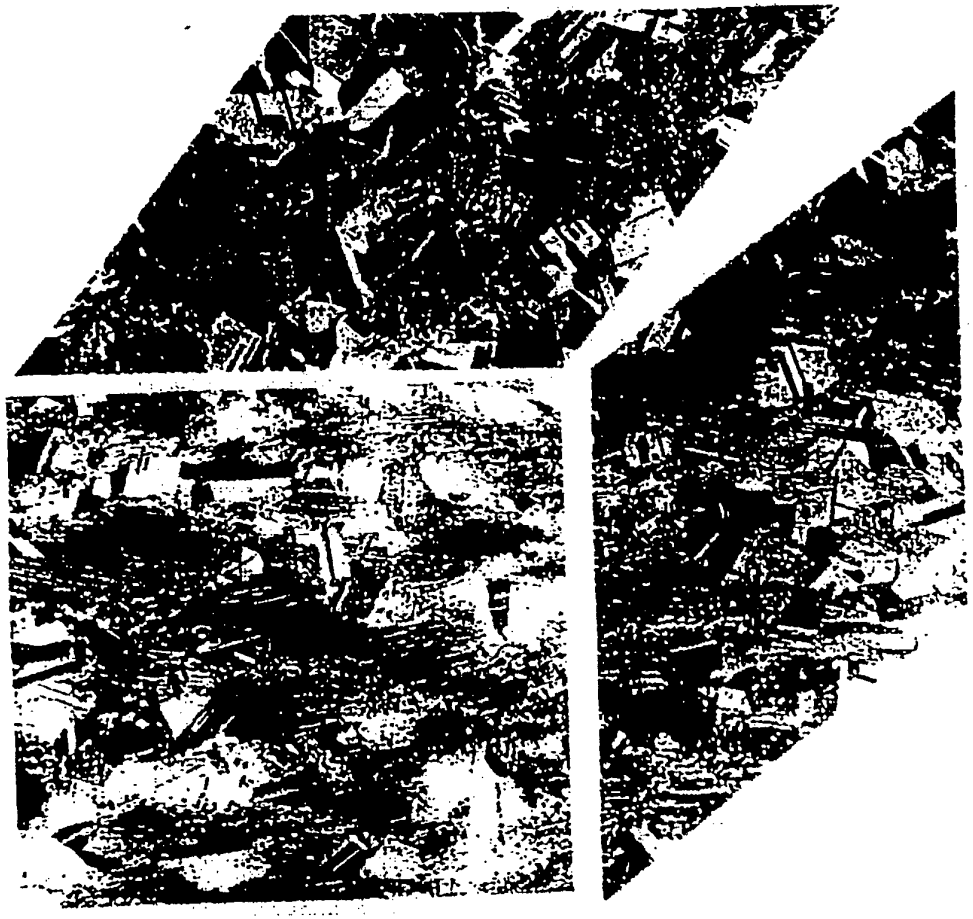

100 µm

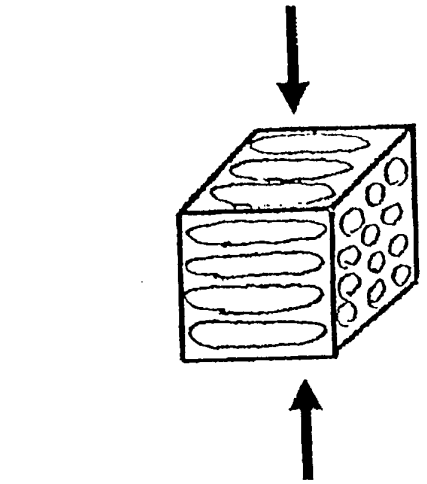

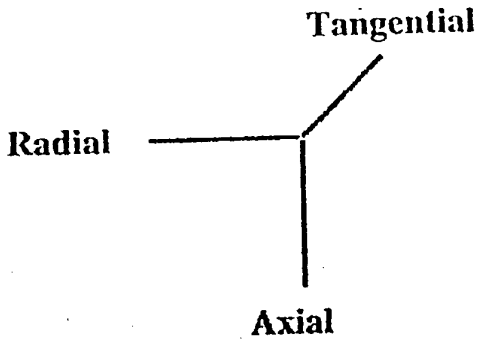

New transformation modes

ONERA

Various transformation modes

- Formation of lamellar structure
  - $\alpha \Rightarrow \alpha+\gamma \Rightarrow \alpha_2+\gamma$ or $\alpha \Rightarrow \alpha_2 \Rightarrow \alpha_2+\gamma$
  - nature of various interfaces :

    γ/α_2 and γ/γ (TB's, ODB's, PTB's, MB's)
- Massive-type transformation
  - $\alpha \Rightarrow \gamma$
  - numerous defects and interfaces including γ APB's
- Discontinuous coarsening of γ lamellae
  - solute redistribution through moving grain boundaries ?
  - mechanism less clarified

- Formation of "Widmannstätten" structure
- Formation of "feathery structure"

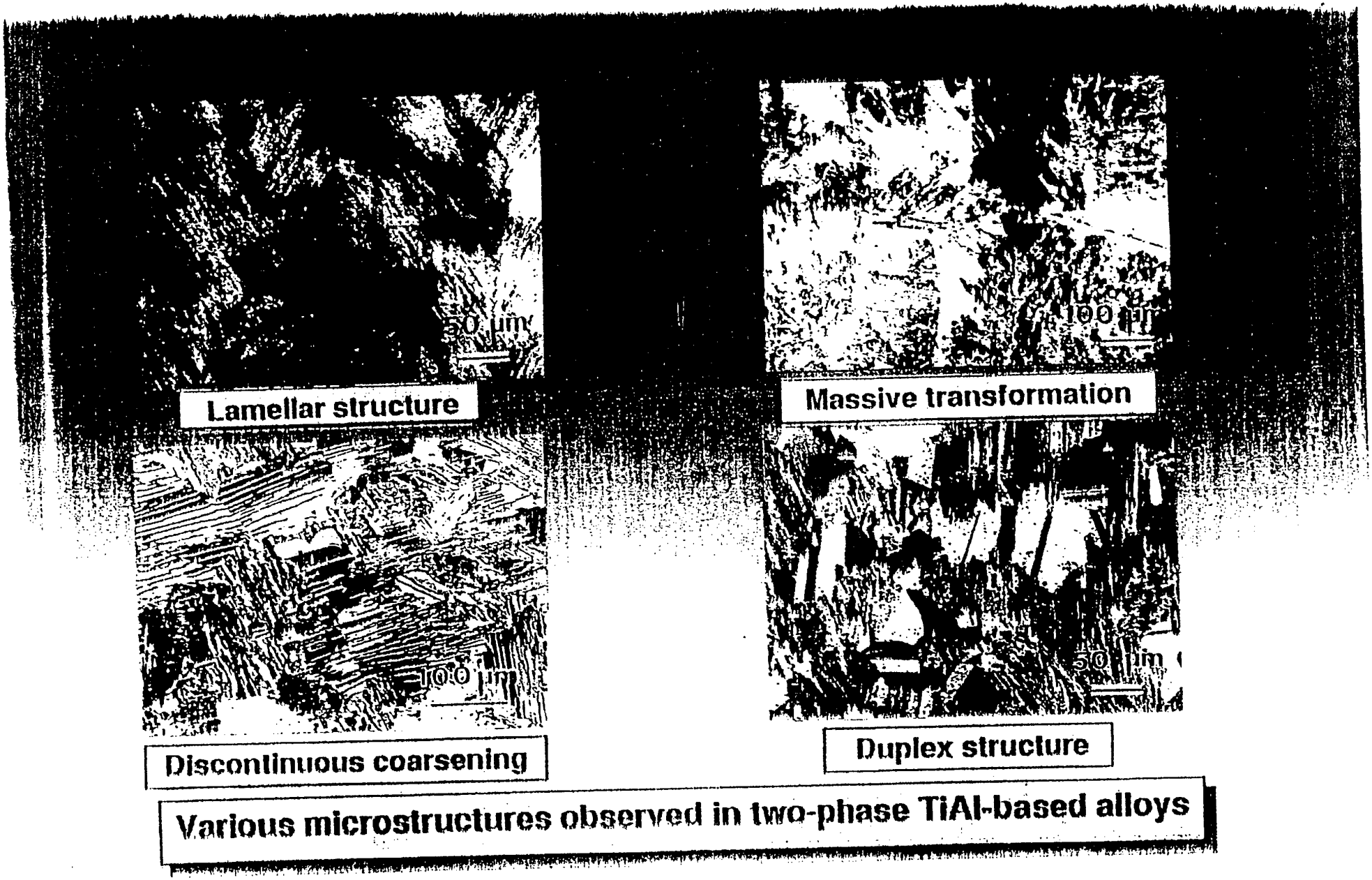

Various microstructures observed in two-phase TiAl-based alloys

ONERA

New types of transformation mode

• These new transformation modes (Widmannstätten and feather-like) can be observed when heat treatments are conducted **at temperatures around the α transus** (both in the α-phase field and in the upper part of the α+γ phase field).

• **Widmannstätten structure**
- observed after slow cooling (eg. furnace cooling) in the alloys initially showing a lamellar structure
- most frequently observed when the alloy has a near γ composition.
- presence, in a lamellar grain, of zones where the orientation of lamellae is different from that of the matrix
- formation mechanism probably related to γ→α transition upon heating

• **Feather-like structure**
- observed after higher-rate cooling (eg. air cooling), but not after highest-rate cooling (eg. oil quenching)
- deviation from the normal lamellar structure?
- formation mechanism less clarified and many further careful experiments required

• Possibility of benefiting the occurrence of these transformation modes in order to obtain the lamellar structure with a small grain size through appropriate heat treatments ?

Widmannstätten structure

Structure "Widmanstätten"

200µm

Feather-like structure

Structure "Plumeaux"

100µm

WIDMANNSTATTEN PLATES.

1,5 µm

$Ti_{48}Al_{48}Cr_2Nb_2$.

1400°C/1h/ furnace cooling.

ONERA

Formation of the Widmannstätten structure

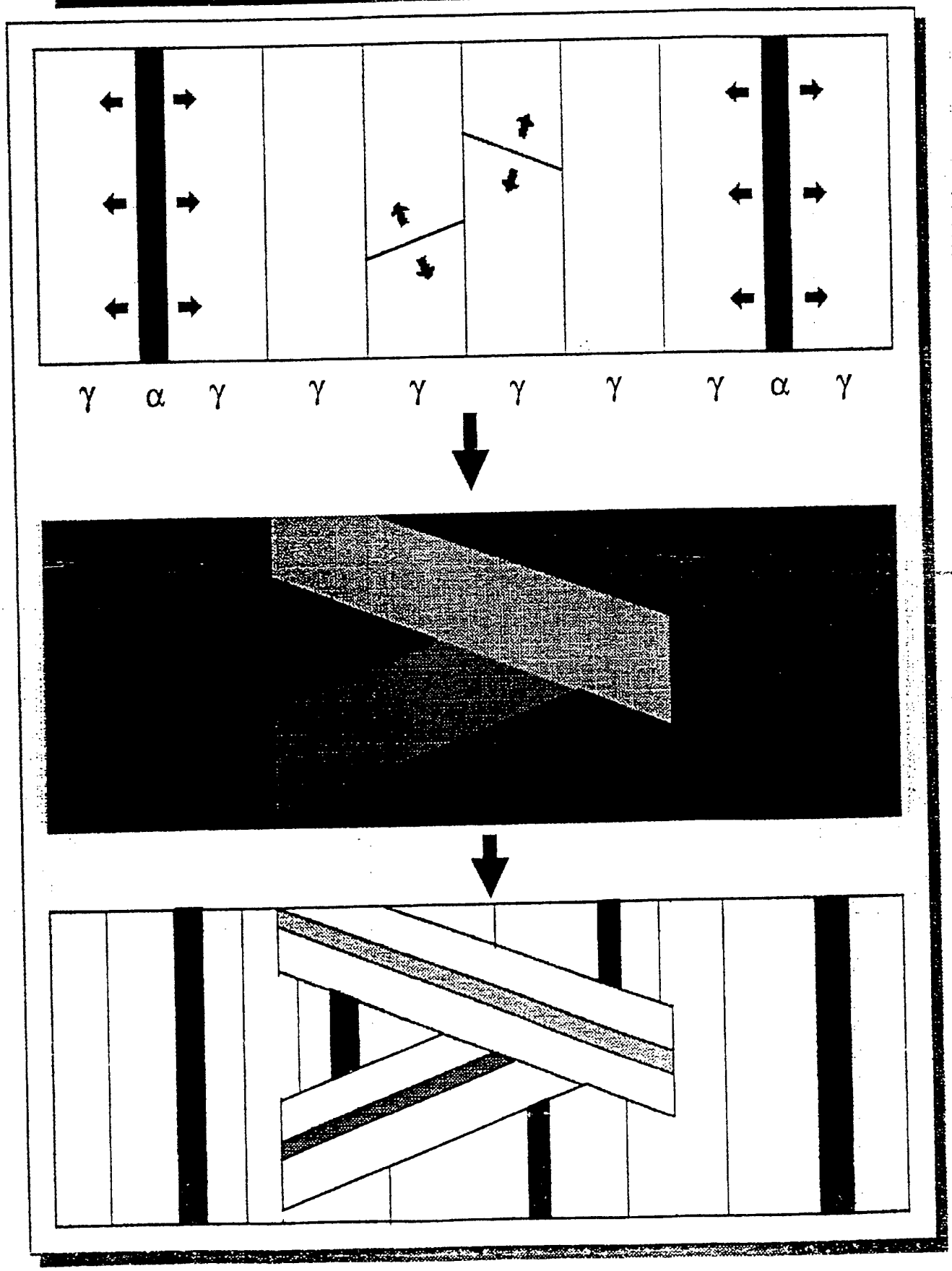

Feather-like structure

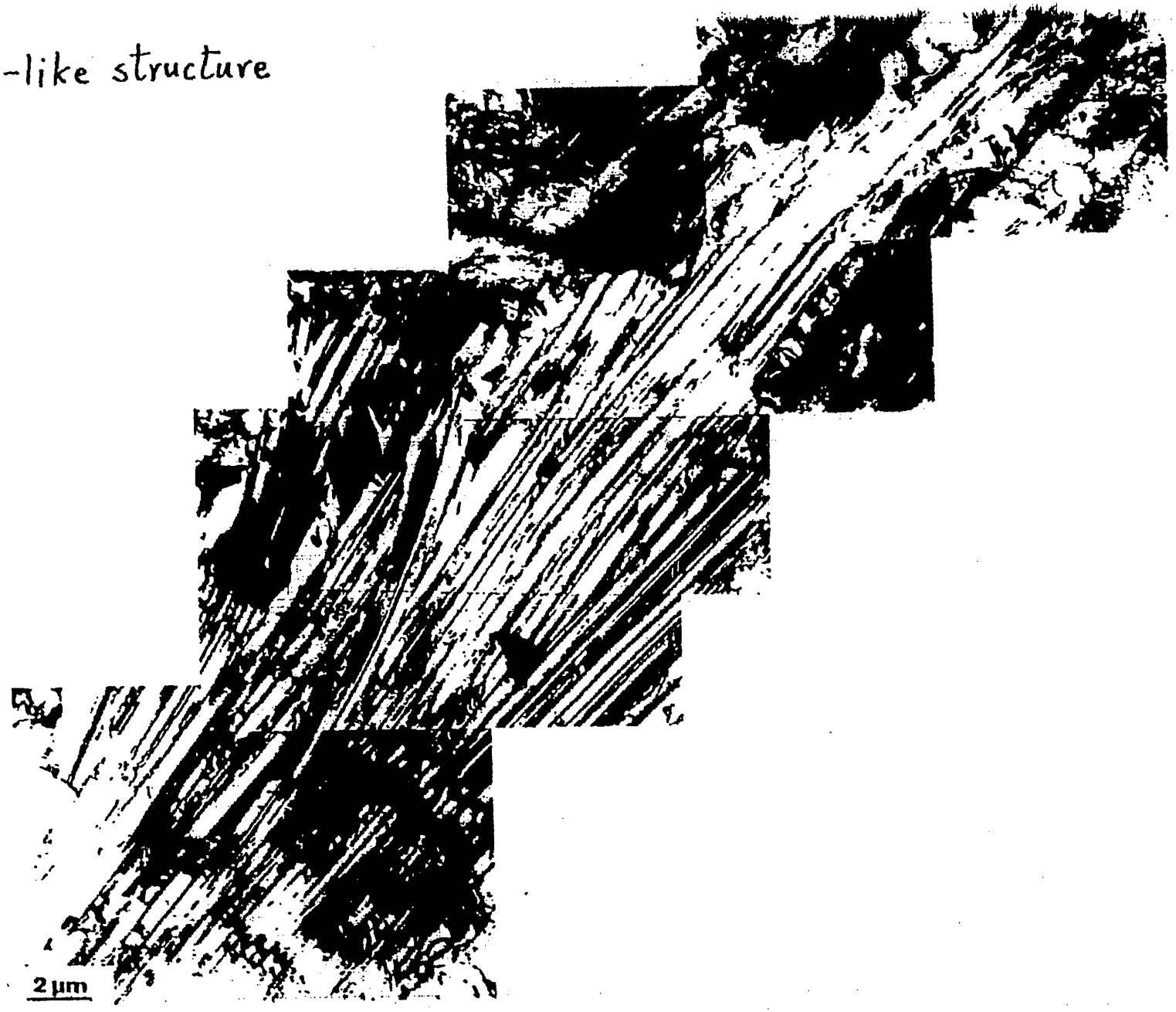

Lamellar structure

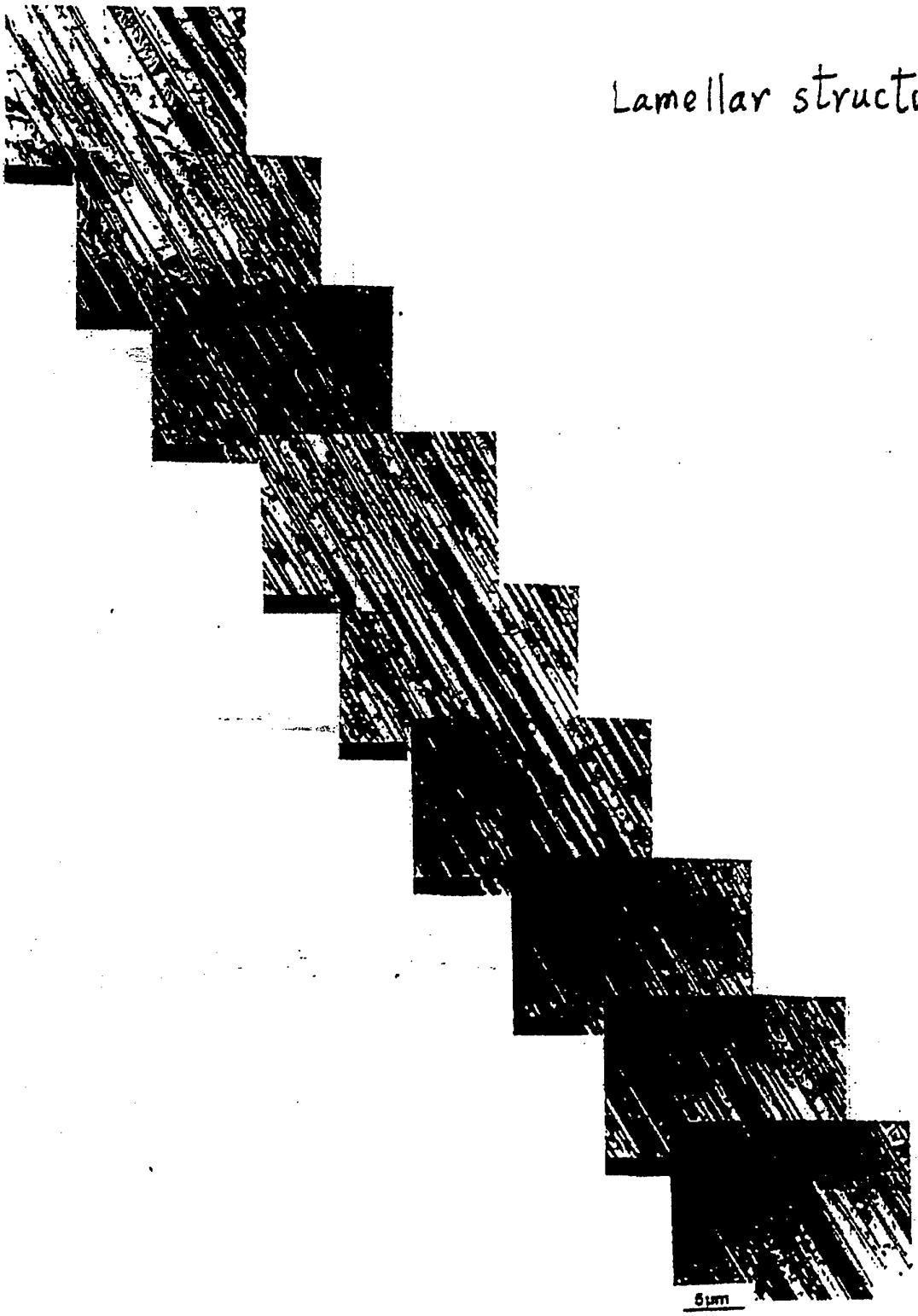

Quantitative analysis of the lamellar structure

Quantitative analysis of the lamellar structure

Collaboration with CEMES-CNRS, Toulouse

- Experiments
  - specimens: an as-cast polycrystalline $Ti_{54}Al_{46}$ alloy and
    a PST $Ti_{50.7}Al_{49.3}$ crystal (provided by Prof. Yamaguchi)
  - TEM: diffraction analyses and dark field imaging
  - in the $Ti_{54}Al_{46}$ alloy: an area of 6.4μm by 9.5μm including 116 lamellae (γ: 77 and α_2: 39)
  - in the PST alloy: several areas of about 20μm by 30μm
- Microstructural parameters examined
  - γ and α_2 lamellae, six γ orientation variants in number and in volume fraction
  - different lamellar interfaces in number and in area fraction

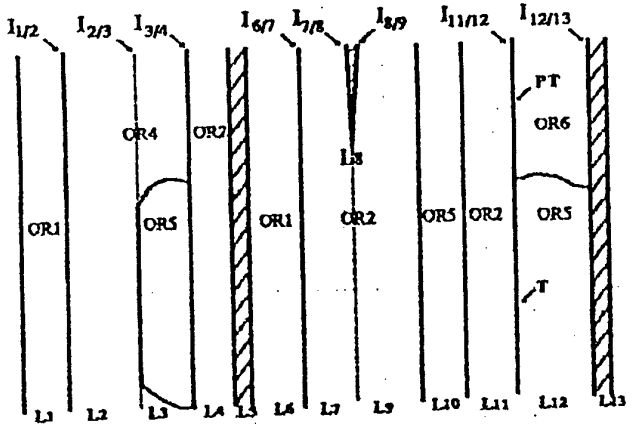

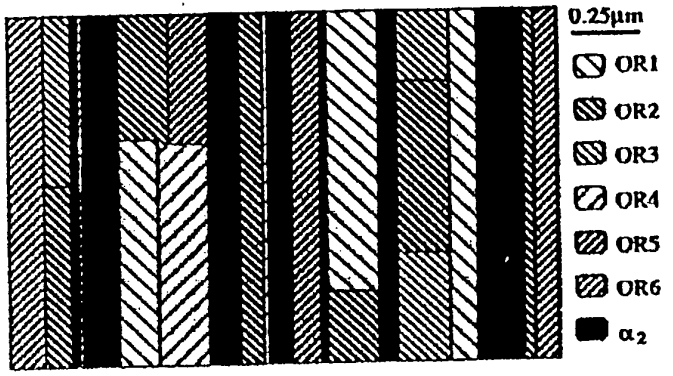

Orientations of the γ domaines in the lamellar structure

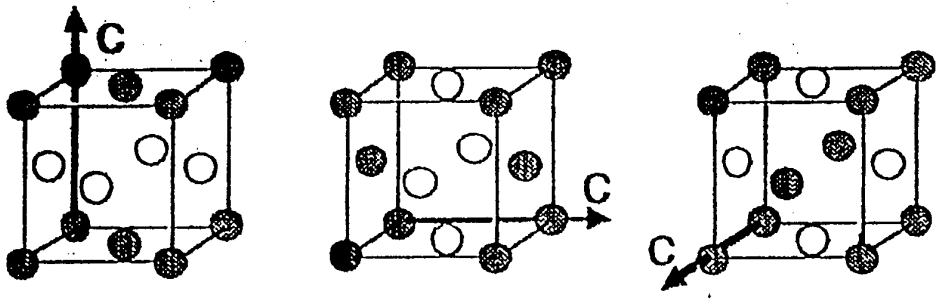

1) non-equivalence of the three <100> axes in γ ($L1_0$)

⇒ **Existence of three variants of orientation**

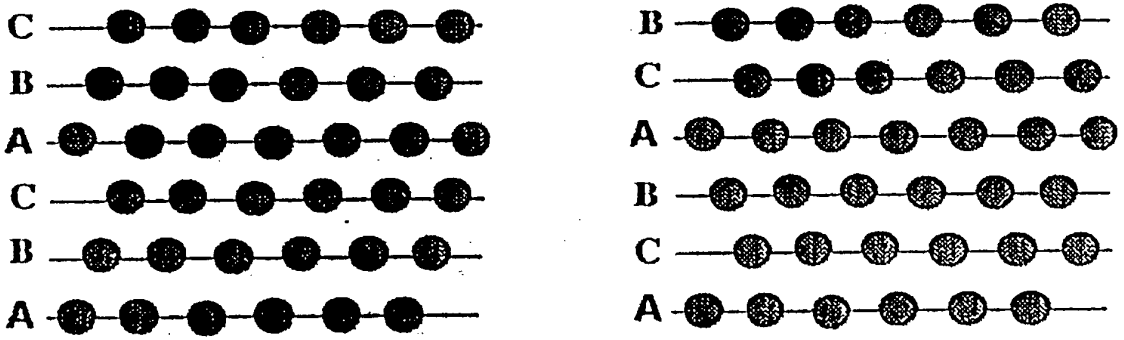

2) Possibility of two stacking sequences for {111} planes of the $L1_0$ structure, ordered on FCC lattice: ABCABC... or ACBACB ...

⇒ **Six (3 X 2) possible orientations of the γ phase**

0,2 µm

Numerous very interesting findings

- In the $Ti_{54}Al_{46}$ alloy, 71% of γ/γ interfaces are twin or psedo-twin boundaries, while 63% of α_2 lamellae are bordered with two γ lamellae of the same stacking sequence.
  - ⇒ During the lamellar structure formation, joining of γ lamellae of the same stacking sequence is more difficult than that of γ lamellae of the opposite stacking sequence due to a repulsive force between two ledge fronts.
  - ⇒ The fact that some interfaces are separating two γ lamellae order-domain related, while order-domain boundaries inside a lamella is wavy, may be explained with a hypothesis that a small number of aomic planes corresponding to the α_2 phase subsist between the two γ lamellae.
- In the two alloys, twin boundaries are more frequently observed than pseudo-twin boundaries both in number and in area fraction, while, theoretically, the latter should form two times more frequently than the former.
  - ⇒ minimization of mismatch energy

Future experiments

- GE alloy before and after heat treatments
- Possible existence of micro(or local)-texture

ONERA

Twining during creep

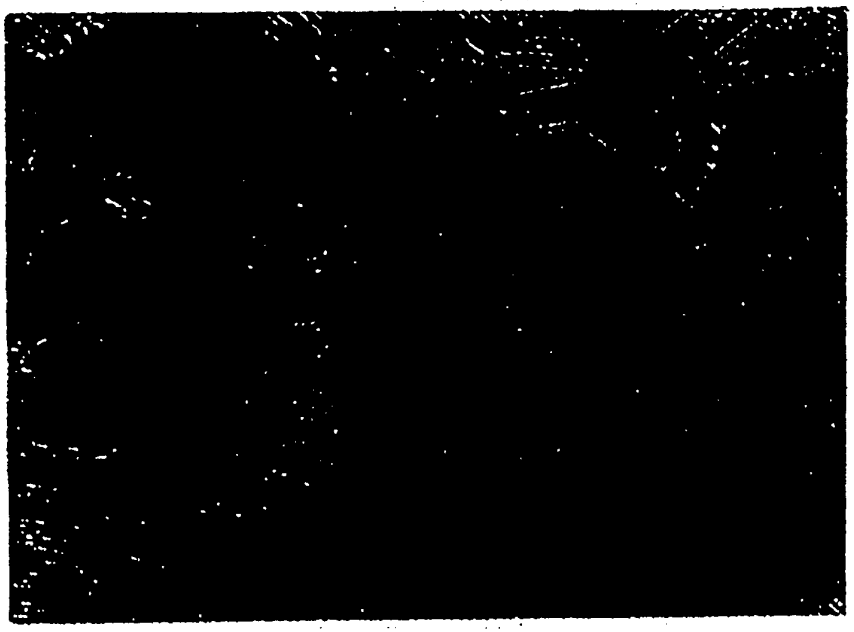

50 µm

Twining in monolithic γ grains

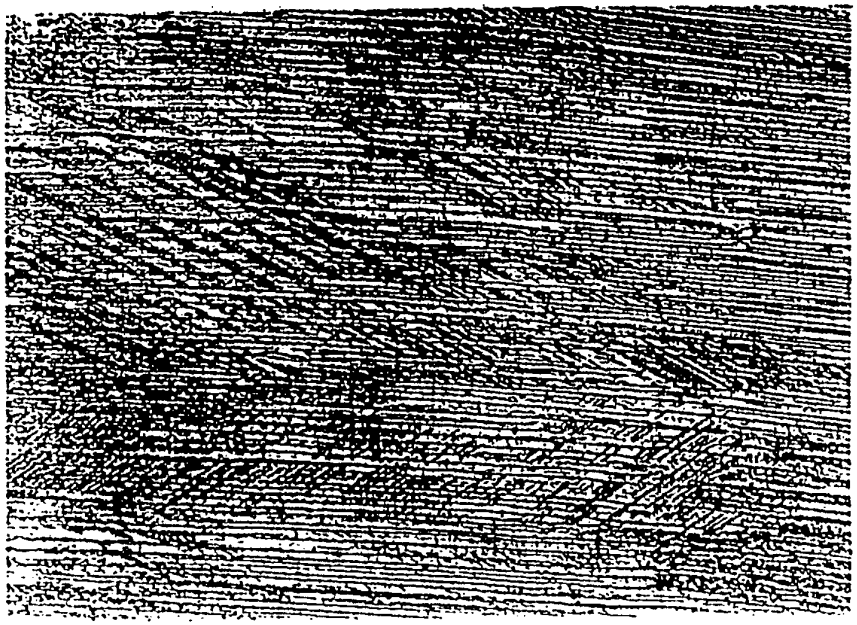

50 µm

Twining in lamellar grains

Three-phase γ+α_2+β alloys

ONERA

Alloys appropriate to casting

- Detailed examinations of the role of solidification paths
  → development of new three-phase (γ+α_2+β) alloys
- Excellent creep properties associated with an acceptable room-temperature tensile ductility

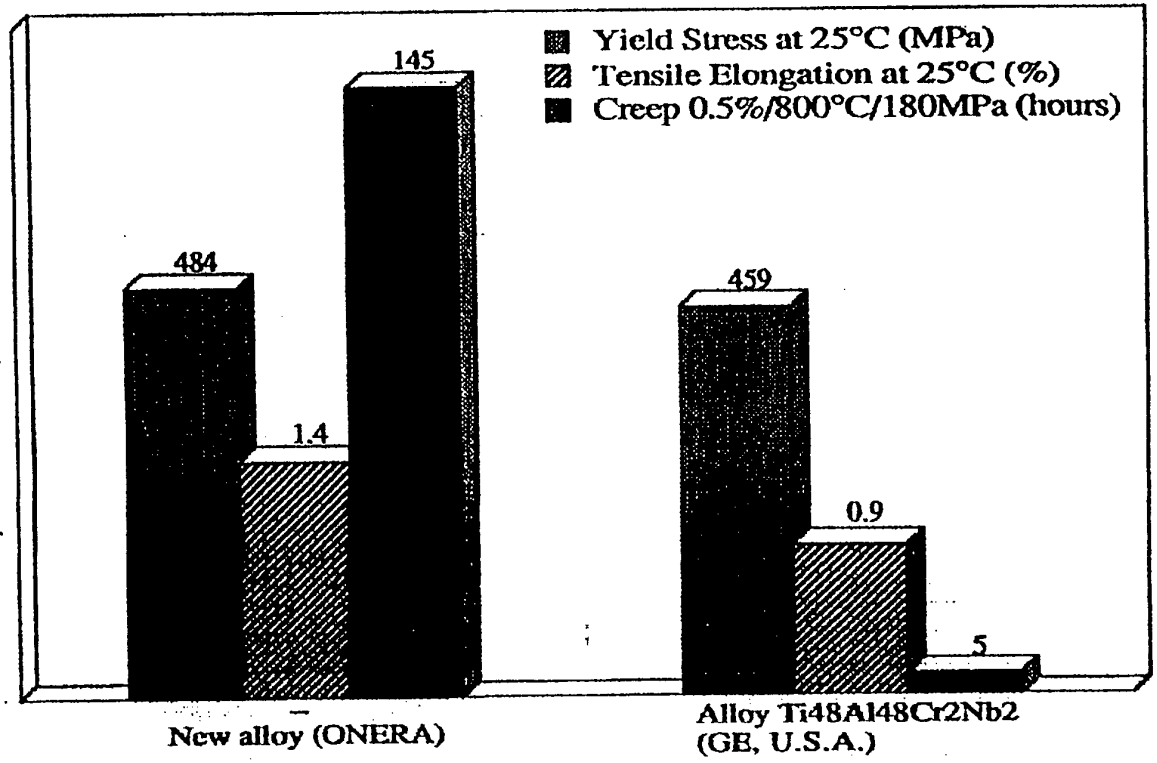

ONERA

Conclusions

- Study of microstructures is very important

not only in order to develop new alloys of higher-performance

but also in order to garantee or improve the minimum value for various mechanical properties by identifying and controlling pertinent microstructural parameters during processing.

- For doing so, it is essential to combine various experimental techniques:

  e.g. - optical microscopy,
  - SEM including EBSD
  - X-ray and neutron diffractions
  - TEM including high resolution lattice imaging
  - atom-probe experiments

Gamma Titanium Aluminide Alloy Technology: Status and Future

Young-Won Kim
UES, Inc., Dayton, OH 45432

(April, 1996)

Gamma alloys are emerging as revolutionary engineering materials for high temperature structural applications. This article discusses the historical background, status and future prospect of gamma alloy technology in the areas of fundamental understanding, alloy development/design, process development, and applications.

Introduction

Since the first measurements of mechanical properties and oxidation resistance in a binary TiAl cast alloy made in the early 1950's, numerous reports have confirmed many properties, beneficial to high temperature structural applications, including low density, high temperature strength retention, high stiffness especially at high temperatures, thermal expansion comparable to current alloys, good oxidation resistance, and hot corrosion resistance comparable to, or better than, those of current alloys. [1-15]

The first major gamma alloy development program was initiated by Air Force Materials Laboratory and conducted by Pratt and Whitney from 1975-1983. This exploratory program evaluated numerous alloy compositions through wrought processing and recommended Ti-48Al-1V-(0.1C) as the best alloy composition on the basis of ductility and creep resistance. Nevertheless, it's properties in the fine duplex microstructure condition were not adequate for the requirements of any engine components. At the end of the program, alloy castings were also evaluated; however, the properties were found to be unsatisfactory as the large-grained cast lamellar microstructures resulted in poor ductility and low strength. A few years later, the second major development program initiated again by the Air Force was performed by General Electric, Schenectady from 1986-1991. Largely based on the knowledge accumulated during the first program effort and other independent investigations, the effort identified Ti-48Al-2(Cr or Mn)-2Nb as the best second-generation alloy composition. The alloys, produced through the rapid-solidification/wrought processing, had a fine duplex microstructure and exhibited ductility/strength and oxidation resistance improved over those of the first-generation gamma alloys. Understanding the effects of alloying elements as well as composition on the properties progressed for both binary compositions and multicomponent alloy systems [6-10].

As in most metallic materials, investment casting was used as the first process route for producing experimental gamma components [6-10, 12, 14]. Since Howmet initiated a major investigation late in the 1980's, several companies worldwide have tried to develop investment casting technology for second generation gamma alloys. For the last few years, the gamma casting technology has advanced considerably through solving various problems such as cracking, hot tearing, surface connected porosity, filling and dimensional accuracy. In addition, much effort now appears to be directed toward establishing low cost, consistent manufacturing processes which incorporate alloy composition and its variations, materials properties, casting conditions and parameters, fillability, HIP'ing and final microstructures of interest. [14].

However, as-cast/HIP'ed Ti-48Al-2Cr-2Nb is unacceptably low in ductility and strength for many applications, due mainly to the coarse and nonuniform cast lamellar microstructure, which is not readily removed by HIP'ing. Empirical efforts have been made to control, through annealing treatments, the lamellar structure into finer mixtures of gamma grains and residual lamellar regions which are called "casting duplex" microstructures of about 100-200μm grain size. The casting duplex form of Ti-47Al-2Cr-2Nb exhibits a reasonable balance of properties (though relatively low levels), and has recently been demonstrated as a viable engineering material through rigorous engine tests. During this period, investigations to refine cast microstructures have been made, resulting in the development of cast XD alloys first at Howmet in 1990. Two XD alloys, Ti-(45, 47)Al-2Mn-2Nb-0.8vol%TiB2, have been tested worldwide and appear to be establishing themselves as engineering alloys. The inoculation ability of boron in cast alloys was also used in Japan (IHI) and Germany (GKSS) to develop cast alloys, Ti-47Al-1.6Fe-1.4V-2.4B and Ti-47Al-3.5(Nb, Cr, Mn)-0.8(B, Si), respectively. [2-5]

Databases for the second-generation cast alloys are being established through extensive property evaluation on a few fixed processing-microstructure conditions. Most of the properties measured at temperatures up to 760°C appear to be comparable to, or better than, when adjusted for density, those of the counterpart Ni-base superalloys which they are to be substituted for. Fatigue crack growth, impact resistance and ductility are of concern, and appropriate measures may be needed in design strategy to accommodate such deficiencies.

Casting Alloys

Various gamma components for turbine engines have been identified for rotational parts such as low pressure turbine (LPT), high pressure compressor (HPC) blades, and high pressure turbine (HPT) blade cover plates, and stationary parts, such as transition duct beams, vanes, swirlers, various cases, and nozzle flaps and tiles.

For the past few years, the databases and damage tolerance of various gamma alloys have been assessed for some of the identified components, through various qualification tests including bench tests, rig tests, and engine tests, by several companies including GE, P&W, MTU, Rolls-Royce, and IHI. Perhaps, the most significant qualification tests were the rigorous engine tests conducted in 1993 and 1994 by GE on a full set wheel of 98 LPT cast gamma blades made of Ti-47Al-2Cr-2Nb. The two successful engine tests including over 1500 simulated flight cycles were a milestone for gamma and planted a definite, though not totally certain, confidence on the material in the gamma TiAl community as well as designers. Through these and other tests, casting gamma alloys are proving to be technologically sound materials and, with some design modifications pertinent to each component, can replace nickel based superalloys in use for selected engine components. Accelerated uses of gamma alloys in replacing the current materials will be warranted when many uncertainties about the performance in the field are cleared or answered and low cost manufacturing processes are demonstrated for important types of components. [3, 14, 15].

Cast TiAl alloys are also intended for use in automotive engine parts such as turbochargers and valves. Recent engine tests show that cast TiAl turbocharger rotors exhibit better acceleration response and higher maximum rotational speed than its counterpart, Inconel rotor. There are some concerns in accepting a TiAl turbocharger, such as low ductility at room temperature and high temperature (above 800°C) oxidation resistance. Nevertheless, its application appears to be imminent, especially, in large diesel engines. Exhaust engine valves appear to be an ideal application for gamma alloys which are expected to replace the current valves made of steel and/or nickel-base (Inconel) alloys. The properties of gamma alloys in most microstructural forms well exceed most of the property requirements, as was demonstrated through series of extensive qualification engine tests conducted at GM recently. The remaining barrier appears to be development of a low-cost, high volume manufacturing method. At present, casting and perhaps reactive sintering are the two most important production methods, and intensive production and alloy modification efforts to reduce the cost is underway worldwide. [3, 14, 15].

Fundamental Advances

While casting gamma technology has been progressing for producing components, the advances in understanding of many fundamental aspects of the alloys has been impressive. The mid-section of Ti-Al binary phase diagram has been established, and some ternary diagram work has progressed. The sequence of transformations involving α decomposition have been qualitatively understood. For the alloy compositions of engineering importance [Ti-(45-48)Al base], decomposition takes place in several paths, depending on cooling rate and method, yielding lamellar structures under relatively slow cooling, "feathery"- type structures under air cooling and massive gamma when water-quenched. Investigations have concentrated on lamellar structures for formation mechanism, growth kinetics and alloy design. Extensive investigations of the deformation behavior of unidirectional lamellar material has been conducted mainly at Kyoto and Osaka Universities to establish the deformation anisotropy. which is extraordinary. Fine details and various mechanical behavior are under continuos investigation worldwide. Advanced understanding of the lamellar structure will be crucial for designing optimal lamellar base microstructures. [4-9, 12-14].

Based on knowledge of the phase relations and transformations, progress has been made for the last several years, in controlling and understanding of microstructures developed in wrought-processed alloys at Wright-Patterson as well as other institutes . Four different types of standard

microstructures were identified: near-gamma, duplex, nearly-lamellar (NL) and fully-lamellar (FL) types. The first two are fine gamma grain based (<60μm), the last two are lamellar based, and FL material in general is large-grained (>350μm). Gamma alloys show the 'so-called' ductility-toughness inverse relation at temperatures below the BDT temperatures. Fine grain microstructures yield improved tensile properties but low fracture toughness, and the reverse is true for large grain FL material. This relation is explained by correlating grain size (GS), pileup-dislocation-density, and the deformation anisotropy of the lamellar structure. However, a critical GS appears to exist, above which further increases of toughness ceases. The anisotropy also appears to be responsible for the abnormally high strength gain with decreasing grain size, as well as the improvements of strength and toughness with decreasing lamellar spacing. Creep resistance is higher for FL than duplex microstructures and appears to increase with grain size. Additions such as Si, C, N, Ta and W appear to improve the creep resistance, although each mechanism is known only qualitatively. High cycle fatigue resistance is excellent at least up to 800°C, but becomes oxidation limited in general at higher temperatures. Relatively low fracture toughness and very fast fatigue crack growth rates are of concern because the material's life will then be limited in the presence of relatively small existing or created defects/flaws. Nevertheless, both properties are improved in FL material and with increasing grain size. [3-5, 12, 14, 15].

Wrought Processing

It is estimated, considering the inverse ductility-toughness relation and the beneficial effects of lamellar structures on fracture toughness, creep, high temperature fatigue properties and fatigue crack growth resistance, that FL material having a grain size roughly in the range from 50-400 μm should show improved balance in properties. The exact magnitude should be a function of property requirements, component configurations and dimensions (thickness) and processing method.

Since such a controlled FL grain size is difficult to produce in Ti-48Al-2Cr-2Nb, and since alloys containing large amounts of boron (such as XD alloys) are not suitable as wrought alloys, extensive investigations have been conducted to design refined lamellar structures in wrought alloys. Such designed materials have been obtained in relatively thin sections: by adding small amounts (<0.3 at%) of boron (yielding TMT lamellar); through appropriate high temperature extrusion (producing TMP lamellar); or by appropriate alloy modifications which widen/lower the high temperature (α+β) phase field (resulting in refined FL). Methods to control lamellar spacing were also developed utilizing the lamellar formation mechanism and growth kinetics. Fundamentally, we are just beginning to sufficiently understand the essential aspects of designing lamellar structures. [3, 4, 14]

Almost at the same time, investigations of workability and texture development during hot working have been extensively investigated in USA, Japan and Germany. On the basis of the fundamental understanding and using concurrently developed process modeling, advances in process development have been realized for wrought processing in areas such as primary processing, secondary processing, and component forming. Ingot conversion through isothermal forging, extrusion and multistep processing has been commonly practiced with and without homogenization treatments on a small scale. Conversion of large ingots (over 250kg) is now possible through multistep processing, although more details have yet to be answered before production scale practices can be implemented. Ingot breakdown by non-isothermal forging has been shown to be feasible using a canned workpiece.

Pack-rolling technology has been advanced using both forged plates as well as prealloyed powder compacts, with sound sheet of 800x300x1.5mm currently produced. The availability of the size and microstructural homogeneity of starting plates appears to limit production of larger sheet. In general, hot-worked gamma material is highly formable, isothermally, at temperatures as low as 900°C. Prototype blades having twisted air foils have been successfully forged isothermally, and rolled sheet has been superplastically formed into various complex-shape parts. Forming by hot-die forging and high rate extrusion, however, is a hurdle for gamma to overcome if wrought gamma components are to be produced cost-effectively. Recent trials of automotive valve extrusion in current production facilities, though limited to canned/insulated material, indicate that such high rate forming of gamma may eventually be feasible if optimum processing conditions and parameters are identified on preconditioned material. [6-10, 14, 15]

Production of gamma ingots has been practiced using various melting and casting methods including induction skull melting (ISM), vacuum arc remelting (VAR), plasma arc melting (PAM) and VIM (vacuum induction melting). Ingots having 30cm diameter are routinely produced by the VAR technique. Ingots with 36 cm diameter and weighing more than 250kg have been produced using

VAR and PAM techniques, and production of larger ingots by PAM appears feasible. The main concerns in scaling-up are cracking, control of chemistry (especially, aluminum level), and compositional variations along the ingot length. In addition, methods to produce ingots having more refined and uniform cast structures are yet to be developed. [15]

Alloy Design

As the importance and necessity of the properties pertinent to specific components is recognized, increasing efforts have been made for the last couple of years to develop specific materials through microstructure control and alloy modification. In this effort focused more on wrought alloys, the thrust was to develop lamellar-based structures which are fine enough for specific component thicknesses and coarse enough to retain the most desirable properties. The important microstructures developed from the effort include TMT, RFL and TMP microstructures. The most dramatic improvements were observed in TMP materials, with strength levels reaching as high as 1000MPa at RT and more than 500MPa at 1000°C.

Nevertheless, considerably more work has to be done in various aspects such as understanding the formation mechanisms, thermal and mechanical stability, process control including heat treatment cycles, establishing data bases, property evaluation, and characterization of damage tolerance. It will also be important to raise the property levels (creep and strength) by adding small amounts of C, Si, N or O, without affecting other properties. With the above modifications, the component-specific gamma materials are expected to exhibit improved balances of properties and/or increased use temperatures by 50-100°C. These types of improvements appear to be possible in cast alloys by alloy modifications (recent results at GE) and refining coarse cast lamellar grains into fine lamellar grains by novel heat treatment cycles (results at Wright-Patterson). [3, 4, 14].

Further increases in use temperature of gamma material to above 850°C could be very profitable in the future and may be accomplished through the development of novel processes, new alloys and effective surface treatments (including protection) methods. The novel processing methods, which are under exploration, are aimed at producing material having aligned lamellar structures by directional solidification (DS) of columnar grains and/or directional extrusion (DE) of lamellar grains. These methods have yet to show their engineering feasibility to produce the intended microstructures and then the resulting microstructures/materials must be shown to demonstrate their expected higher temperature capabilities as well as the damage tolerance comparable to those of current gamma alloys. In the end, however, it appears inevitable to protect the surface of any gamma alloys if they are to be used at temperatures above 800-850°C. Several preliminary or developmental efforts in this area, however, suggest that this is most challenging and will not happen quickly [14].

Increases in both oxidation resistance and higher temperature strength levels may require drastic departures in composition from the current gamma alloys. One example can be alloys containing large amounts of Niobium. Development of such new alloys requires prolonged research efforts which nevertheless are very much worthwhile.

Summary and Future

Gamma alloys are emerging as important engineering materials. These alloys are a rare example of how the research community, developers, producers, and users can work closely to speed up and steer a materials technology in the right directions. The current alloys, basically cast alloys, developed under such remarkable collaboration meet property requirements of selected turbine, as well as automotive, engine components. With the development of appropriate design methodologies and cost effective manufacturing methods, these alloys are certain to be implemented for selected applications in the near future. In the meantime, the research community faces (new) challenges: designing engineering wrought alloys, controlling new and/or improved processing/microstructures for immediate, specific applications, and development of new materials/alloys for higher performance and temperature applications. This surely will be a long road, but should be rewarding as their past effort. There is increasing evidence that the research community is no longer naive or close-minded as too many are quick to assume. When both the research and producer/user communities work closely together, posturing to learn from each other, the gamma technology will be advanced even faster, finding more diversified application areas which will benefit all communities.

References

1. M.J. Blackburn and M.P. Smith, AFWAL Technical Report, 80-4175 and 82-4086(1980-82).
2. H.A. Lipsitt, Advanced High-Temperature Alloys (ASM, 1986), pp. 157-164.
3. Y-W. Kim, JOM, 14 (7) (1989), pp. 24-30 and 46 (7) (1994), pp. 30-40.
4. Y-W. Kim and D.M. Dimiduk, JOM, 43 (8) (1991), pp. 40-47.
5. M. Yamaguchi and H. Inui, Structural Intermetallics (Warrendale, Pa, TMS), pp. 127-142.

6-9 *High Temperature Ordered Intermetallic Alloys* II-V (1989-1995),(Pittsburgh, Pa, MRS).

10. *Microstructure/Property relationships in Titanium Aluminides and Alloys*, TMS proceedings (Warrendale, Pa, TMS, 1990).
11. *High Temperature Aluminides $ Intermetallics* (Warrendale, Pa, TMS, 1990).
12. *Structural Intermetallics* (Warrendale, Pa, TMS, 1993).
13. *Intermetallic Compounds*, Proc. 3rd Japan International SAMPE Symp. (Chiba, Japan, 1993).
14. Proc. on International Symp. on *Gamma Titanium Aluminides*, ed. Y-W. Kim, R. Wagner and M.Yamaguchi (Warrendale, Pa, TMS) 1995
15. Communications: C. Austin (GEAE), M.J. Blackburn (P&W), P. Bowen (IRC), K. Chan [SwRI], H. Clemens (Plansee), D. Davidson (P&W), D. Dimiduk (Wright Lab.), D. Furrer (Ladish), S. Hartfield-Wünsch (GM), H. Huang (GE), W. Konkel (W-G), D. Larsen, Jr. (Howmet), J. Larsen (Wright Lab.), C. T. Liu (ORNL), P. Bowen (IRC), S. Naka (ONERA), Y. G. Nakagawa (IHI), S. Ram (PCC), S. Reed (Duriron), S. Schwenker (Wright Lab.), L. Semiatin (Wright Lab.), D. Shih (MD), W. Smarsley (MTU), R. Wagner (GKSS), and M. Yamaguchi (Kyoto U.).

Overview of joining gamma alloys

P Threadgill

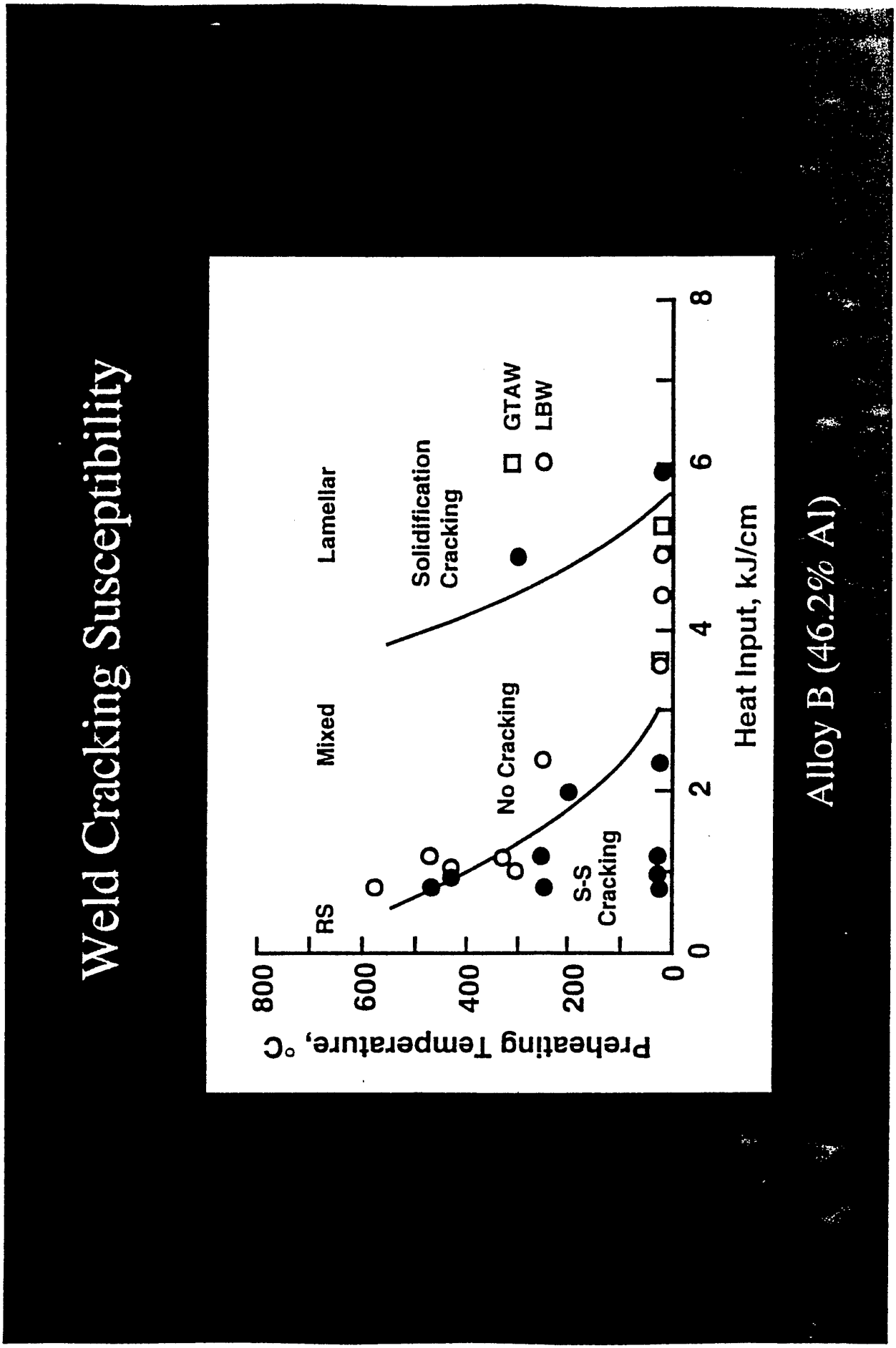

J Lee, W A Baeslack and T J Kelly: Weld fusion zone phenomena in Ti (45-48)Al-Nb-Cr γ titanium aluminides, submitted to Welding Journal.

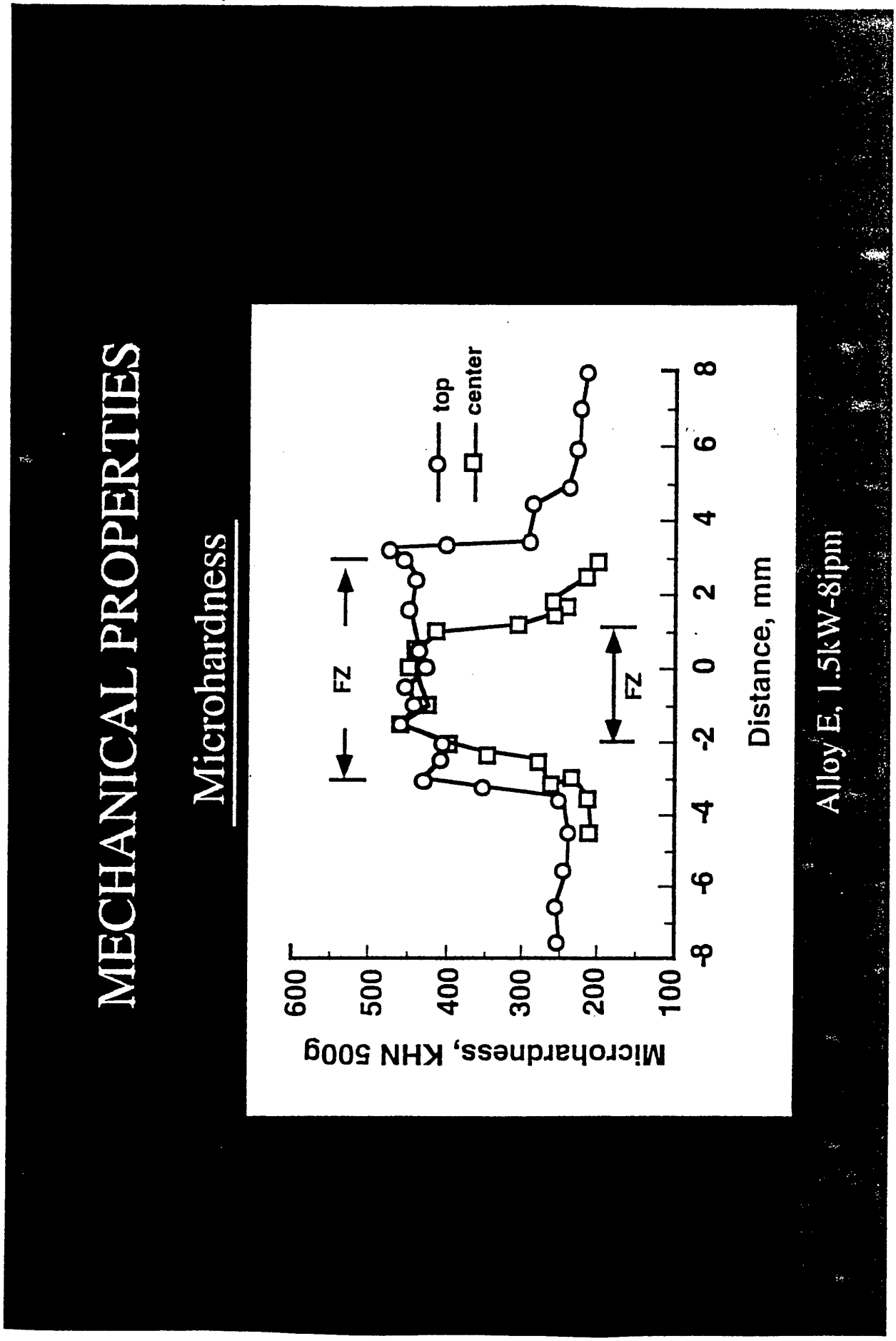

J Lee, W A Baeslack and T J Kelly: Weld fusion zone phenomena in Ti (45-48)Al-Nb-Cr γ titanium aluminides, submitted to Welding Journal.

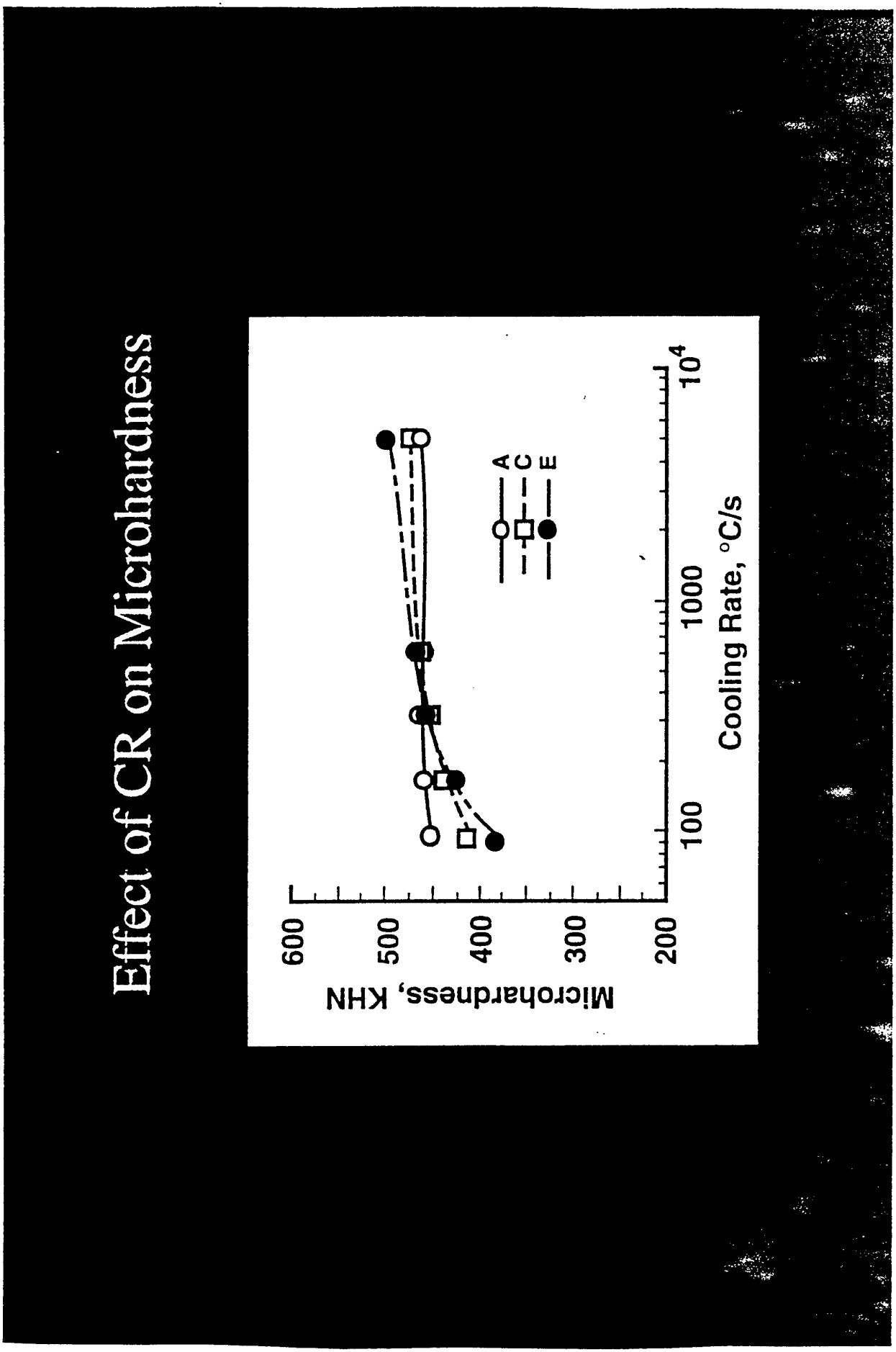

J Lee, W A Baeslack and T J Kelly: Weld fusion zone phenomena in Ti (45-48)Al-Nb-Cr-Y titanium aluminides, submitted to Welding Journal.

Effect of Heat Input, Al content and PWHT

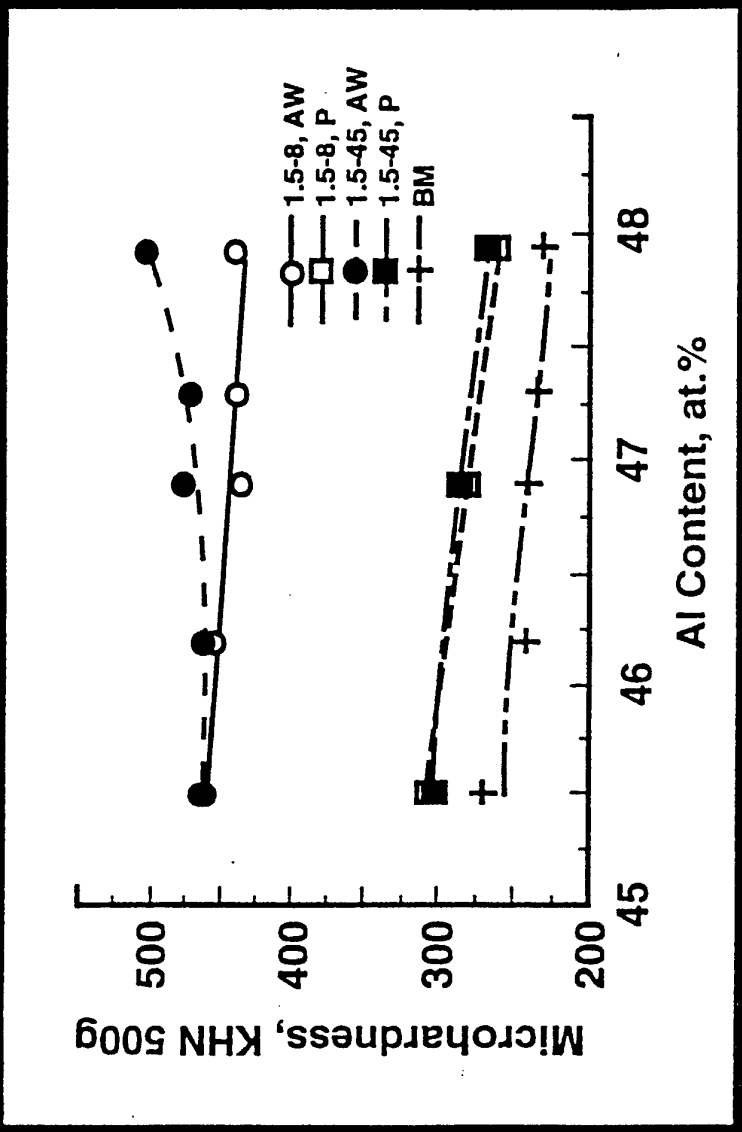

J Lee, W A Baeslack and T J Kelly: Weld fusion zone phenomena in Ti (45-48)Al-Nb-Cr γ titanium aluminides, submitted to Welding Journal.

CONCLUSIONS

- Gamma titanium aluminides were found to be susceptible to solidification cracking. Solidification cracking occurred along centerline and cracking susceptibility was determined by fusion zone morphology.
- Solidification cracking susceptibility increased as heat input and Al content increased.
- Solid-state cracking susceptibility decreased as cooling rate decreased and Al content increased. Process windows for crack-free sound LB welds were established in this study.

J Lee, W A Baeslack and T J Kelly: Weld fusion zone phenomena in Ti (45-48)Al-Nb-(1-3)V titanium aluminides, submitted to Welding Journal.

CONCLUSIONS

- Microhardness of the as-welded fusion zone was much higher than the base material but weld cooling rate did not influence microhardness of fusion zone significantly.
- PWHT reduced microhardness of the fusion zone to the level of the base material.
- Based on fractography, it was apparent that PWHT increased the fusion zone ductility.

J Lee, W A Baeslack and T J Kelly: Weld fusion zone phenomena in Ti (45-48)Al-Nb-Cr γ titanium aluminides, submitted to Welding Journal.

MICROSTRUCTURE EVOLUTION IN THE FUSION ZONE

- FZ with fast cooling rates:
  Low Al Alloy; Incipient Lamellar + α_2 Grains +(B_2 phase)
  High Al Alloy; Incipient Lamellar + γ Grains +(B_2 phase)
- FZ with slow cooling rates:
  Low Al Alloy; Fully Lamellar + Fine GB γ +(B_2 phase)
  High Al Alloy; Lamellar + Blocky γ Grains +(B_2 phase)
- Lamellar spacing increase with H.I.
- Dendrite and columnar grain size increase with H.I.

J Lee, W A Baeslack and T J Kelly: Weld fusion zone phenomena in Ti (45-48)Al-Nb-Cr γ titanium aluminides, submitted to Welding Journal.

SOLIDIFICATION OF GAMMA TITANIUM ALUMINIDES

- Fusion zone: cored dendritic structure
- Primary solidification mode change from single phase BCC β solidification to duplex solidification(α+β) with increasing Al content and/or CR
- Solute redistribution during solidification:
  - -Al segregation to interdendritic regions
  - -Cr enrichment and Al depletion on dendrite cores

J Lee, W A Baeslack and T J Kelly: Weld fusion zone phenomena in Ti (45-48)Al-Nb-Cr γ titanium aluminides, submitted to Welding Journal.

WELD CRACKING SUSCEPTIBILITY OF GAMMA TITANIUM ALUMINIDES

- Susceptible to both solidification cracking and solid-state cracking.
- Solidification crack: parallel to the welding direction
  propagate along centerline
  Solid-state crack: perpendicular to the welding direction
  propagate along alpha-two phase preferentially
- As Al content and H.I. increased, solidification cracking susceptibility increased while solid-state cracking susceptibility decreased.
- Process windows for sound LB welds were established.

J Lee, W A Baeslack and T J Kelly: Weld fusion zone phenomena in Ti (+5-48)Al-Nb-Cr γ titanium aluminides, submitted to Welding Journal.

EXPERIMENTAL PROCEDURE

Materials

HT	Ti	Al	Nb	Cr	Si	Fe	O
A	50.6	45.5	1.9	1.8	.028	.028	.221
B	49.8	46.2	2.0	1.7	.04	.04	.13
C	49.4	46.9	1.9	1.5	.03	.03	.14
D	48.6	47.3	1.9	1.9	.03	.03	.14
E	48.4	47.9	1.9	1.5	.03	.03	.15

J Lee, W A Baeslack and T J Kelly: Weld fusion zone phenomena in Ti (45-48)Al-Nb-Cr γ titanium aluminides, submitted to Welding Journal.

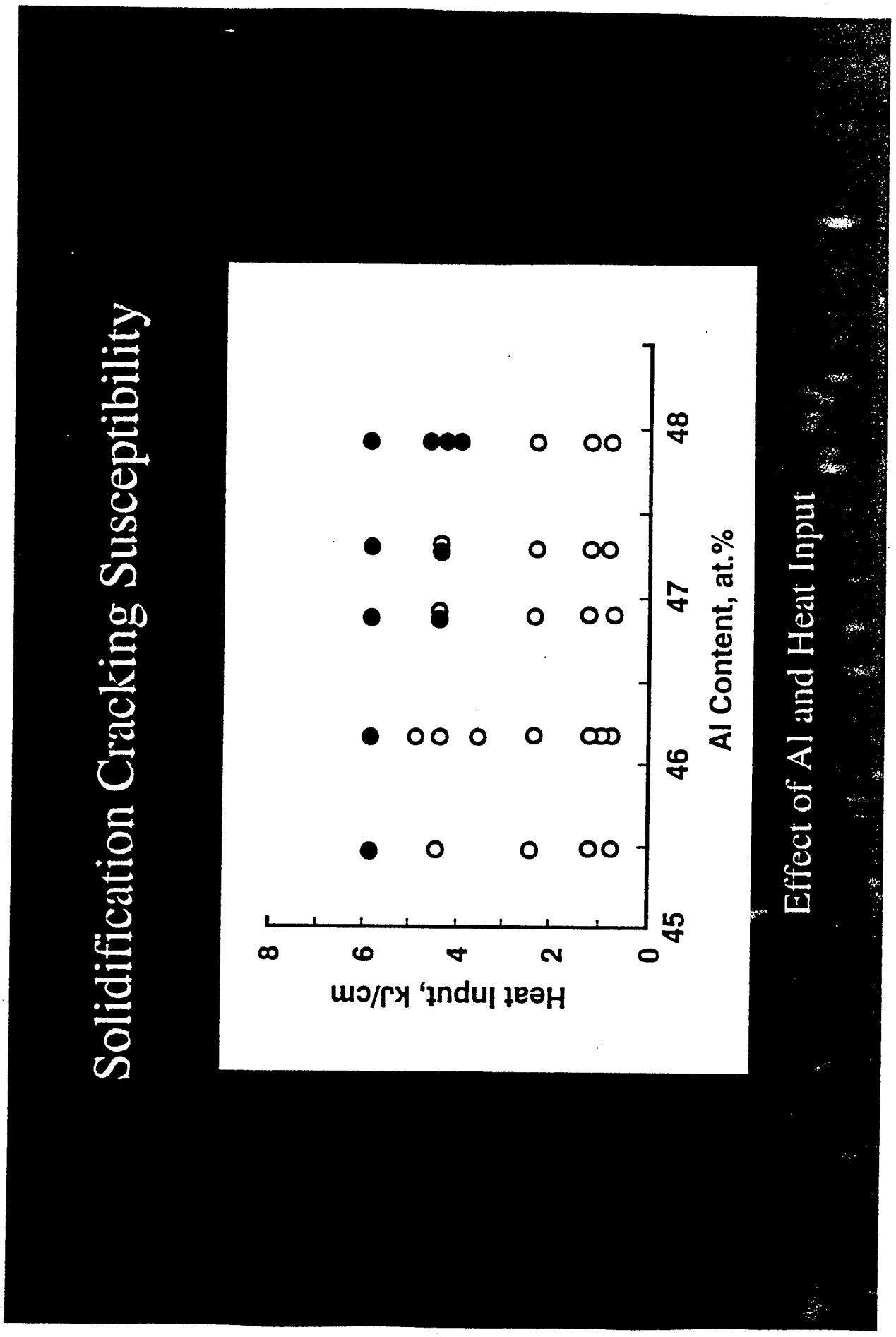

J Lee, W A Baeslack and T J Kelly: Weld fusion zone phenomena in Ti (45-48)Al-Nb-Cr γ titanium aluminides, submitted to Welding Journal.

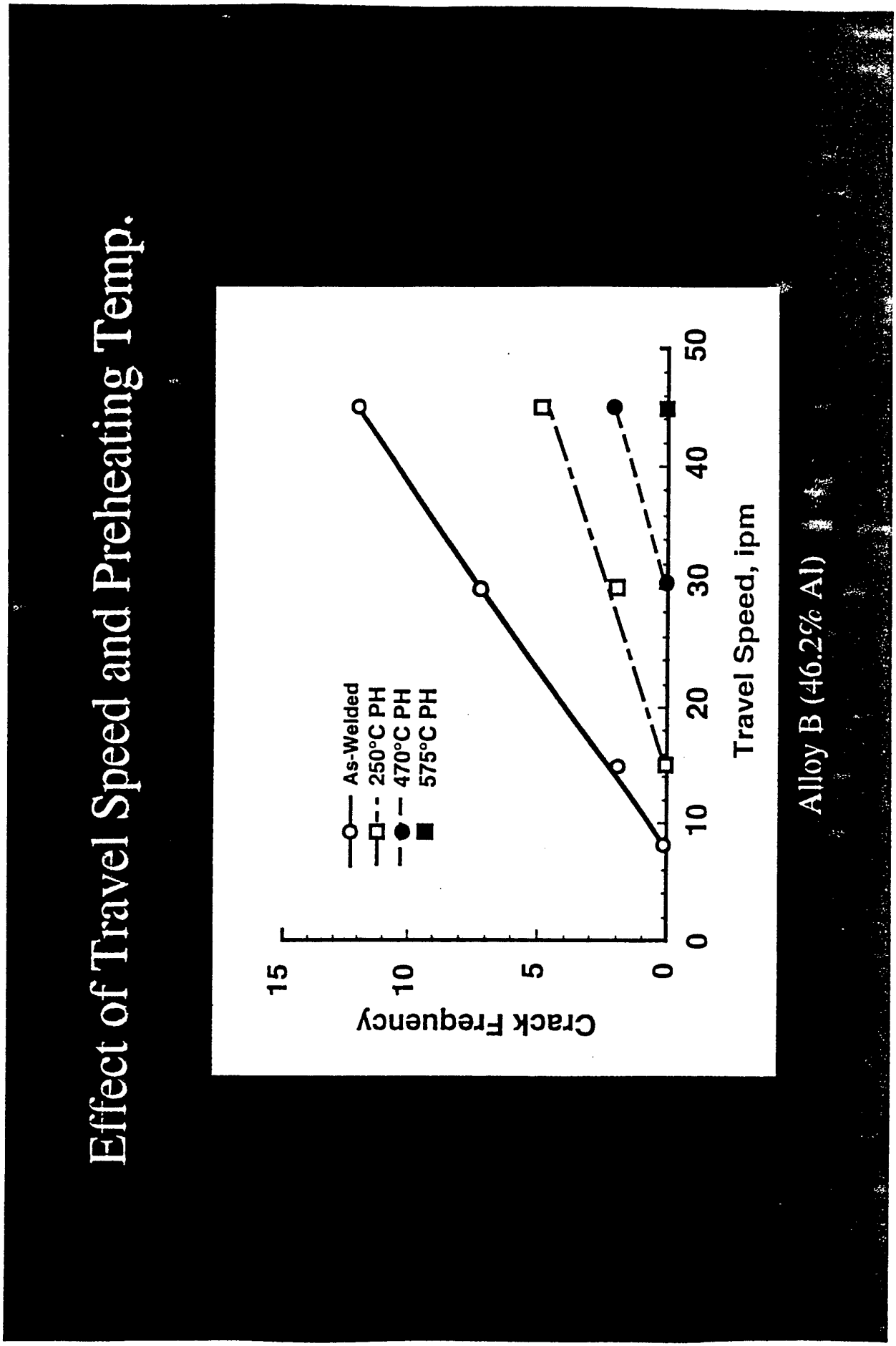

J Lee, W A Baeslack and T J Kelly: Weld fusion zone phenomena in Ti (45-48)Al-Nb-Cr γ titanium aluminides, submitted to Welding Journal.

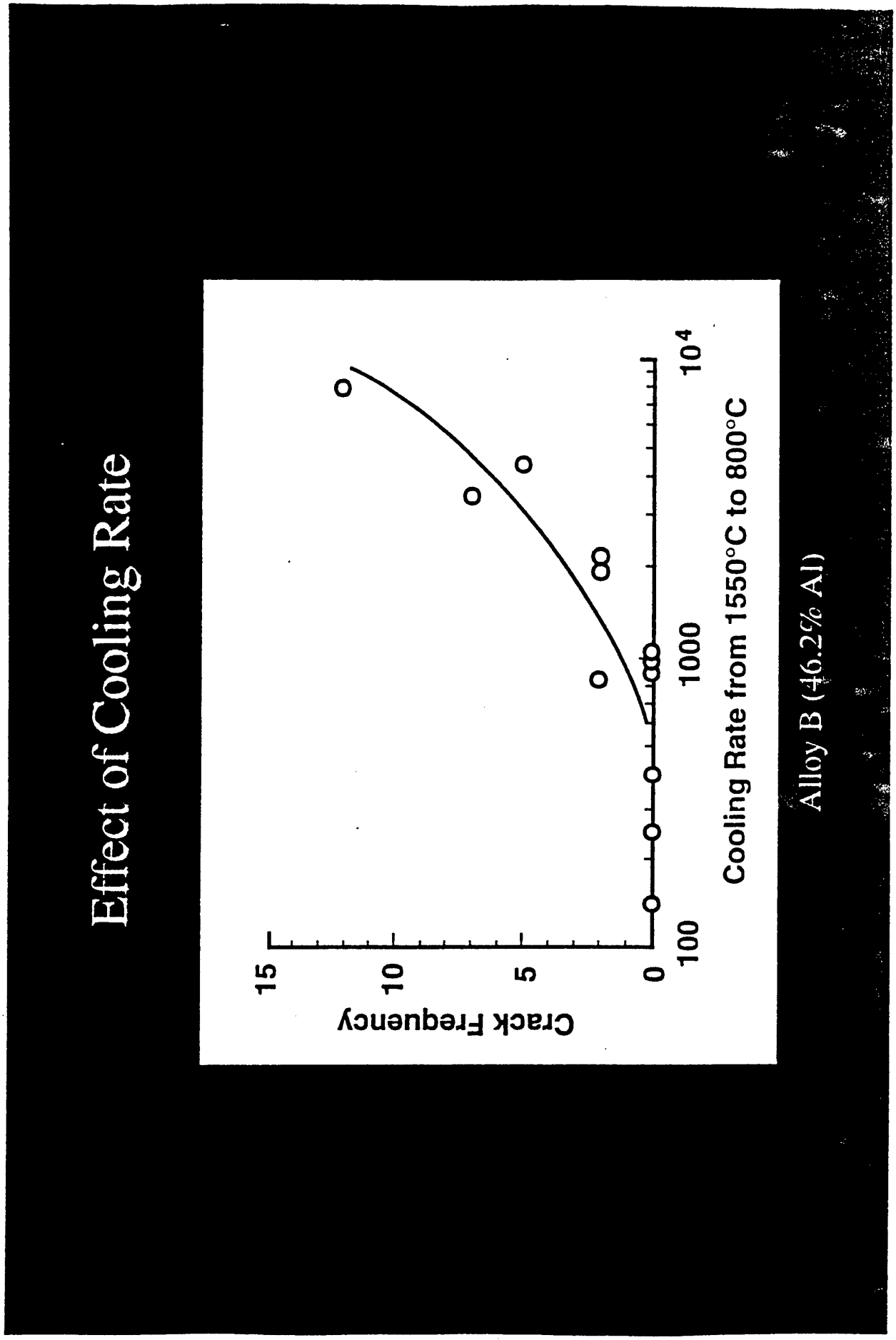

J Lee, W A Baeslack and T J Kelly: Weld fusion zone phenomena in Ti (45-48)Al-Nb-Cr γ titanium aluminides, submitted to Welding Journal.

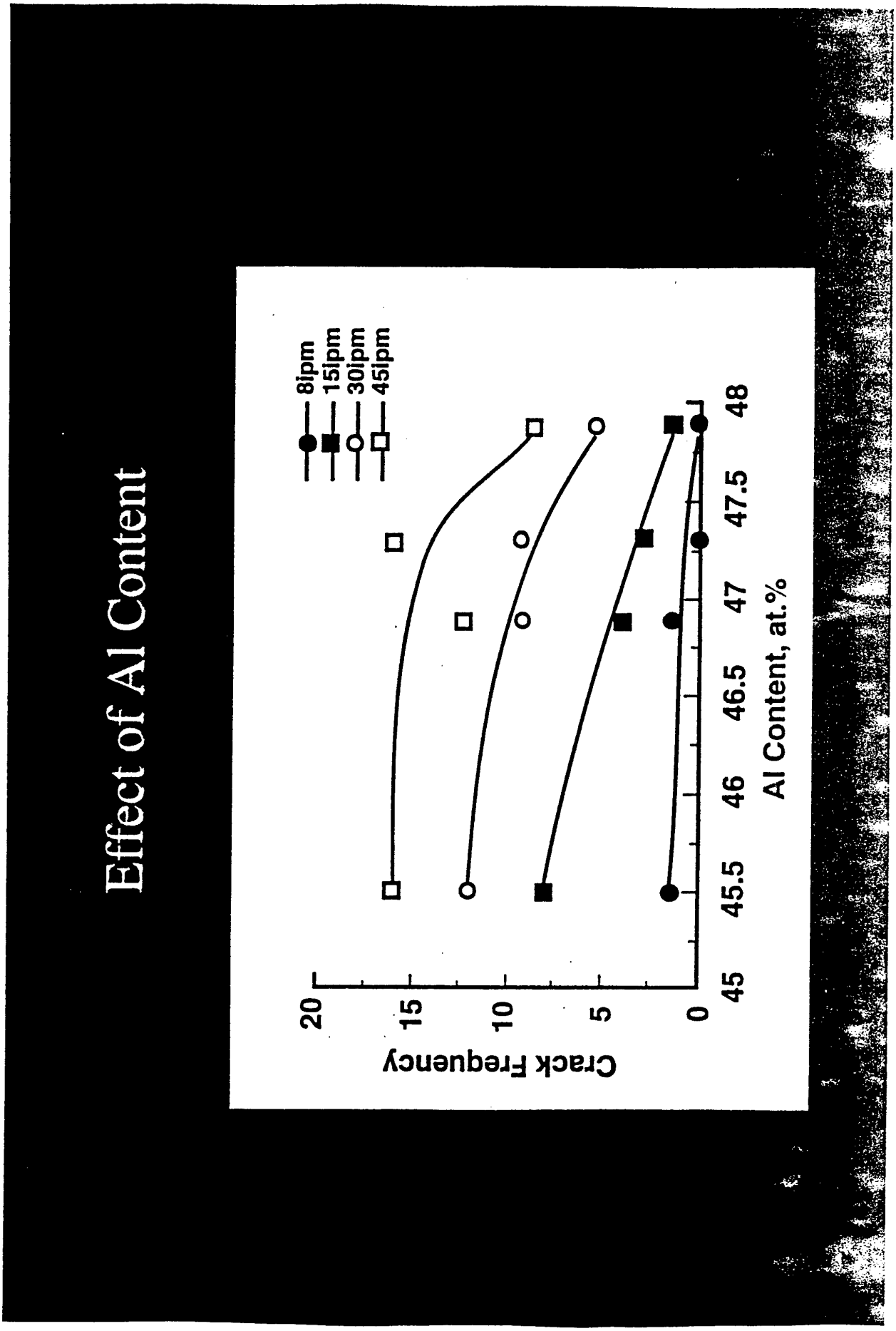

J Lee, W A Baeslack and T J Kelly: Weld fusion zone phenomena in Ti (45-48)Al-Nb-Cr γ titanium aluminides, submitted to Welding Journal.

Partitioning of Alloying Elements during Solidification

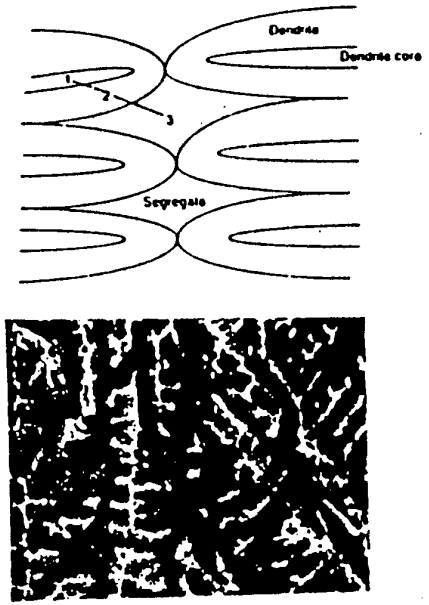

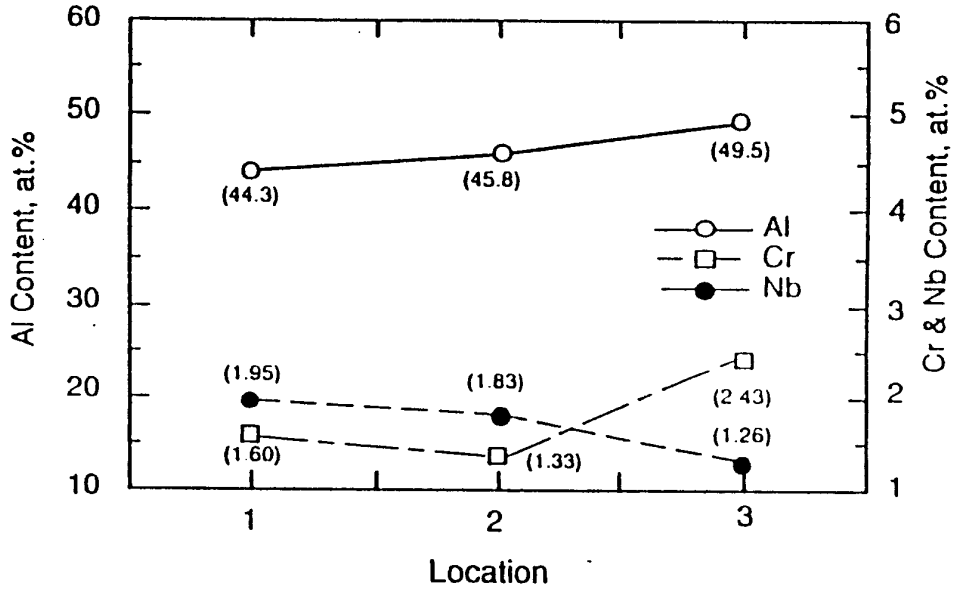

Alloy E, 1.5kW-8ipm

J Lee, W A Baeslack and T J Kelly: Weld fusion zone phenomena in Ti (45-48)Al-Nb-Cr γ titanium aluminides, submitted to Welding Journal.

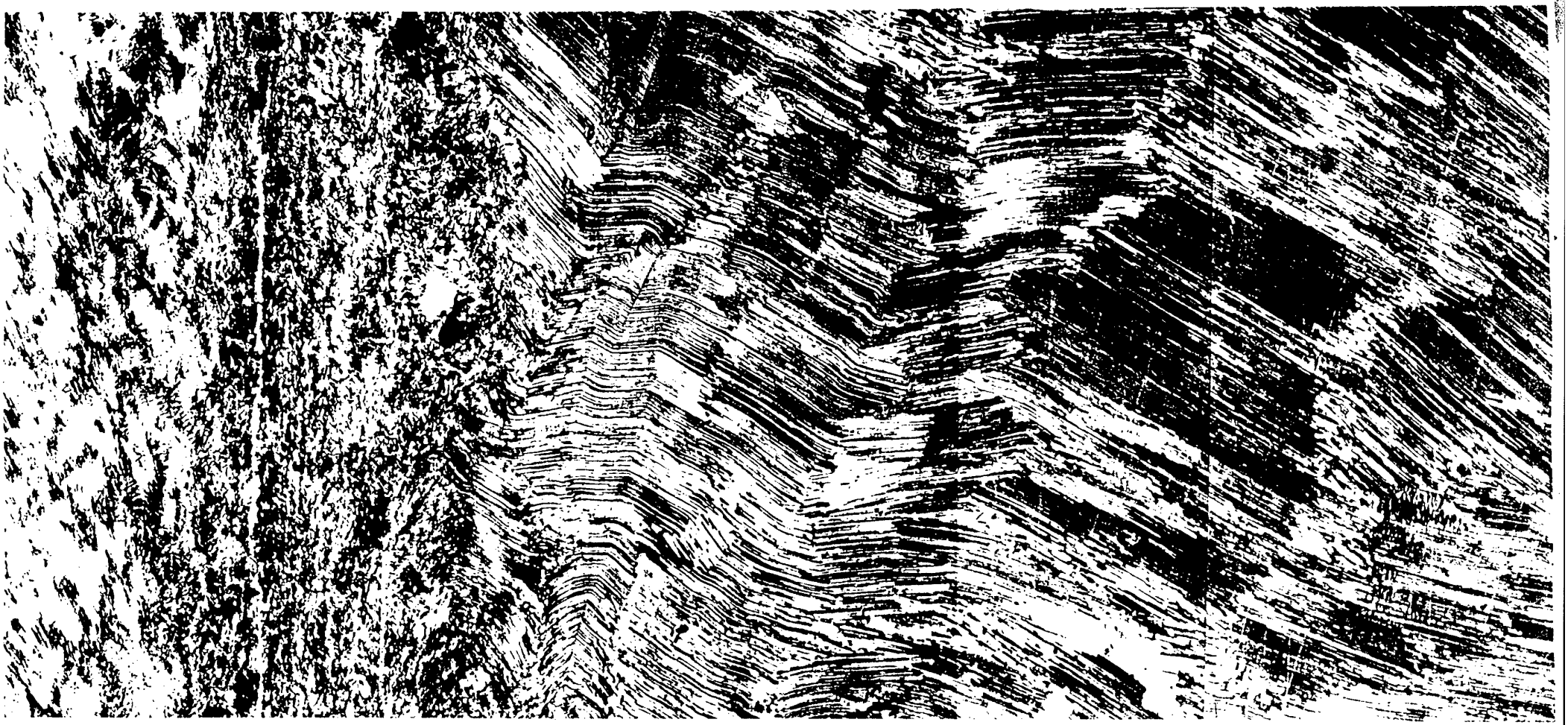

Linear friction weld in 10mm Ti-48Al-2Mn-2Nb, FW10, x100. AG2210 (top) - AG2213

Backscattered electron image of HAZ microstructure of linear friction weld FW10 in Ti-48Al-2Mn-2Nb casting, in unetched condition, x500. Negs 42676,-77,-78,-80

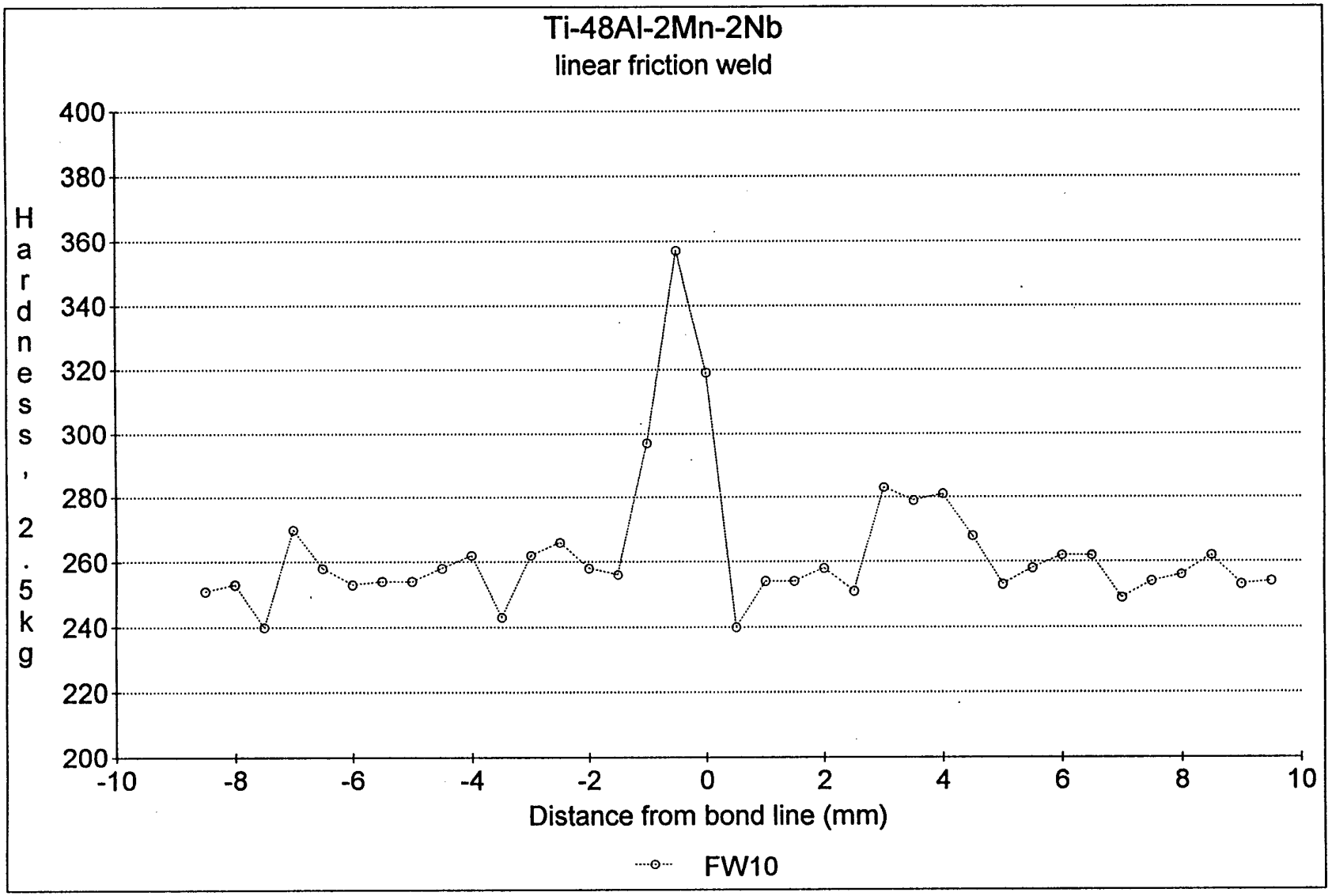
Ti-48Al-2Mn-2Nb
linear friction weld
Hardness, 2.5kg
400
380
360
340
320
300
280
260
240
220
200
-10
-8
-6
-4
-2
0
2
4
6
8
10
Distance from bond line (mm)
FW10

(a)

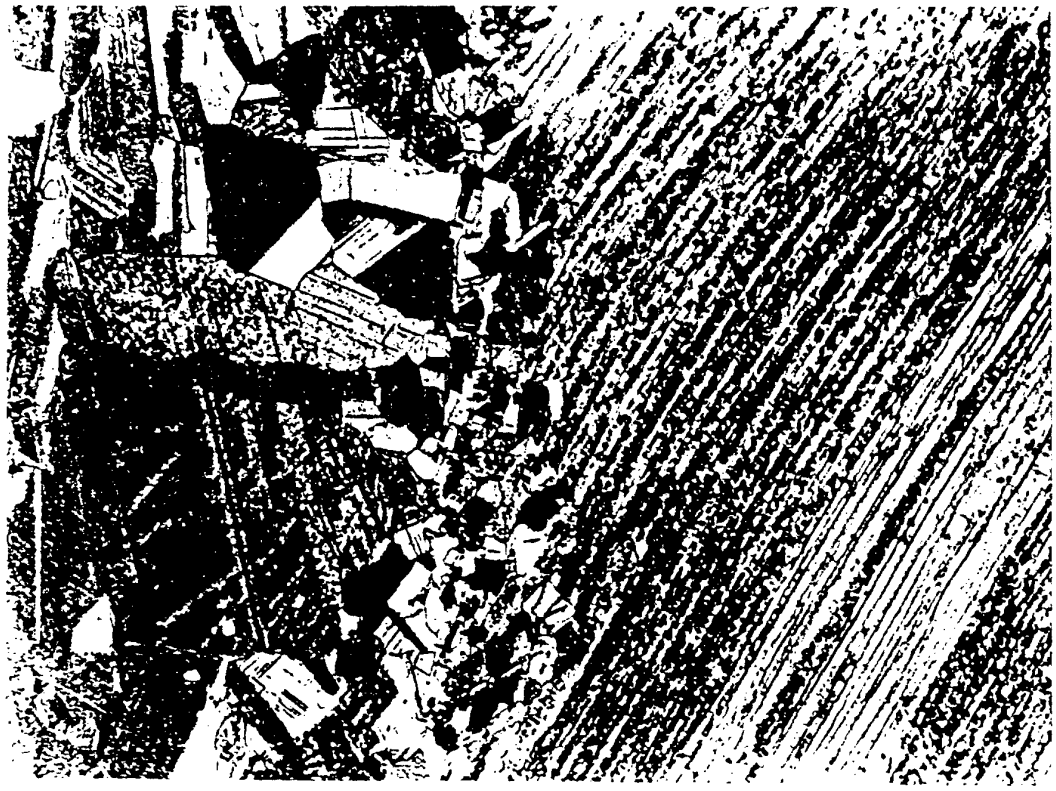

(b)

Electron beam diffusion bond in Ti-48Al-2Mn-2Nb, W81, 1200°C, 20MPa.
(a) x500, AG2021 (b) x1000, AG2022

150 nm

Bright field electron micrograph showing fine laths in 'retained α' regions of electron beam welded Ti-48at.%Al-2at.%Mn-2at.%Nb. Arrows indicate possible growth steps on the laths

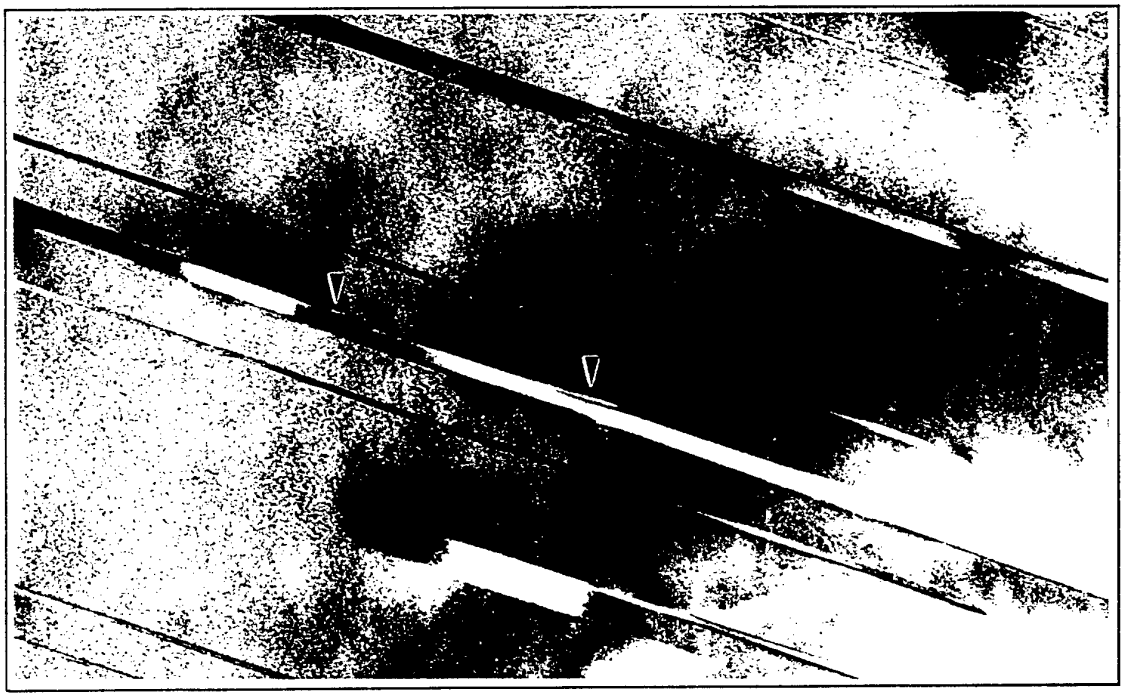

50 nm

Bright field electron micrograph showing fine laths in 'retained α' regions of electron beam welded Ti-48at.%Al-2at.%Mn-2at.%Nb. Arrows indicate possible growth steps on the laths

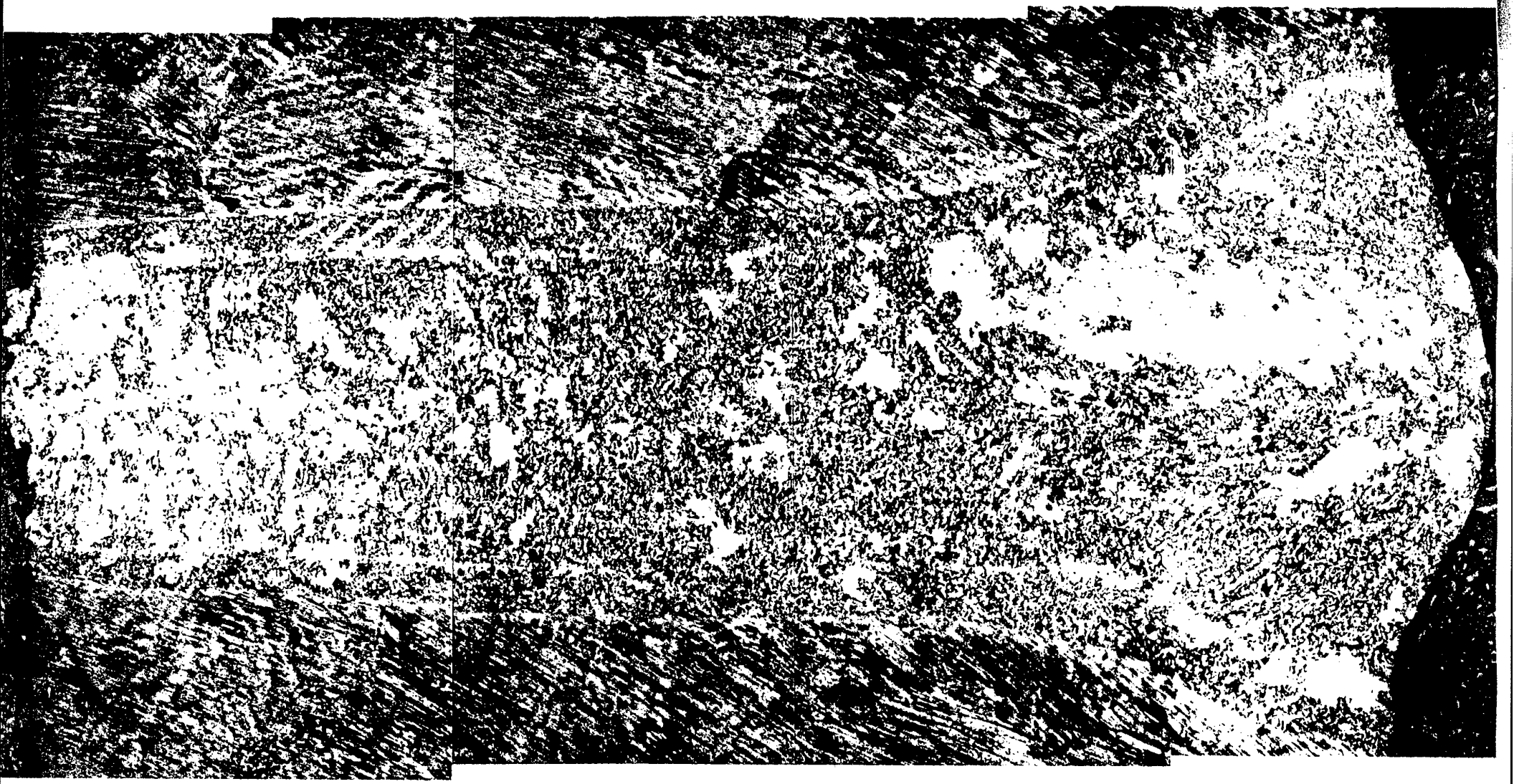

Electron beam weld in 5mm Ti-48Al-2Mn-2Nb, no preheat, x50. (Birmingham University)

Autogenous keyhole plasma weld in Ti-48Al-2Mn-2Nb casting, x10

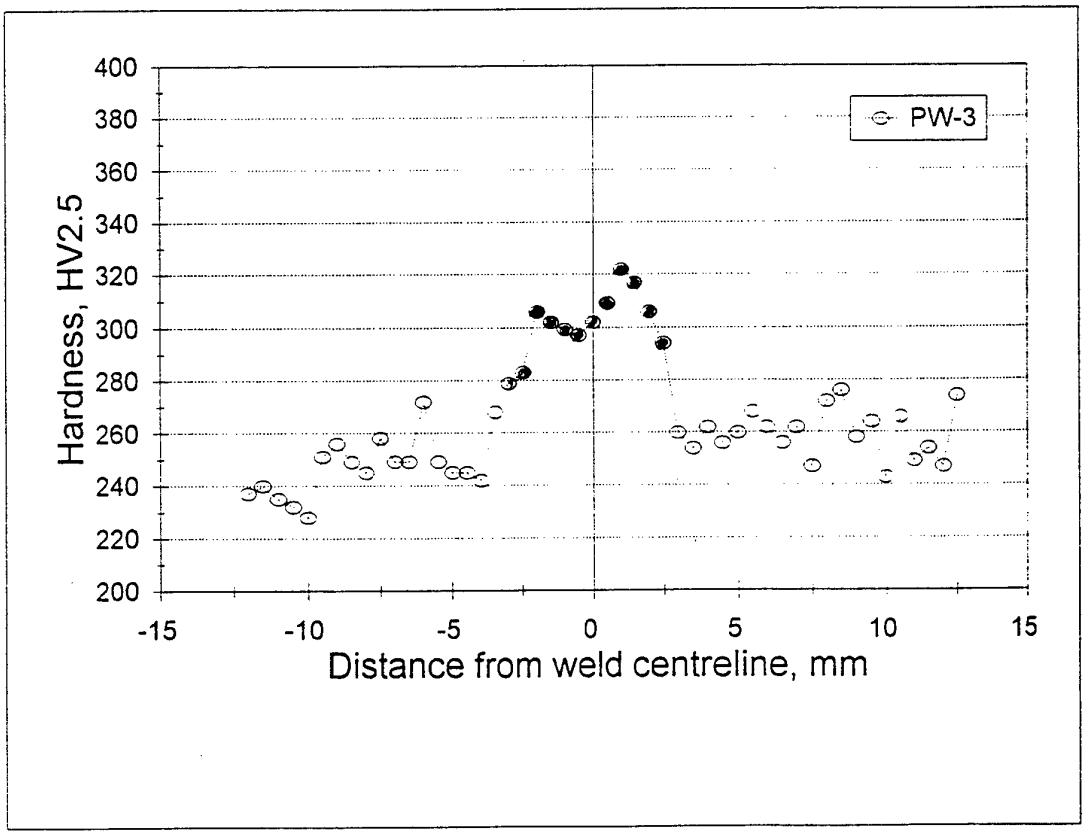

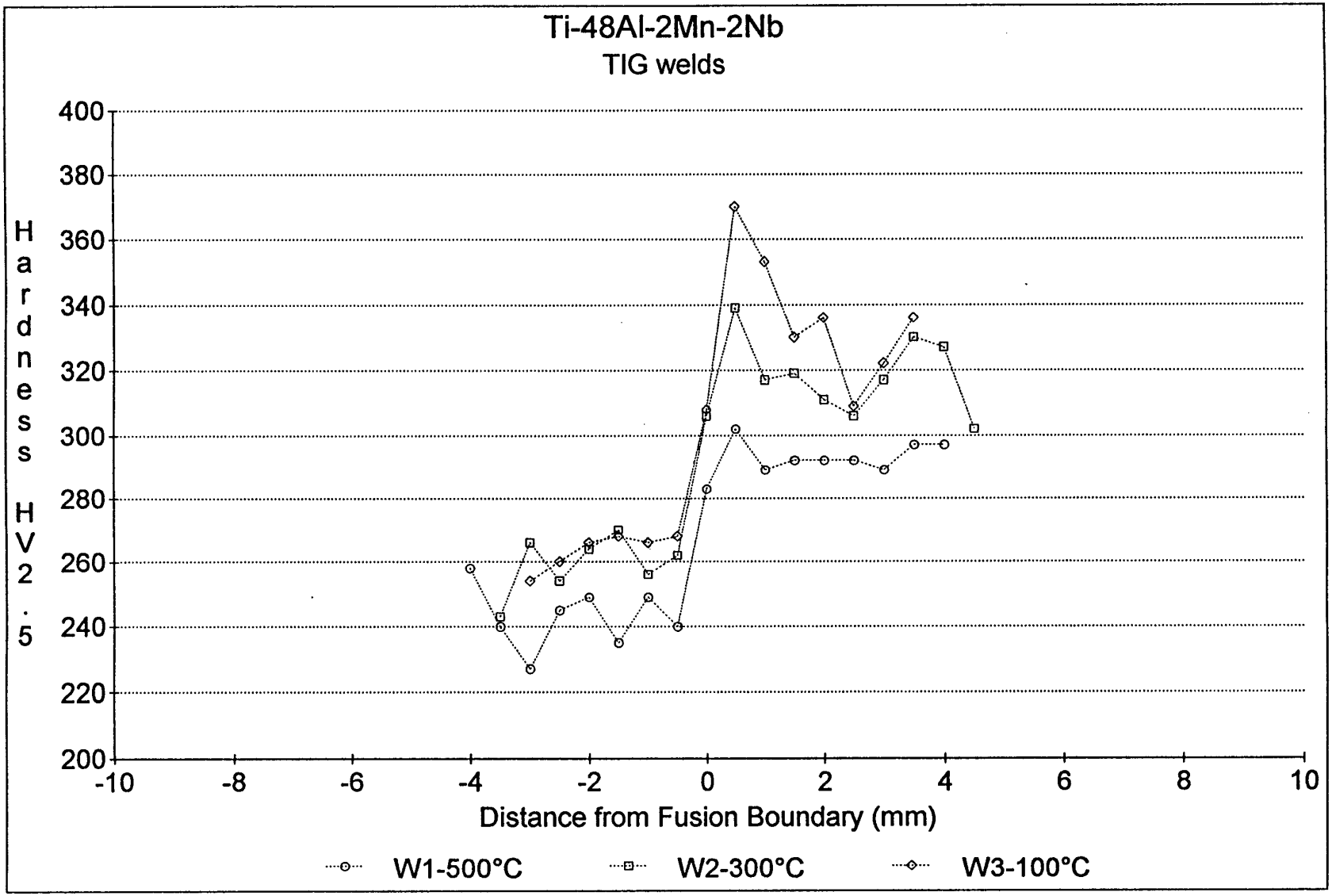
Ti-48Al-2Mn-2Nb
TIG welds
Hardness HV2.5
400
380
360
340
320
300
280
260
240
220
200
-10
-8
-6
-4
-2
0
2
4
6
8
10
Distance from Fusion Boundary (mm)
W1-500°C
W2-300°C
W3-100°C

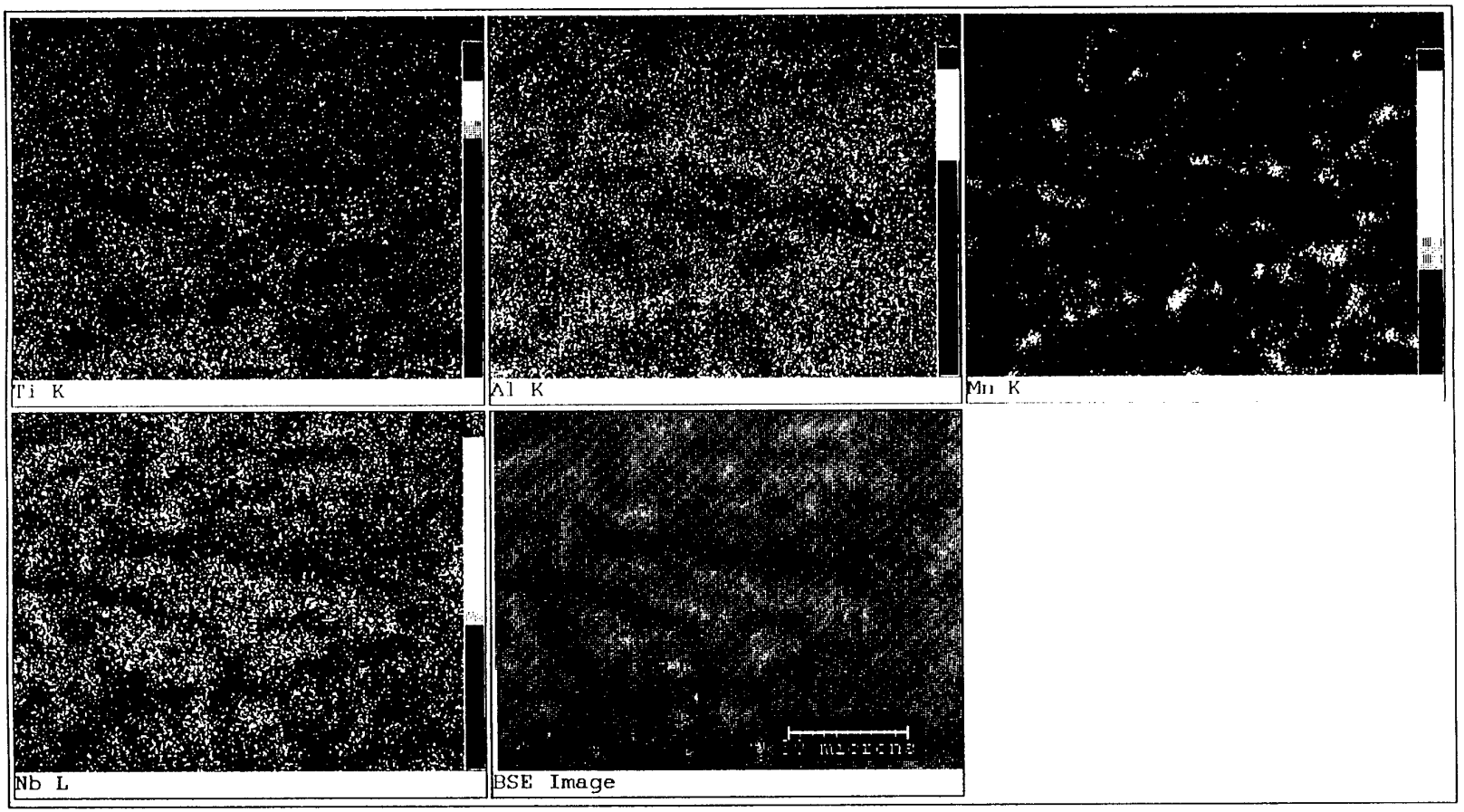

Element distributions in TIG weld W2 in Ti-48Al-2Mn-2Nb

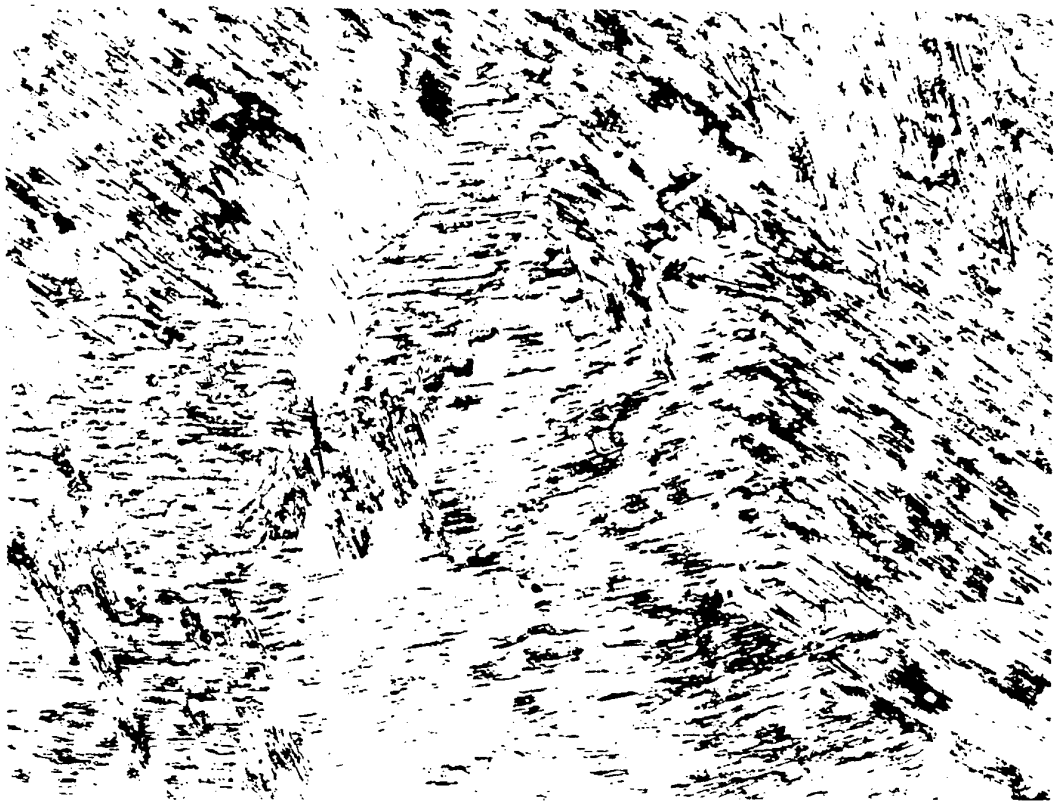

Fusion zone microstructure of TIG melt W2 (300°C) run in Ti-48Al-2Mn-2Nb, close to surface. x500. AG1620

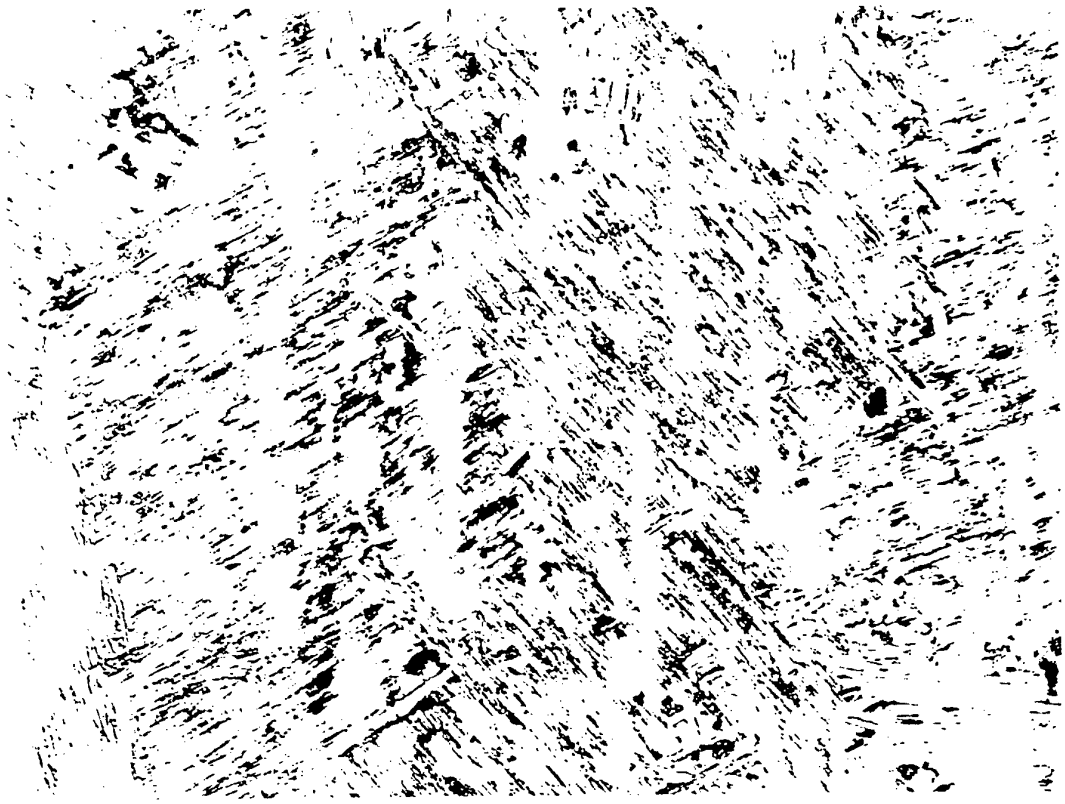

Fusion zone microstructure of TIG melt W3 (100°C) run in Ti-48Al-2Mn-2Nb, close to surface. x500. AG1621

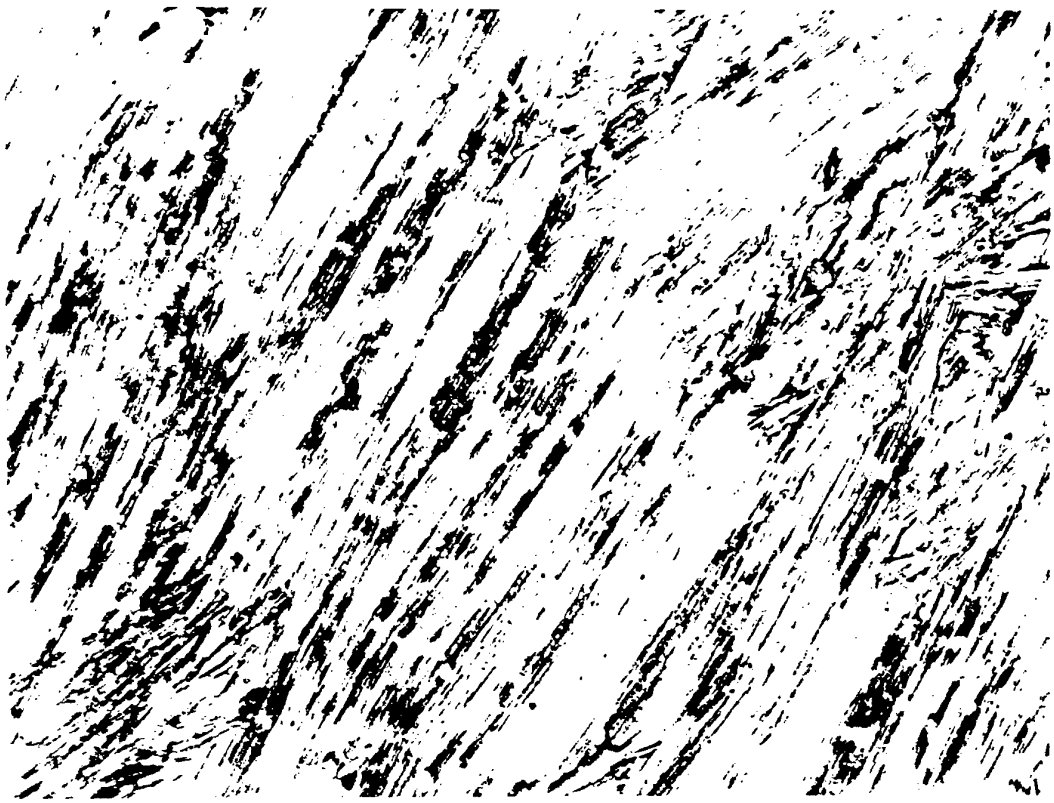

Fusion zone microstructure of TIG melt W1 (500°C) run in Ti-48Al-2Mn-2Nb, close to surface. x500. AG1619

(a)

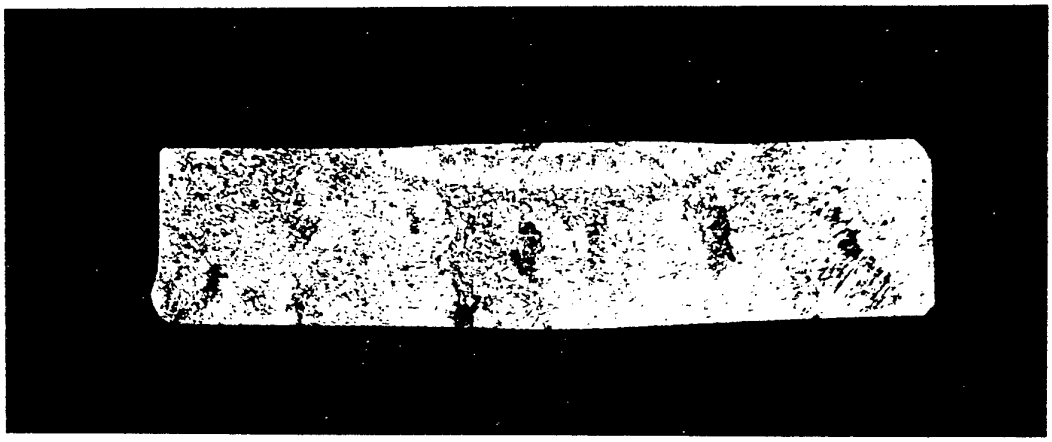

(b)

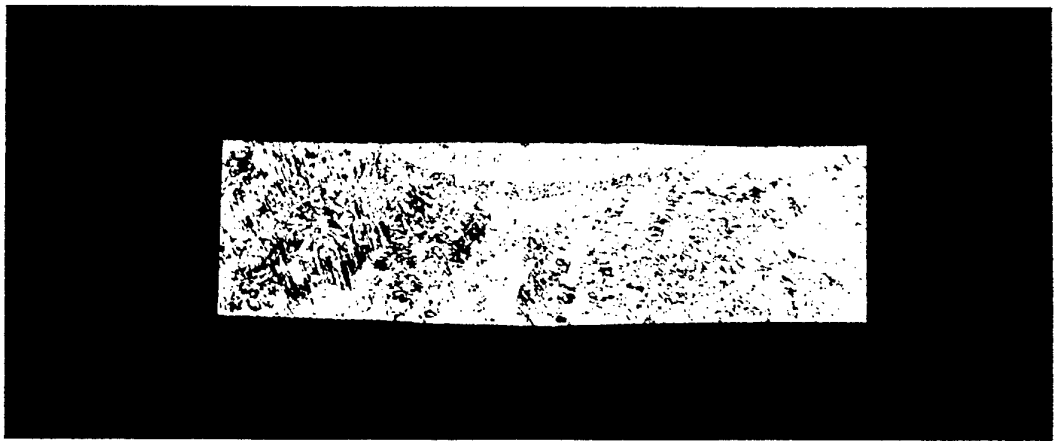

(c)

TIG melt runs in Ti-48Al-2Mn-2Nb, x5
(a) W1, 500°C, AG1630. (b) W2, 300°C, AG1629. (c) W3, 100°C, AG1628.